UNIWERSYTET ŚLĄSKI W KATOWICACH
WYDZIAŁ NAUK ŚCISŁYCH I TECHNICZNYCH
INSYTUT CHEMII

SARA IZABELA ZIMNY
9005

Badanie dynamiki molekularnej wybranych polisiloksanów o różnych topologiach w zmiennych warunkach termodynamicznych

PRACA DOKTORSKA

PROMOTOR:
Prof. dr hab. Kamil Kamiński

Chorzów 2025

Składam serdeczne podziękowania
Panu prof. dr hab. Kamilowi Kamińskiemu
za cenne wskazówki, cierpliwość, poświęcony czas
oraz nieocenione wsparcie merytoryczne
na każdym etapie przygotowania niniejszej rozprawy doktorskiej.

Składam również podziękowania
Pani dr hab. Magdalenie Tarnackiej
za opiekę i wiedzę, którą mi przekazała.

Pragnę także podziękować całej grupie badawczej
za pomoc oraz stworzenie przyjaznej i twórczej atmosfery,
a moim Najbliższym za wyrozumiałość i ogromne wsparcie.

NARODOWE CENTRUM NAUKI

Badania przeprowadzone na potrzeby niniejszej rozprawy doktorskiej finansowane były w ramach projektów Narodowego Centrum Nauki - OPUS 17, pt. *„Korelacja między ograniczoną rozmiarowością i oddziaływaniami z powierzchnią i ich wpływ na dynamikę molekularną materiałów ograniczonych przestrzennie dwuwymiarowo. Czy rozmiar zastosowanego ograniczenia przestrzennego ma znaczenie?”* (nr decyzji: 2019/33/B/ST3/00500), którego kierownikiem była dr hab. Magdalena Tarnacka, prof. UŚ; oraz OPUS 24, pt. *„Badanie dynamiki molekularnej i oddziaływań międzymolekularnych w miękkich materiałach infiltrowanych do nanostrukturyzowanych mezoporowatych membran”* (nr decyzji: 2022/47/B/ST4/00236), którego kierownikiem jest prof. dr hab. Kamil Kamiński.

SPIS TREŚCI

WYKAZ SKRÓTÓW

ATRP – metoda polimeryzacji rodnikowej z przeniesieniem atomu

BDS – szerokopasmowa spektroskopia dielektryczna

Đ – dyspersyjność

d – gęstość

DLS – dynamiczne rozpraszanie światła

DSC – Różnicowa kalorymetria skaningowa

dTg/dp – współczynnik ciśnieniowy temperatury przejścia szklistego

f - częstotliwość

G" – moduł stratności

HN - Havriliaka-Negami (funkcja, model)

HO-PDMS-OH – poli(dimetylosiloksan) z hydroksylowymi grupami terminalnymi

IUPAC – Międzynarodowa Unia Chemii Czystej i Stosowanej

M_n – Masa cząsteczkowa

O – symbol chemiczny tlenu

p – ciśnienie

PCS - spektroskopia korelacji fotonowej

PI – cis-1,4-poliizopren

PIB – poli(izo-butylen)

PLAs – poli(laktydy)

PMMS – poli(merkaptopropylometylosiloksan)

PMMS-*graft*-HA - poli[merkapto(heksylo-3-propaniano)propylometylosiloksan]

PMMS-*graft*-HMA - poli[merkapto(heksylo-3-(2-metylo)-propaniano)propylometylosiloksan]

PMMS-*graft-izo*BA - poli[merkapto(izo-butylo-3-propaniano)propylometylosiloksan]

PMMS-*graft*-MA – poli[merkapto(metylo-3-propaniano)propylometylosiloksan]

PMMS-*graft*-MBA - poli[merkapto(butylo-3-(2-metylo)-propaniano)propylometylosiloksan]

PMMS-*graft*-MMA - poli[merkapto(metylo-3-(2-metylo)-propaniano)propylometylosiloksan]

PMMS-*graft-n*BA - poli[merkapto(n-butylo-3-propaniano)propylometylosiloksan]

PMMS-*graft-tert*BA - poli[merkapto(tert-butylo-3-propaniano)propylometylosiloksan]

PMPS - poli(metylofenylosiloksan)

PMpTS – poli(metylo-para-tolilosiloksan)

POB - poli(tlenek 1,2-butylenu)

PPG - poli(glikol propylenowy)

-SH – grupa tiolowa

Si – symbol chemiczny krzemu

T – temperatura

T_g – temperatura przejścia szklistego

T_g^{BDS} – temperatura zeszklenia uzyskana z badań dielektrycznych

T_g^{DSC} – temperatura zeszklenia uzyskana z badań kalorymetrycznych

TTPS – reguła superpozycji czasowo-temperaturowo-ciśnieniowej

α,α’ – procesy relaksacyjne

ΔV – objętość aktywacji

ε'' – straty dielektryczne

η – lepkość

τ_{Debye} – czas relaksacji procesu Debye’a

$\tau_{sub\text{-}Rouse}$ – czas relaksacji procesu *sub-Rouse*

τ_T – czas relaksacji terminalnej z badań mechanicznych

τ_α – czas relaksacji segmentalnej

WYKAZ RYSUNKÓW I TABEL

I. WSTĘP

Zgodnie z definicją Międzynarodowej Unii Chemii Czystej i Stosowanej (IUPAC) polimery to klasa związków chemicznych składająca się z makrocząsteczek. Makrocząsteczka to molekuła o wysokiej masie cząsteczkowej, która zbudowana jest z wielokrotnie powtarzanych jednostek pochodzących z cząsteczek o niskiej masie cząsteczkowej (tzw. merów).[1] W ostatnich dekadach polimery zaczęły stanowić dominującą klasę materiałów, dzięki temu, iż oferują znacznie lepsze właściwości fizyczne i chemiczne niż materiały konwencjonalne. Znajdują szerokie zastosowanie we współczesnej gospodarce, od przemysłu, przez motoryzację i elektronikę, aż po medycynę. Wykorzystywane są m.in. jako smary,[2] bezrozpuszczalnikowe elastomery,[3] modyfikatory powierzchni,[4] kryształy fotoniczne,[5] w litografii[6] lub jako nośniki leków oraz w produktach codziennego użytku – kosmetykach, produktach higienicznych, środkach gospodarstwa domowego.[7,8] Tak znaczna ekspansja polimerów ma swoje źródło bezpośrednio w tym, iż bardzo łatwo można modyfikować i kontrolować ich masę cząsteczkową (M_n), dyspersyjność (Đ), gęstość (d), strukturę i skład chemiczny, produkując materiały o pożądanych właściwościach użytkowych.

W ostatnich latach dokonano ogromnego postępu technologicznego w dziedzinie chemii polimerów, a tym samym rozwoju metod ich przetwarzania, takich jak – odwracalnej dezaktywacji polimeryzacji rodnikowej, zwłaszcza polimeryzacji rodnikowej z przeniesieniem atomu (ATRP).[9–15] Metody te umożliwiają dostęp do bardziej zaawansowanych materiałów polimerowych, które charakteryzują się pożądanymi i kontrolowanymi architekturami makromolekularnymi, posiadającymi inną topologię niż liniowa, takie jak kopolimery, struktury gwiaździste, szczotkowe, usieciowane czy też hiperrozgałęzione/dendrymeryczne (**Rys. 1**).[16,17]

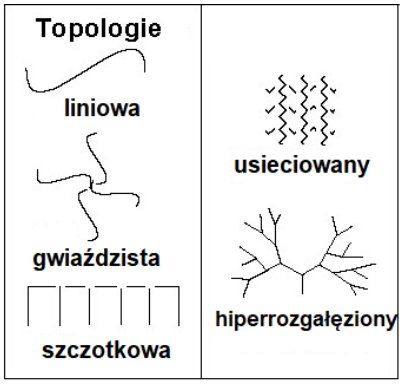

Rys. 1. Rodzaje topologii wśród polimerów.

Z biegiem lat materiały polimerowe stały się interesującymi obiektami badań dla naukowców pracujących na całym świecie. Szczególnego znaczenia nabrało poznanie i zrozumienie zachowania polimerów semikrystalicznych bądź całkowicie amorficznych w pobliżu przejścia szklistego (T_g). Jest to istotne, gdyż wiele takich makrocząsteczek, stosowanych w różnych gałęziach przemysłu, zmienia swoje podstawowe właściwości fizyczne na skutek starzenia i procesów związanych z reorganizacją molekularną w nich zachodzących, które mają wpływ na szybsze ich zużywanie, utratę odpowiednich własności mechanicznych. Warto tutaj nadmienić, iż przejście szkliste opisuje zakres temperaturowy, w którym właściwości mechaniczne materiałów zmieniają się ze stanu twardego/kruchego ciała stałego na bardziej miękkie, gumowate o właściwościach lepko-sprężystych, które jest bardziej odkształcalne, elastyczne.[18] Tak dramatyczna zmiana lepkości, elastyczności i twardości polimerów w pobliżu T_g jest ważnym zagadnieniem fizyki materii skondensowanej, ale również ma duże znaczenie w kontekście projektowania i przetwórstwa polimerów amorficznych. Z pewnością systematyczne badania nad zrozumieniem natury przejścia szklistego prowadzone w różnych warunkach termodynamicznych pozwolą optymalizować procesy przetwórcze oraz określić wpływ czynników zewnętrznych, takich jak temperatura czy ciśnienie na degradację oraz fizyczne starzenie się polimerów.[19,20]

Fizyczne zrozumienie przemiany szklistej jest obecnie aktualnym problemem fizyki materii skondensowanej.[18,21,22] Gdy układ tworzący szkło zostaje przechłodzony poniżej temperatury krystalizacji, jego dynamika molekularna ulega silnemu spowolnieniu na skutek gwałtownego wzrostu lepkości (η). W kontekście polimerów, za proces zeszklenia odpowiedzialna jest relaksacja segmentalna (α-relaksacja) odzwierciedlająca kooperatywne przegrupowanie cząsteczek cieczy przechłodzonej, które odbywa się z charakterystycznym czasem, zwanym czasem relaksacji α, τ_α.[23,24] Z kolei temperaturę, z której układ przechodzi ze stanu metastabilnego, równowagowego do stanu metastabilnego, nierównowagowego określa się jako temperaturę zeszklenia (T_g). Jest ona definiowana jako temperatura, w której lepkość i czas relaksacji osiągają odpowiednio wartości $\eta = 10^{13}$ Pa × s, i $\tau_\alpha = 100$ s.[25–29] Do badania zachowania polimerów w pobliżu przejścia szklistego[18] wykorzystuje się szereg komplementarnych metod eksperymentalnych takich jak: Dynamiczne Rozpraszanie Światła (DLS), Spektroskopię Rozpraszania Neutronów, Spektroskopię Mechaniczną oraz Szerokopasmową Spektroskopię Dielektryczną (BDS). Ostatnia z wymienionych technik jest szczególnie użytecznym narzędziem do badania dynamiki molekularnej polimerów ze względu na rejestrację procesów relaksacyjnych odzwierciedlających ruchliwość molekularną makrocząsteczek o skrajnie różnych skalach czasowych, w szerokim zakresie częstotliwości, temperatur i ciśnień.

Za pomocą wymienionych metod eksperymentalnych, wnikliwie zbadano dynamikę molekularną makrocząsteczek, takich jak: cis-1,4-poliizopren (PI),[30–32] poli(tlenek 1,2-butylenu) (POB),[33] poli(tlenek etylenu) (PEO),[34] poli(laktydy) (PLAs),[35] poli(tlenek styrenu),[36] poli(izocyjanian heksylu),[37] poli(glikol propylenowy) (PPG).[38–44] Warto nadmienić, iż w/w makrocząsteczki są bardzo atrakcyjne z punktu widzenia badań dielektrycznych, ponieważ posiadają wypadkowy moment dipolowy ułożony równolegle do łańcucha głównego, to tzw. polimery typu A według klasyfikacji Stockmayera.[45] Wynika

z tego, że oprócz obecności procesu segmentalnego związanego z ruchami kooperatywnymi powtarzających się jednostek łańcucha (relaksacja α), na widmach strat dielektrycznych obserwuje się również dodatkowy proces relaksacyjny, tzw. *normal-mode*, związany z fluktuacjami wektora łączącego dwa końce łańcucha (ang. *end-to-end*). Co ciekawe, jeżeli porówna się czasy relaksacji procesu *normal-mode* wyznaczone z pomiarów dielektrycznych z czasami relaksacji terminalnej otrzymanymi z pomiarów mechanicznych, stwierdzić można bardzo dobrą zgodność między nimi.[46–49] To proste porównanie jasno pokazuje, że ta dodatkowa mobilność zarejestrowana na widmach dielektrycznych jest związana z dynamiką całego łańcucha polimeru. To jasno sugeruje, że w przypadku polimerów typu A istnieje możliwość śledzenia dielektrycznie globalnej dynamiki łańcucha całej makrocząsteczki.

Jednakże obserwacja w pomiarach BDS *normal-modu*, który daje informację o globalnej dynamice (dyfuzji) polimerów nie jest możliwa dla wszystkich układów. Makrocząsteczki, dla których moment dipolowy jest ułożony prostopadle względem łańcucha głównego, tzn. polimery typu B, nie wykazują obecności na widmach strat dielektrycznych relaksacji *normal-mode*.[50] Przykładem może być poli(metylofenylosiloksan) (PMPS).[51–58] Warto nadmienić, iż PMPS jest przedstawicielem polisiloksanów, polimerów o dość unikalnym charakterze, który związany jest z ich budową – łańcuch główny składa się z połączenia tlenu (O) oraz krzemu (Si), co sprawia, że cały szkielet makrocząsteczki jest o wiele bardziej elastyczny i charakteryzuje się większą swobodą rotacji w porównaniu do polimeru o budowie węglowej. Co więcej, w zależności od długości łańcucha głównego i charakteru przyłączonych grup bocznych do atomów krzemu, polisiloksany mogą przybierać różne formy – od ciężkich, smaropodobnych cieczy po stałe żywice. Związki te są bardzo stabilne chemicznie oraz termicznie, charakteryzują się słabymi oddziaływaniami między-łańcuchowymi, wynikającymi z niskoenergetycznych wiązań Si-O, mają niskie napięcie

powierzchniowe oraz wykazują niską toksyczność i reaktywność chemiczną.[59,60] W efekcie znajdują powszechnie zastosowanie w medycynie (np. wyroby medyczne, takie jak implanty, opatrunki hydrożelowe, itp.), w budownictwie (jako kleje, uszczelniacze, itp.), w kosmetykach, produktach higienicznych, tworzywach sztucznych, a także w przemyśle spożywczym.[61–65]

PMPS był obiektem badań spektroskopowych przez różne grupy. Najwcześniejsze badania wykonane dla tego polimeru przy użyciu spektroskopii korelacji fotonowej (PCS) pozwoliły zaobserwować dwa procesy relaksacyjne powyżej temperatury zeszklenia. Co ważne czasy relaksacji otrzymane dla szybszego procesu wyznaczone z badań PCS dobrze zgadzały się z czasami relaksacji procesu segmentalnego z badań dielektrycznych. Natomiast drugi, wolniejszy proces, tzw. relaksacja α', nie posiadał swojego odpowiednika w badaniach dielektrycznych. Stąd autorzy postulowali, że proces α' jest związany z dyfuzją całego łańcucha polimerowego.[58,66] Nowe spojrzenie na dynamikę molekularną PMPS przyniosły badania podjęte przez prof. Adrjanowicz i wsp., która zmierzyła dielektrycznie dwie próbki PMPS o różnych ciężarach cząsteczkowych.[56,57] Pomiary te ujawniły istnienie dodatkowego procesu relaksacyjnego, wolniejszego niż relaksacja segmentalna, którego dynamika była zależna od masy cząsteczkowej polimeru. Dodatkowo z racji tego, że czasy relaksacji nowego modu nie zgadzały się z czasami relaksacji terminalnej (τ_T) wyznaczonymi z pomiarów mechanicznych, jak również biorąc pod uwagę to, że PMPS jest polimerem typu B, dodatkowy proces dielektryczny został zaklasyfikowany jako *sub-Rouse*.[56] Warto tutaj wspomnieć, iż badania z wykorzystaniem metody PCS oraz pomiarów mechanicznych ujawniły obecność procesu typu *sub-Rouse* w poli(izo-butylenie) (PIB),[67,68] czy też poli(metylo-para-tolilosiloksanie) (PMpTS).[69,70]

W niniejszej rozprawie przeprowadzono badania dynamiki molekularnej substancji wielkocząsteczkowych z grupy polisiloksanów i ich pochodnych, które formują fazę szklistą, za pomocą szerokopasmowej spektroskopii dielektrycznej (BDS). Ta metoda badawcza

umożliwia rejestrację ruchów relaksacyjnych wielu nisko- i wielkocząsteczkowych układów w szerokim zakresie częstotliwości 10^{-2} – 10^{6} Hz i w różnych warunkach temperatury (T) i ciśnienia (p). Szczególną uwagę skupiono na detekcji procesu relaksacyjnego typu *sub-Rouse* w badanych układach oraz jego zachowania, właściwości dynamicznych w zmiennych warunkach termodynamicznych.

II. CEL PRACY

Celem niniejszej pracy doktorskiej było scharakteryzowanie dynamiki molekularnej badanych polimerów z grupy polisiloksanów – poli(merkaptopropylometylosiloksanu) (PMMS) oraz syntezowanych na bazie PMMS kopolimerów szczepionych otrzymanych metodą fotopolimeryzacji, w których w łańcuchu bocznym poprzez grupę tiolową -SH zostały przyłączone różne monomery.

Przede wszystkim główną motywacją niniejszych badań było znalezienie wyjaśnienia dotyczącego natury dodatkowych ruchów molekularnych, jakie obserwuje się w pomiarach dielektrycznych polisiloksanów. Natomiast dla polimerów modyfikowanych grupami chemicznymi o różnej strukturze i topologii szczególnie ważne wydało się określenie wpływu architektury polimeru na dynamikę molekularną w zmiennych warunkach termodynamicznych. Dielektryczne badania temperaturowe i ciśnieniowe rozpatrywanych w niniejszej rozprawie doktorskiej układów były wspierane przez komplementarne techniki eksperymentalne, takie jak różnicowa kalorymetria skaningowa (DSC) czy też dynamiczna analiza mechaniczno-termiczna (DMTA).

Rezultaty prowadzonych badań zostały opublikowane w prestiżowych czasopismach naukowych z listy filadelfijskiej:

A1. S. Zimny, M. Tarnacka, E. Kamińska, R. Wrzalik, K. Adrjanowicz, M. Paluch, K. Kamiński. **Studies on the Molecular Dynamics at High Pressures as a Key Identify the Sub-Rouse Mode in PMMS.** *Macromolecules, 2022, 55 (13), 5581-5590.*

A2. S. Zimny, M. Tarnacka, Ż. Wojnarowska, D. Heczko, P. Maksym, M. Paluch, K. Kamiński. **Impact of the Graft' Structure on the Behavior of PMMS-Based Brushes. High Pressure Studies.** *Polymer, 2023, 271, 125790.*

A3. S. Zimny, M. Tarnacka, P. Maksym, Ż. Wojnarowska, M. Paluch, K. Kamiński. **The Influence of Graft Rigidity on the Dynamical Behavior of PMMS-Based Polymer Brushes at Ambient and High Pressures.** *Macromolecules, 2024, 57 (22), 10754-10766.*

Treść powyższych publikacji stanowiących podstawę niniejszej pracy doktorskiej można znaleźć w **Rozdziale IV**. Wyniki uzyskane w trakcie mojego doktoratu zostały zaprezentowane na konferencjach naukowych:

1. „XV. Kopernikańskie Seminarium Doktoranckie" (2022), Toruń, Polska.
2. „IV. Seminarium Ogólnoakademickie „Metody fizykochemiczne w badaniach naukowych" (2023), Sosnowiec, Polska.
3. „65. Zjazd Naukowy Polskiego Towarzystwa Chemicznego" (2023), Toruń, Polska.
4. „V. Seminarium Ogólnoakademickie „Metody fizykochemiczne w badaniach naukowych" (2024), Sosnowiec, Polska.
5. „12th Conference on Broadband Dielectric Spectroscopy and its Applications" (2024), Lizbona, Portugalia.
6. "VI. Seminarium Ogólnoakademickie "Metody fizykochemiczne w badaniach naukowych" (2025), Sosnowiec, Polska.

Ponadto jestem współautorem dwóch artykułów naukowych, które nie zostały włączone do rozprawy:

1. A. Górny, M. Tarnacka, S. Zimny, M. Geppert-Rybczyńska, A. Brzózka, G.D. Sulka, M. Paluch, K. Kamiński. **Impact of Nanostructurization of The Pore Walls on the Dynamics of a Series of Phenyl Alcohols Incorporated Within Nanoporous Aluminum Oxide Templates.** *The Journal of Physical Chemistry C, 2022, 126 (43), 18475-18489.*

2. S. Zimny, M. Tarnacka, M. Geppert-Rybczyńska, K. Kamiński. **Is There a Relationship Between Wettability and the Rates of Equilibration of Hydrogen-Bonded Oligomer Poly(mercaptoproylmethylsiloxane) Under Confinement?** *The Journal of Physical Chemistry C, 2023, 127 (47), 23034-23043.*

III. OMÓWIENIE OTRZYMANYCH WYNIKÓW

A. Wysokociśnieniowe badania dielektryczne poli(merkaptopropylo-metylosiloksanu) (PMMS) w celu identyfikacji dodatkowych procesów relaksacyjnych

W artykule **A1** w celu zbadania dynamiki molekularnej polimeru asocjacyjnego z grupy polisiloksanów wybrano poli(merkaptopropylometylosiloksan) (PMMS). Polimer ten do każdego monomeru w szkielecie ma przyłączony łańcuch alkilowy zakończony grupą -SH, która wpływa na zdolność makrocząsteczki do tworzenia słabych wiązań wodorowych. Wykorzystany w badaniach homopolimer PMMS charakteryzuje się M_n = 2400 g/mol oraz Đ = 1,26, jest cieczą o dość rzadkiej konsystencji podobnej do wody. Jego temperatura zeszklenia (T_g) wynosi 178 K, a ponadto nie wykazuje on tendencji do krystalizacji. Podstawowe informacje dotyczące struktury i nazewnictwa przedstawiono na **Rys. 2.** Wybór tego polimeru nie był przypadkowy, ponieważ poprzednio przeprowadzone badania dielektryczne ujawniły obecność dodatkowego procesu relaksacyjnego, dla którego jednoznaczne określenie jego pochodzenia było trudne do ustalenia.[71]

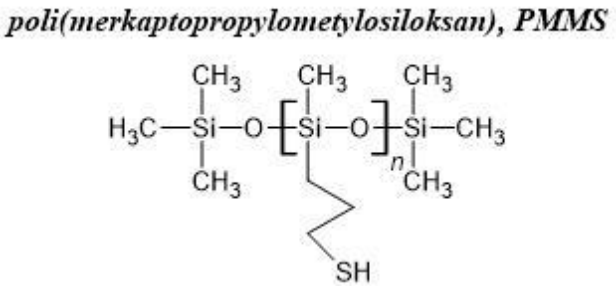

Rys. 2. Struktura i nazewnictwo badanej substancji.

W pierwszej kolejności przeprowadzono badania za pomocą szerokopasmowej spektroskopii dielektrycznej w szerokim zakresie temperatur (T = 173 – 213 K), w warunkach ciśnienia atmosferycznego (p = 0,1 MPa). Otrzymane widma strat dielektrycznych (**Rys. 3a)** badanej substancji ujawniły obecność przewodnictwa stałoprądowego związanego

z transportem ładunków oraz procesu relaksacyjnego o szerokim, bimodalnym kształcie, widocznego przy najwyższych częstotliwościach. Bimodalny charakter krzywej strat dielektrycznych wskazywał na obecność dwóch niezależnych procesów relaksacyjnych - α i α' (**Rys. 3b**), których skale czasowe stawały się coraz bardziej zbliżone do siebie wraz ze spadkiem temperatury. W efekcie, w pobliżu przejścia szklistego obserwowany był pojedynczy proces relaksacyjny.

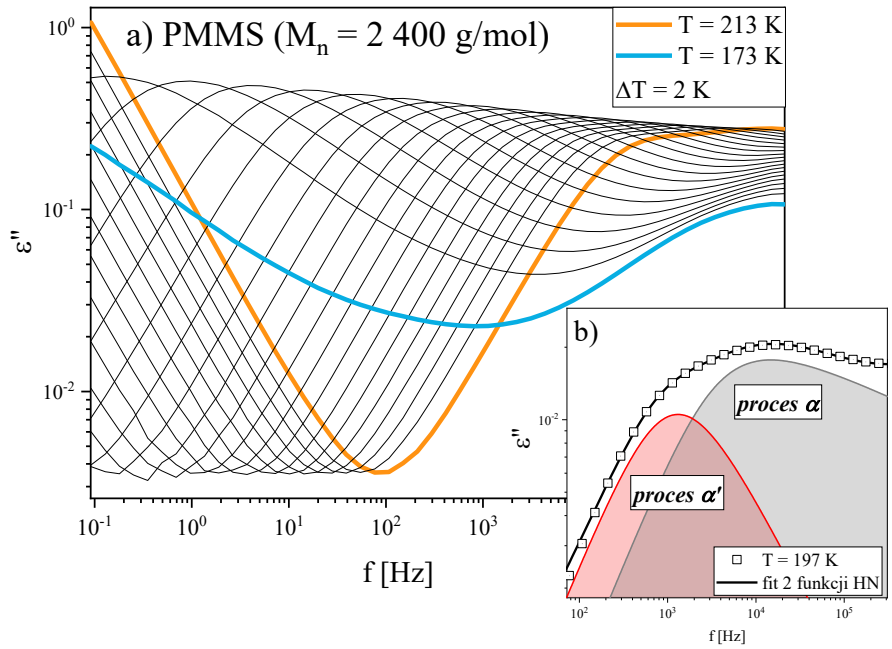

Rys. 3. a) Widma strat dielektrycznych badanego PMMS zarejestrowane powyżej T_g. **b)** Dopasowanie dwóch funkcji Havriliaka-Negamiego (HN) do widm strat dielektrycznych zmierzonych w T = 197 K.

W celu wyjaśnienia natury obu procesów widocznych na widmach dielektrycznych, wykonano dynamiczne pomiary mechaniczne. Badania te wykazały obecność relaksacji segmentalnej oraz relaksacji związanej z globalną dynamiką łańcucha (relaksację terminalną). Należy jednak zauważyć, że separacja skali czasowej obu procesów była znacznie większa niż w przypadku procesów relaksacyjnych obserwowanych w badaniach dielektrycznych. Następnie, z analizy widm dielektrycznych za pomocą modelu Havriliaka-Negamiego, wyznaczono czasy relaksacji τ_α i $\tau_{\alpha'}$, które porównano z czasami relaksacji uzyskanymi z analizy badań mechanicznych (τ_α i τ_T). Wartości czasów relaksacji wykreślono w funkcji

temperatury na **Rys. 4a**. Przedstawione dane ujawniły wyraźną rozbieżność między czasami relaksacji wyznaczonymi obiema technikami. W przypadku τ_α, mimo ogólnej rozbieżności z czasami relaksacji segmentalnej z badań mechanicznych, w pobliżu przejścia szklistego zaobserwowano większą zgodność. Dlatego założono, że proces relaksacyjny widoczny na widmach dielektrycznych przy wyższych częstotliwościach to relaksacja segmentalna (α). Potwierdzeniem tego była zgodność wartości T_g uzyskanych z badań kalorymetrycznych (T_g^{DSC} = 178 K) i dielektrycznych (T_g^{BDS} = 177 K). Natomiast, tak znaczna rozbieżność dla zależności temperaturowych $\tau_{\alpha'}$ i τ_T sugerowała, że wolniejszy proces α' charakteryzuje się inną dynamiką molekularną niż relaksacja całego łańcucha monitorowana w badaniach mechanicznych. Aby wyjaśnić pochodzenie wolniejszego procesu α', zestawiono zależności temperaturowe czasów relaksacji dla PMMS z danymi literaturowymi innych polisiloksanów, tj. poli(metylofenylosiloksanu) (PMPS) oraz poli(dimetylosiloksanu) z hydroksylowymi grupami terminalnymi (HO-PDMS-OH).[56,72] Dane zostały przeskalowane względem wartości T_g (**Rys. 4b**). W przebiegu zależności czasów relaksacji α od T_g/T zauważono, że wykresy $\tau_\alpha(T_g/T)$ dla PMMS i PMPS nakładają się na jedną krzywą, co dodatkowo potwierdziło identyfikację procesu α jako relaksacji segmentalnej. Ponadto, $\tau_{\alpha'}$ badanego PMMS i $\tau_{sub\text{-}Rouse}$ dla PMPS nałożyły się na drugiej krzywej. To porównanie pozwoliło stwierdzić, iż dodatkowy proces α' obserwowany w badaniach dielektrycznych dla polimeru PMMS jest relaksacją typu *sub-Rouse*, tak jak zostało to stwierdzone dla polimeru PMPS.

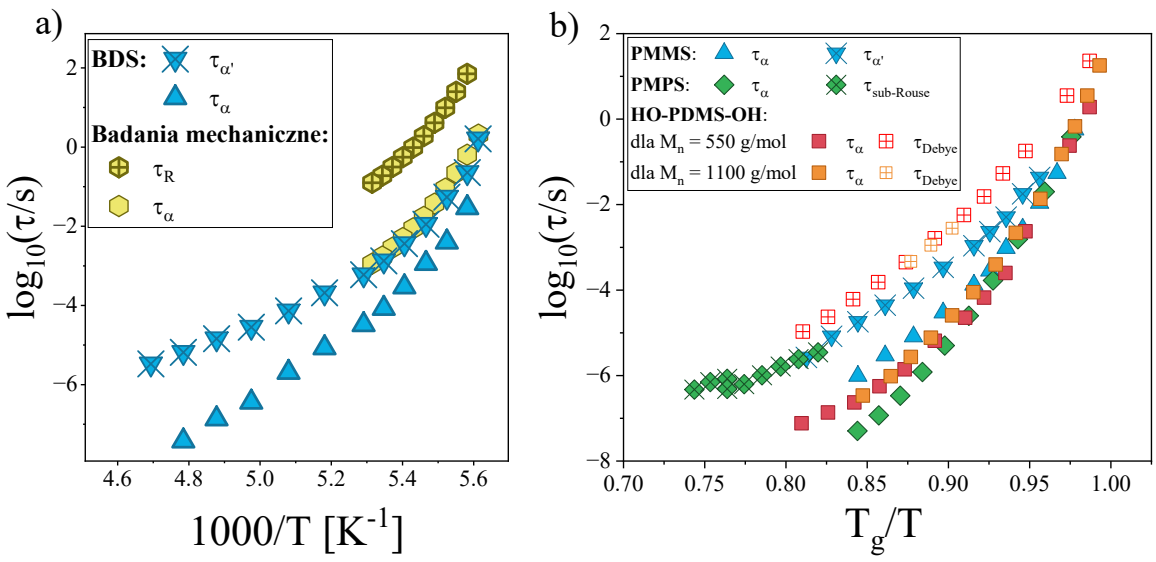

Rys. 4. a) Temperaturowe zależności czasów relaksacji uzyskanych z pomiarów dielektrycznych i mechanicznych. **b)** Porównanie ewolucji temperaturowej czasów relaksacji wyznaczonych dla różnych procesów obserwowanych w PMPS, HO-PDMS-OH i PMMS. Przedstawione dane zostały przeskalowane względem wyznaczonych wartości T_g.

Następnie, na podstawie zarejestrowanych widm strat dielektrycznych uzyskanych z wysokociśnieniowych badań dielektrycznych w różnych warunkach T i p, dokonano porównania kształtu krzywych strat dielektrycznych o zbliżonej częstotliwości maksimum procesu relaksacji segmentalnej (**Rys. 5**). Zauważono, że krzywe strat dielektrycznych są identyczne dla tych samych czasów relaksacji α, w zmiennych warunkach T i p. Zatem spełniona jest superpozycja czasowo-temperaturowo-ciśnieniowa (TTPS). Co istotne, dla PMMS istnieje superpozycja wolniejszego procesu α' oraz relaksacji segmentalnej α, niezależnie od warunków termodynamicznych. Podobne wyniki uzyskano dla poli(glikolu propylenowego) (PPG) oraz cis-1,4-poliizoprenu (PI),[42,73] dla których również przeprowadzono pomiary ciśnieniowe. Zaobserwowano, że niezależnie od warunków termodynamicznych, widma strat dielektrycznych zestawione dla tego samego τ_α wykazują superpozycję procesu *normal-mode* (związanego z fluktuacjami wektora łączącego końce łańcucha, odzwierciedlającego globalną, łańcuchową dynamikę) i relaksacji segmentalnej α.

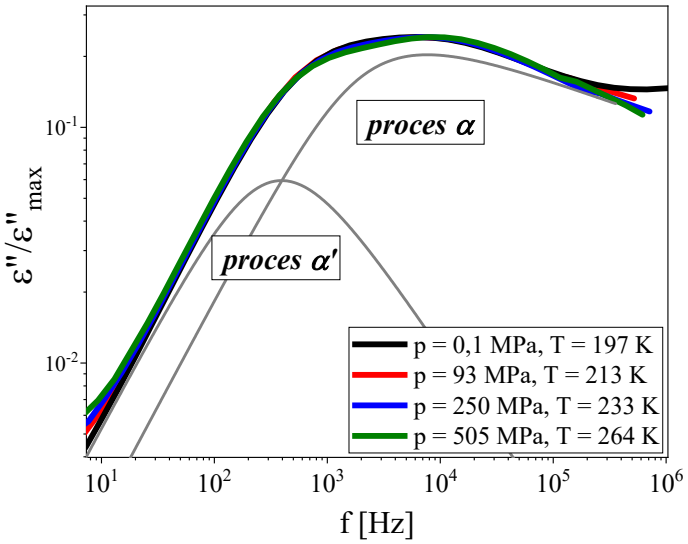

Rys. 5. Widma strat dielektrycznych zarejestrowane dla PMMS w różnych warunkach termodynamicznych, charakteryzujące się stałym τ_α.

Oznaczało to, że dla PMMS zachowana jest ta sama zasada co w przypadku PPG i PI. Otrzymany wynik był kolejnym argumentem potwierdzającym, że dodatkowy proces α' jest związany z częściowymi ruchami molekularnymi łańcucha polimeru (*sub-Rouse*), o dużo większej skali czasowej niż relaksacja segmentalna, jednak mniejszej niż mobilność całego łańcucha polimerowego. Ponadto oszacowano objętość aktywacji (ΔV) dla obu procesów relaksacyjnych (**Rys. 6**). Otrzymane wartości ΔV dla modów α i α' były bardzo zbliżone, co stanowiło kolejne podobieństwo procesu α' do zachowania relaksacji *normal-mode* i istotnie wzmacniało interpretację, że dodatkowa mobilność wykryta w PMMS jest procesem typu *sub-Rouse*.

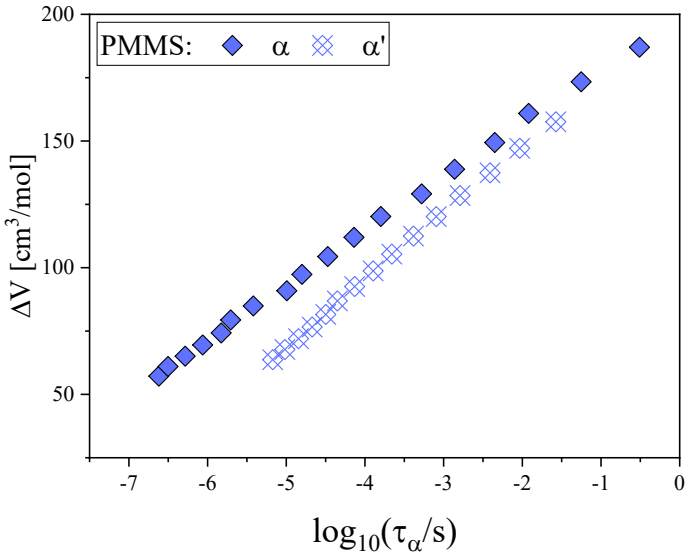

Rys. 6. Objętość (ΔV) oszacowana dla relaksacji segmentalnej i sub-Rouse, wykreślona od czasów segmentalnej (τ_α) dla PMMS.

B. Wpływ struktury szczepów na zachowanie dynamiki molekularnej kopolimerów szczepionych w różnych warunkach termodynamicznych

Podobne badania dynamiki molekularnej przeprowadzono w pracy **A3** dla kopolimerów szczepionych, w których do głównego łańcucha poli(merkaptopropylo-metylosiloksanu) poprzez sfunkcjonalizowaną grupę tiolową -SH zostały przyłączone boczne odgałęzienia wybranych homologicznych monomerów akrylanów i metakrylanów. Struktury chemiczne tych związków oraz ich pełne nazwy zostały przedstawione na **Rys. 7** i **8**. Z uwagi na bardzo rozbudowane nazwy systematyczne badanych kopolimerów szczepionych, w dalszej części korzystano z ich form skróconych. W pierwszej kolejności dla badanych związków wyznaczono T_g z pomiarów metodą DSC, które zestawiono w **Tabeli 1** oraz dokonano ich porównania z wartościami T_g wyznaczonymi z badań dielektrycznych (**Rys. 9)**.

Kopolimery PMMS szczepione wybranymi monomerami akrylanów

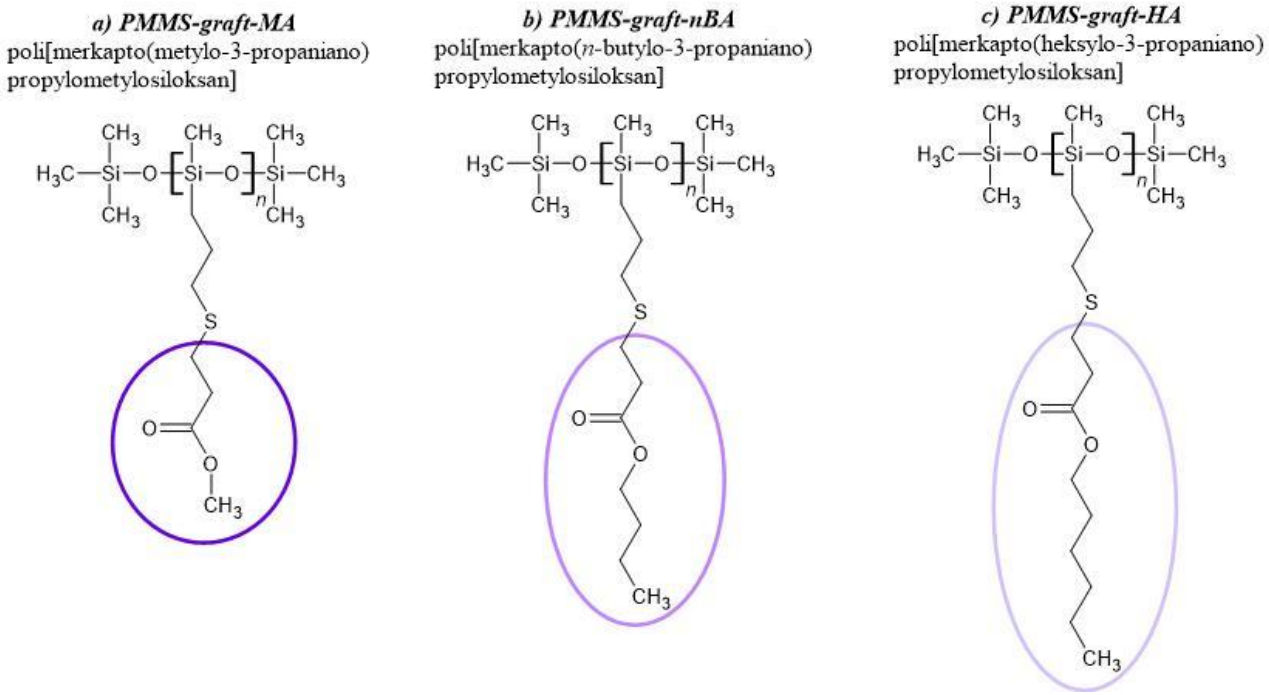

Rys. 7. Struktury chemiczne i nazewnictwo badanych kopolimerów PMMS szczepionych homologicznymi monomerami akrylanów.

Kopolimery PMMS szczepione wybranymi monomerami metakrylanów

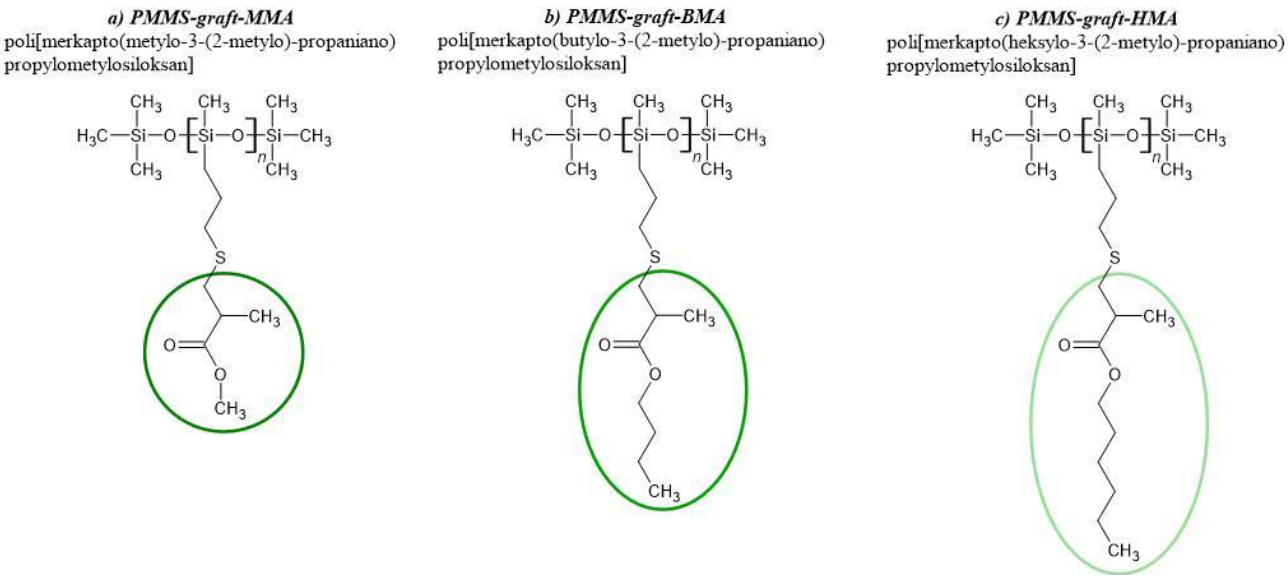

Rys. 8. Struktury chemiczne i nazewnictwo badanych kopolimerów PMMS szczepionych homologicznymi monomerami metakrylanów.

Tabela 1. Masy cząsteczkowe (M_n) i temperatury zeszklenia (T_g) wyznaczone z pomiarów kalorymetrycznych i dielektrycznych dla badanych kopolimerów szczepionych. Dane dla PMMS zostały zaczerpnięte z pracy [74].

	M_n [g/mol]	T_g^{BDS} [K] dla τ_α = 1 s	T_g^{DSC} [K]
PMMS	2 400	177	178
Kopolimery PMMS szczepione monomerami akrylanów			
PMMS-*graft*-MA	3 400	231	224
PMMS-*graft*-*n*BA	4 100	204	201
PMMS-*graft*-HA	4 600	198	196
Kopolimery PMMS szczepione monomerami metakrylanów			
PMMS-*graft*-MMA	3 600	244	244
PMMS-*graft*-BMA	4 100	218	215
PMMS-*graft*-HMA	4 700	206	198

Zaobserwowano, że wartości T_g dla kopolimerów szczepionych są znacznie wyższe niż dla homopolimeru PMMS (T_g = 178 K) (**Rys. 9**). Najwyższe T_g wykazywały kopolimery szczepione homologicznymi monomerami metakrylanów, które cechowały się dużo większą sztywnością łańcucha niż kopolimery szczepione homologicznymi monomerami akrylanów. Ponadto, wartości temperatury zeszklenia malały wraz ze zwiększającą się długością łańcucha szczepu. Sugerowało to, że na zmiany temperatur zeszklenia wyraźny wpływ ma zwiększona zawada steryczna spowodowana zarówno wydłużeniem, jak i sztywnością dołączonych łańcuchów bocznych.

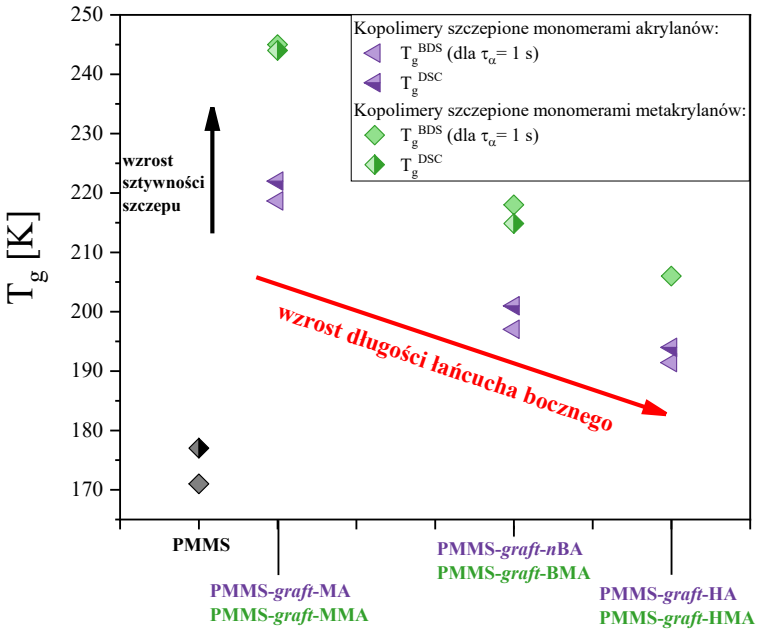

Rys. 9. Temperatury zeszklenia wyznaczone za pomocą różnych technik eksperymentalnych wykreślone w funkcji długości łańcucha szczepu.

Przeprowadzone badania dielektryczne w szerokim zakresie temperatur w warunkach ciśnienia atmosferycznego (**Rys. 10**) pozwoliły stwierdzić obecność na widmach przewodnictwa stałoprądowego (przy niższych częstotliwościach, f) oraz przy najwyższych f relaksację segmentalną α dla kopolimerów PMMS szczepionych akrylanami o różnej długości łańcucha alkilowego. Co zaskakujące, dla kopolimerów PMMS szczepionych homologicznymi monomerami metakrylanów wykryto bimodalny proces relaksacyjny, będący złożeniem dwóch niezależnych relaksacji – α i α', dla których skale czasowe stawały się bardzo zbliżone w pobliżu przejścia szklistego – podobnie jak w przypadku homopolimeru PMMS.

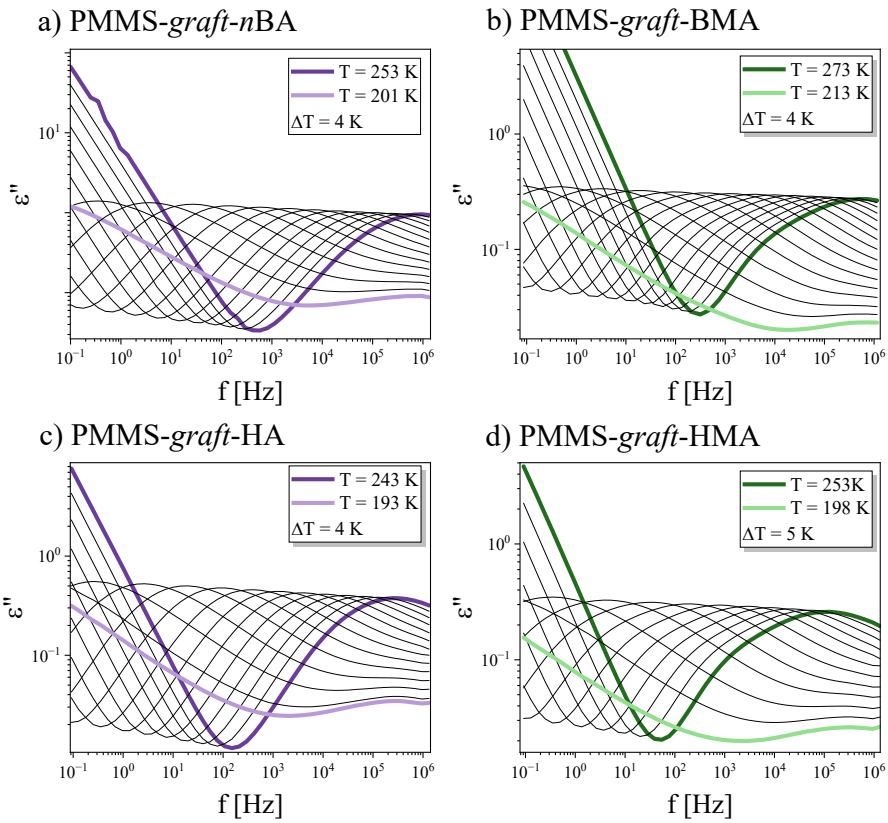

Rys. 10. Reprezentatywne widma strat dielektrycznych zmierzone powyżej T_g dla wybranych kopolimerów szczepionych monomerami akrylanów: **a)** PMMS-*graft*-*n*BA, **c)** PMMS-*graft*-HA oraz metakrylanów: **b)** PMMS-*graft*-BMA, **d)** PMMS-*graft*-HMA; o różnych długościach łańcuchów alkilowych.

Następnie wykonano pomiary mechaniczne, które pozwoliły na obserwację dwóch procesów – relaksacji segmentalnej oraz relaksacji terminalnej. Co więcej, wykryte procesy relaksacyjne występowały dla wszystkich badanych układów niezależnie od zastosowanego szczepu. Porównując temperaturowe zależności czasów relaksacji wyznaczonych z analizy widm dielektrycznych modelem HN (τ_α i $\tau_{\alpha'}$) oraz z analizy danych mechanicznych (τ_α i τ_T) (**Rys. 11**) zauważono bardzo dobrą zgodność τ_α uzyskanych z pomiarów dielektrycznych i mechanicznych zarówno dla reprezentatywnego kopolimeru PMMS szczepionego akrylanem butylu (PMMS-*graft*-*n*BA) jak i szczepionego metakrylanem butylu (PMMS-*g*-BMA). Jednak, co ciekawe zauważono wyraźną rozbieżność skali czasowej relaksacji α' z relaksacją terminalną. Dokonana analiza wykazała, że dodatkowy proces relaksacyjny obserwowany w kopolimerach PMMS szczepionych homologicznymi monomerami metakrylanów nie jest

powiązany z globalną dynamiką łańcucha ze względu na inne skale czasowe obu zarejestrowanych procesów.

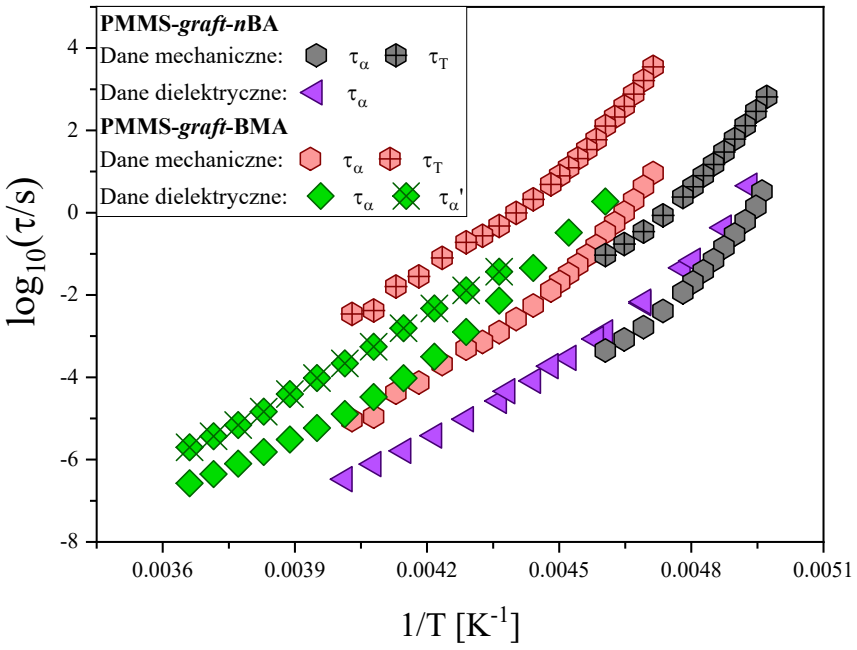

Rys. 11. Temperaturowe zależności czasów relaksacji uzyskanych z pomiarów dielektrycznych i mechanicznych dla dwóch reprezentatywnych kopolimerów PMMS szczepionych akrylanem butylu i metakrylanem butylu.

Ze względu na duże podobieństwo zaobserwowanego dodatkowego procesu α' w badanych kopolimerach szczepionych homologami metakrylanów z procesem *sub-Rouse* wykrytym w homopolimerze PMMS, wykonano wysokociśnieniowe badania dielektryczne w różnych warunkach temperatury i ciśnienia w celu lepszego wyjaśnienia obserwowanego zjawiska. Podobnie jak w przypadku badań dielektrycznych przeprowadzonych w ciśnieniu atmosferycznym, w badaniach ciśnieniowych również wykryto obecność pojedynczego procesu relaksacyjnego dla kopolimerów szczepionych homologicznymi monomerami akrylanów oraz wyraźny bimodalny proces relaksacyjny dla kopolimerów PMMS szczepionych monomerami metakrylanów.

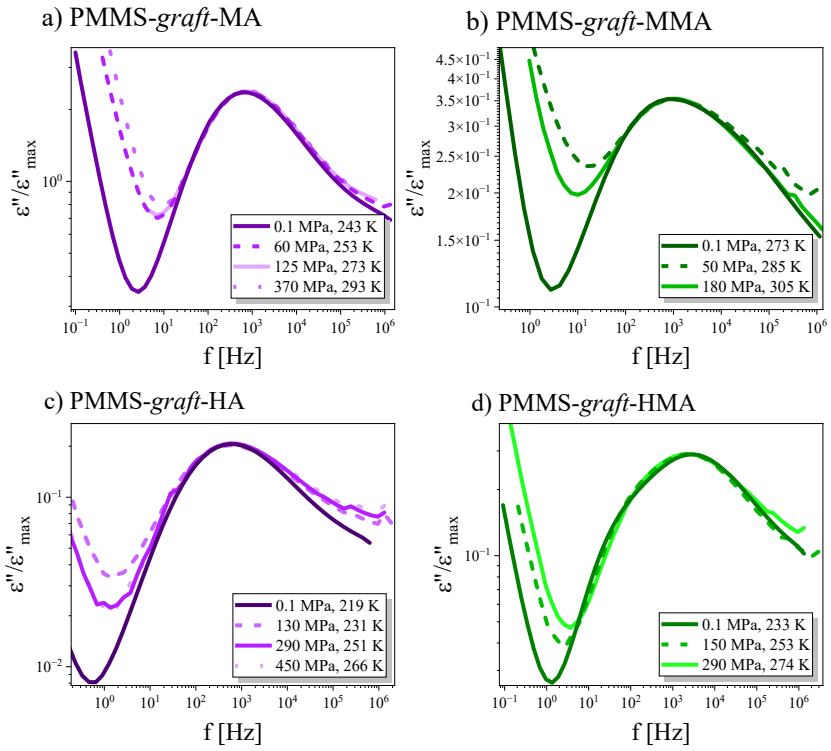

Rys. 12. Widma strat dielektrycznych zarejestrowanych w różnych warunkach termodynamicznych charakteryzujące się stałym τ_α, dla wybranych kopolimerów PMMS szczepionych homologicznymi monomerami akrylanów (a i c) oraz homologicznymi monomerami metakrylanów (b i d).

Co istotne, porównując krzywe strat dielektrycznych w różnych warunkach termodynamicznych (**Rys. 12**), zauważono, że ich kształt jest identyczny dla tych samych wartości czasów relaksacji segmentalnej, τ_α. Zatem również i w tym przypadku została spełniona reguła superpozycji czasowo-temperaturowo-ciśnieniowej (TTPS). Także stwierdzono, że dla kopolimerów PMMS szczepionych monomerami metakrylanu istnieje superpozycja wolniejszego procesu α' oraz relaksacji segmentalnej α, niezależnie od warunków termodynamicznych. Przeprowadzona analiza badań ciśnieniowych sugeruje, że dodatkowy proces relaksacyjny wykryty w kopolimerach PMMS szczepionych monomerami metakrylanów jest związany z częściowymi ruchami molekularnymi łańcucha polimeru, typu *sub-Rouse*. Jednakże, nie można całkowicie wykluczyć, że dodatkowy proces α' może być przejawem ruchów molekularnych pochodzących od szczepów monomerów metakrylanów

z grupy bocznej kopolimerów, które cechuje znacznie większa sztywność łańcucha niż w przypadku szczepów monomerów akrylanów.

C. Określenie wpływu struktury „ramienia" i zawady sterycznej na zachowanie się dynamiki molekularnej kopolimerów szczepionych. Badania dielektryczne w wysokim ciśnieniu.

Biorąc pod uwagę silny wpływ struktury szczepów w łańcuchach bocznych na dynamikę molekularną całego polimeru, przedmiotem dalszych badań w artykule **A2** były również kopolimery szczepione PMMS, do których poprzez sfunkcjonalizowaną grupę -SH przyłączono izomery akrylanu butylu – akrylanu *n*-butylu (PMMS-*graft*-*n*BA), *izo*-butylu (PMMS-*graft*-*izo*BA) oraz *tert*-butylu (PMMS-*graft*-*tert*BA), z coraz bardziej rozgałęzioną strukturą chemiczną szczepu. Wzory strukturalne badanych kopolimerów szczepionych oraz ich nazewnictwo zostały przedstawione na **Rys. 13.**

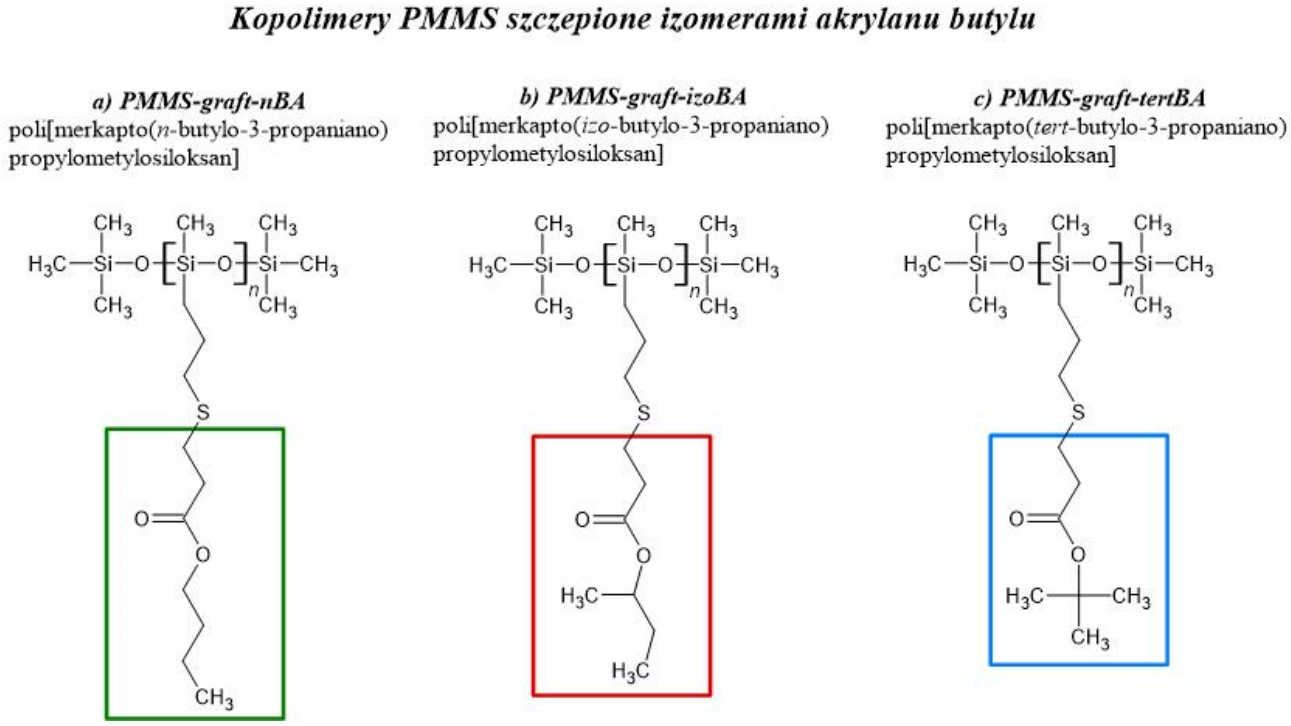

Rys. 13. Struktura chemiczna i nazewnictwo badanych kopolimerów PMMS szczepionych izomerami akrylanu butylu.

W pierwszym etapie przeprowadzono badania kalorymetryczne. Reprezentatywne termogramy badanych kopolimerów przedstawione na **Rys. 14** uwidoczniły endotermiczne skoki ciepła właściwego wskazujące na przejście do fazy szklistej. Wyznaczone temperatury zeszklenia były znacznie wyższe w porównaniu z T_g homopolimeru PMMS (T_g = 178 K). Ponadto ich wartości wzrastały wraz ze wzrostem rozgałęzienia szczepu, np. PMMS-*graft*-*tert*BA cechował się najwyższą wartością T_g. Sugerowało to, że na obserwowane zmiany T_g ma wpływ zwiększająca się zawada steryczna związana z wydłużeniem się łańcuchów bocznych kopolimerów. Podobne zjawisko obserwowano w przypadku kopolimerów PMMS szczepionych homologicznymi monomerami akrylanów i metakrylanów.[75]

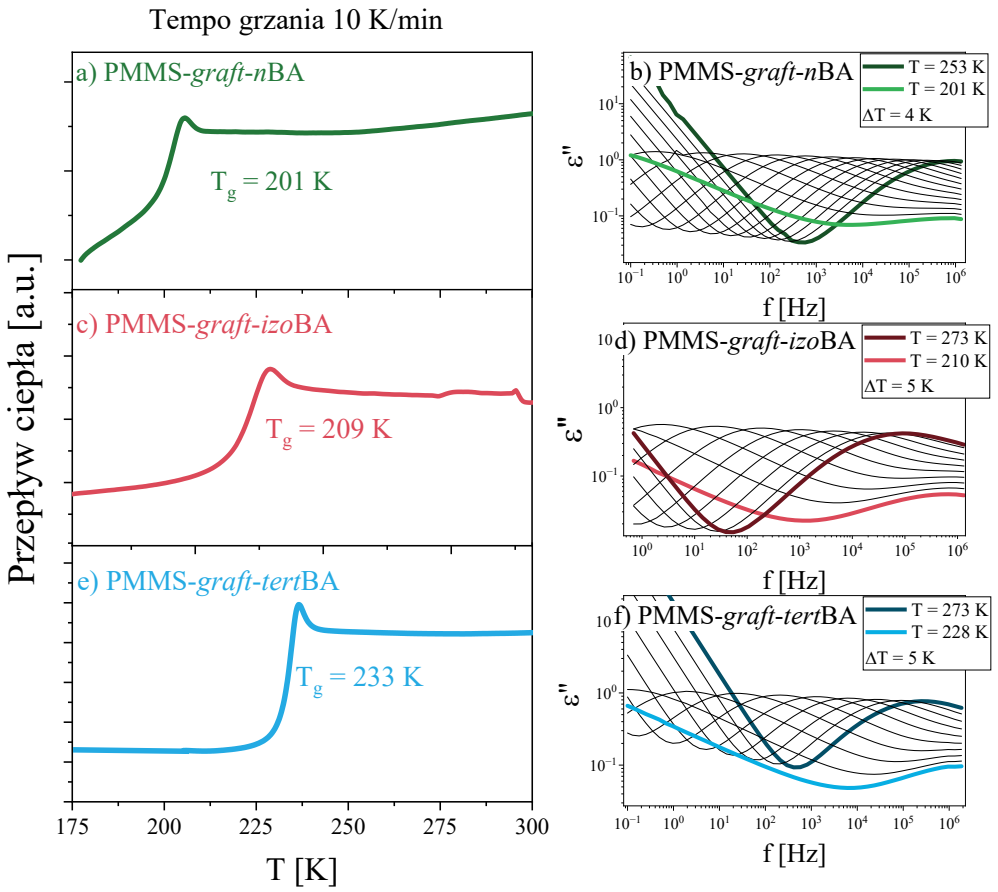

Rys. 14. a,c,e) Termogramy i **b,d,f)** reprezentatywne widma strat dielektrycznych dla badanych kopolimerów szczepionych.

W następnym kroku wykonano badania dielektryczne w warunkach ciśnienia atmosferycznego i szerokim zakresie temperatur. Uzyskane widma strat dielektrycznych ujawniły obecność przewodnictwa stałoprądowego oraz jednego, szerokiego procesu relaksacji segmentalnej α (**Rys. 14b,d,f**). Podobny scenariusz był obserwowany dla szczepionych homologicznymi monomerami akrylanów w artykule **A3**. Dodatkowo wykonano badania mechaniczne, które wskazały na obecność relaksacji segmentalnej i terminalnej. Na podstawie uzyskanych danych eksperymentalnych, dokonano porównania widm strat dielektrycznych ε”(f) z widmami modułu stratności G”(f) z badań mechanicznych (**Rys. 15**). Okazało się, że pierwsze z wymienionych są znacznie szersze niż widma modułu G”, w szczególności dla PMMS-*graft*-*tert*BA.

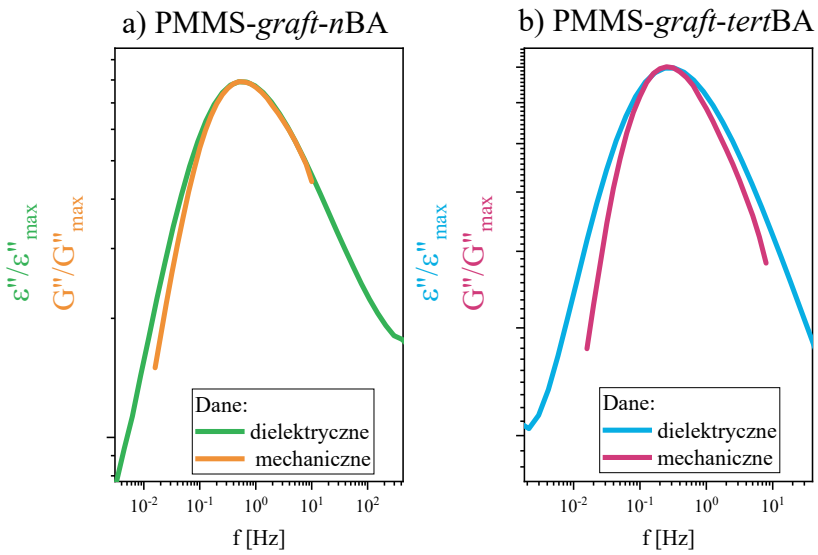

Rys. 15. Porównanie widm ε”/ε”$_{max}$ i G”/G”$_{max}$ od częstotliwości (f) charakteryzujących się stałym τ_α dla kopolimerów PMMS szczepionych **a)** akrylanem *n*-butylu oraz **b)** akrylanem *tert*-butylu.

Ostatnim etapem badań były wysokociśnieniowe pomiary dielektryczne. Wykorzystując zmierzone dane w różnych warunkach termodynamicznych (T i p) porównano je tak, aby maksima strat dielektrycznych dla procesu segmentalnego były takie same (**Rys. 16**). Takie porównanie wykazało, że kształt procesu relaksacyjnego jest identyczny, a zatem zasada superpozycji (TTPS) w zmiennych warunkach T i p jest spełniona.

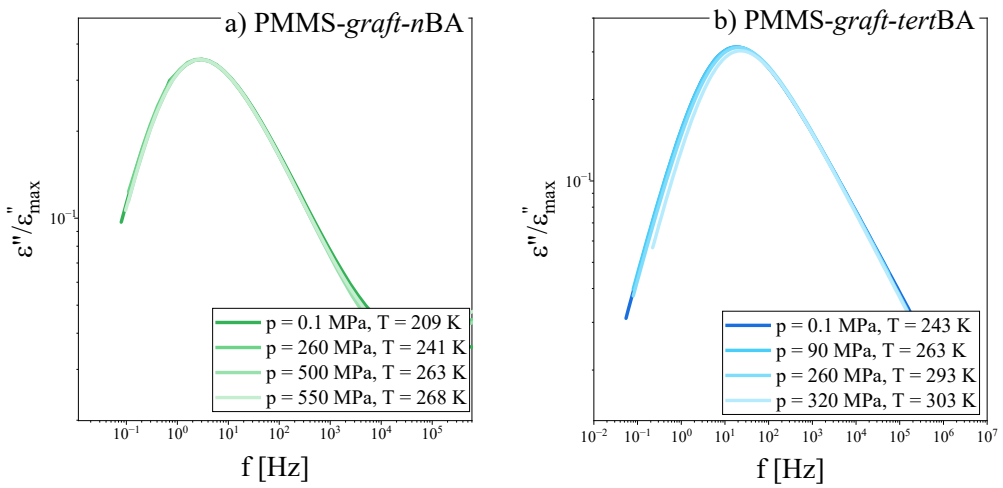

Rys. 16. Porównanie widm strat dielektrycznych zmierzonych w różnych warunkach termodynamicznych, charakteryzujących się takim samym czasem relaksacji segmentalnej τ_α.

Ciekawych wyników dostarczyły współczynniki ciśnieniowe temperatury przejścia szklistego (dT_g/dp) oszacowane w granicy ciśnienia atmosferycznego (**Rys. 17a**) oraz wartości objętość aktywacji (ΔV) wyznaczone dla różnych τ_α (**Rys. 17b).** Wartości obu parametrów były znacznie wyższe dla badanych kopolimerów szczepionych niż dla homopolimeru PMMS. Zachowanie to może być związane bezpośrednio z budową przyłączonych szczepów w łańcuchu bocznym. Można wnioskować, iż coraz większa ilość podstawników oraz rosnąca zawada steryczna uniemożliwia tworzenie się wiązań wodorowych makrocząsteczce.

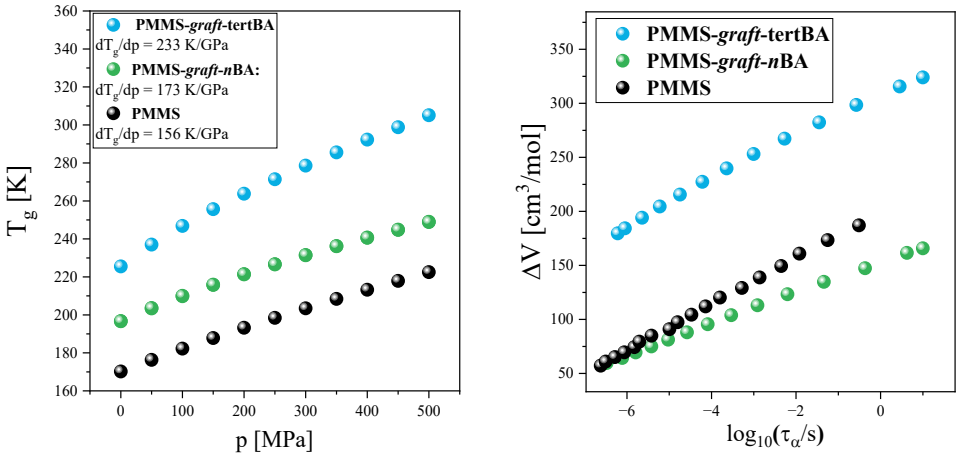

Rys. 17. a) Zależności T_g od p_g wyznaczone z równania Avramova, **b)** Objętość aktywacji ΔV w funkcji czasu relaksacji segmentalnej α dla badanych kopolimerów szczepionych i homopolimeru PMMS, dla którego dane zaczerpnięto z pracy [74].

IV. TREŚCI ARTYKUŁÓW STANOWIĄCYCH PODSTAWĘ ROZPRAWY DOKTORSKIEJ WRAZ Z OŚWIADCZENIAMI WSPÓŁAUTORÓW

A1. Studies on the Molecular Dynamics at High Pressures as a Key Identify the Sub-Rouse Mode in PMMS.

AUTORZY: S. Zimny, M. Tarnacka, E. Kamińska, R. Wrzalik, K. Adrjanowicz, M. Paluch, K. Kamiński.

REFERENCJA: Macromolecules, 2022, 55 (13), 5581-5590.

DOI: 10.1021/acs.macromol.2c00378

Impact Factor czasopisma z roku opublikowania: 5.5

Liczba punktów ministerialnych MNiSW czasopisma (2022): 140

Mój udział w pracy polegał na przygotowaniu próbek, wykonaniu pomiarów dielektrycznych i analizie otrzymanych wyników, współtworzeniu manuskryptu (przeprowadzenie przeglądu literaturowego, przygotowanie tekstu manuskryptu i rysunków, opis wyników i sformułowanie wniosków), formułowaniu odpowiedzi na uwagi recenzentów oraz korekcie manuskryptu po otrzymanych recenzjach.

Macromolecules

pubs.acs.org/Macromolecules Article

Studies on the Molecular Dynamics at High Pressures as a Key to Identify the Sub-Rouse Mode in PMMS

Sara Zimny, Magdalena Tarnacka,* Ewa Kamińska, Roman Wrzalik, Karolina Adrjanowicz, Marian Paluch, and Kamil Kamiński

Cite This: *Macromolecules* 2022, 55, 5581−5590 Read Online

ACCESS | Metrics & More | Article Recommendations | Supporting Information

ABSTRACT: In this paper, we have investigated the molecular dynamics of the associating polymer, poly(mercaptopropyl)methylsiloxane (PMMS), at high pressure (up to $p \sim 505$ MPa) by means of broadband dielectric spectroscopy. Previous studies revealed that PMMS exhibits two dielectric relaxation processes observed above the glass transition temperature related, most likely, to either the mobility within self-assemblies or the sub-Rouse mode (α'-slower process) and segmental (α-faster process) dynamics, whereas mechanical measurements revealed only the presence of terminal and segmental relaxations [Tarnacka et al. *Macromolecules* **2020**, *53* (22), 10225−10233]. In order to determine the origin of the dielectric α'-process, further high-pressure experiments were performed. It was found that the timescale separation between relaxation times of segmental (α) and α'-processes is invariant to the compression, and activation volume calculated for both kinds of motions is comparable. These dynamical features are characteristic of the chain relaxation (called usually normal mode) found in *type-A* polymers. However, because mechanical data excluded identification of the slow dielectric relaxation as normal mode, we assigned it as the sub-Rouse process. This assignment is in the line with previous studies on poly(methylphenyl)siloxane. Further density functional theory computations revealed that the detection of the relatively strong sub-Rouse process is most likely possible due to the presence of a highly polar side group (thiol, −SH, moiety) that gives a strong contribution to dipole moment along the main polymer backbone. Additionally, we demonstrated that the pressure coefficient of the glass transition temperature, dT_g/dp, in PMMS is one of the smallest among those reported to date for various polymers ($dT_g/dp = 156$ K/GPa). This quite surprising finding was assigned to the specific interactions formed by the thiol group. Finally, it should be emphasized that high-pressure experiments turned out to be the key element to identify the sub-Rouse mode in dielectric spectra—a process that might provide important information about the chain dynamics in polysiloxanes. However, to finally prove this hypothesis, further studies are required to discard the eventual possibility that the slow mode is somehow related to the nanoscopic organization in PMMS.

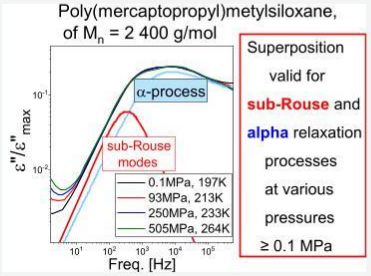

1. INTRODUCTION

In recent years, there is a growing interest in new polymer-based systems. It is because they very often offer enhanced physical and chemical features compared to traditional materials. Moreover, one can easily tune/modify mechanical, rheological, and other properties of macromolecules by varying their molecular weight (M_n), dispersity, chemical composition, topology, and so forth. An intriguing group of polymers is polysiloxanes, whose unique character is solely related to the connection between oxygen (O) and silicon (Si) in the basic unit/mer, making the overall backbone very flexible. Importantly, depending on the length of the chain and the nature of pendant groups attached to the Si atoms, the mentioned compounds can take different forms from heavy, grease-like oil-line fluids to solid resins.[1,2] Moreover, they are chemically/thermally stable and are characterized by low surface tension, toxicity, and chemical reactivity.[3,4] It is also worth mentioning that such kinds of macromolecules are commonly used in medicine (e.g., medical devices), polishes, adhesives, cosmetics, hygiene products, coating, plastics, households, and so forth.[5,6]

Over the years, polysiloxanes have become interesting objects for molecular dynamics studies because, in the vicinity of the glass transition temperature (T_g), one can observe multiple relaxation processes in the spectra of these materials. Previous photon correlation spectroscopy (PCS) investigations on model poly(methylphenylsiloxane) (PMPS) have clearly demonstrated that there are two relaxation modes above T_g in this polymer irrespective of M_n.[7] Correlation relaxation times,

Received: February 21, 2022
Revised: May 26, 2022
Published: June 27, 2022

https://doi.org/10.1021/acs.macromol.2c00378
Macromolecules 2022, 55, 5581−5590

τ, of the faster process corresponded very well with the segmental ones determined from dielectric measurements. On the other hand, the slower mode, not detected in dielectric loss spectra, was assigned to the normal mode, reflecting the global chain dynamics.[8] However, it was postulated that due to the lack of the dipole component parallel to the backbone, the chain-related processes are not visible in dielectric spectra. Interestingly, later studies have proved that this hypothesis was wrong.[9−11] Studies on PMPS of varying molecular weight, M_n ∼ 2.5 kg/mol and M_n ∼ 27.8 kg/mol, revealed that their loss spectra exhibit, apart from the segmental process (α), the slow mode (α') of much lower amplitude at the low-frequency side of the main dielectric relaxation peak.[9] Moreover, as M_n of PMPS increases, the time scale separation between α and α' processes becomes greater. Note that the presence of α'-process in PMPS was also observed by creep compliance and PCS.[7] This process detected in a series of PMPS was assigned as the so-called sub-Rouse mode because it was not related to the global chain dynamics.[9−11] It should be highlighted that the presence of the new relaxation process of similar features as that seen for PMPS was, for the first time, discovered in high molecular weight polyisobutylene by creep compliance and PCS.[12−14] Because its dynamical features did not agree with those determined for the terminal relaxation from mechanical studies, the new process was named the sub-Rouse mode, characterized by the time and length scales intermediate between the Rouse and segmental ones.[12,15,16] After that the sub-Rouse modes were also identified in various polysiloxanes.[17] Apart from PMPS, the sub-Rouse modes have been also reported in poly(methyl-*para*-tolylsiloxane) (PMpTS) polymers.[17,18] PCS measurements revealed that there are two relaxation modes in PMpTS, for which the time scale separation between both modes is molecular weight dependent. Importantly, it turned out that the relaxation times of the faster (α)-process agree well with those determined from mechanical and dielectric investigations. On the other hand, the dynamics of the slow (α') mode was much faster than that of the terminal relaxation monitored by mechanical spectroscopy.[18] Further shear creep compliance measurements on a high molecular weight PMpTS confirmed the presence of the α'-mode, which was assigned as the sub-Rouse modes.[17]

As can be deduced from the abovementioned discussion, in the case of ordinary/classical polysiloxanes, the data obtained from different experimental techniques agree very well when we consider the dynamics of the segmental relaxation, while some significant discrepancies are noted in the interpretation of the slow (α') mode. Nevertheless, it seems that the latter process provides information about the (sub)chain dynamics and can be treated as the sub-Rouse mode. A much more complicated situation is found when we deal with polysiloxanes having polar moieties, such as −OH, $-NH_2$, or −SH, which can form effective H-bonds and consequently supramolecular structures. As shown for hydroxyl-terminated polydimethylsiloxane (HO−PDMS−OH),[19] except for the segmental process, one can detect an additional slow mode in dielectric loss spectra. Its amplitude decreased with the molecular weight of the polymer. Moreover, this relaxation was absent in the macromolecules without OH moieties. It was argued that the origin of the slow relaxation is similar to that of the Debye (D) process detected in low-molecular-weight glass formers (monohydroxy alcohols) and is strictly connected to the motions occurring within nanoassociates.

Recently, we have studied the dynamics of poly(mercaptopropyl)methylsiloxane (PMMS), belonging to the polysiloxane group and having a thiol (−SH) moiety (which can form very weak H-bonds) attached to each monomer in the polymer backbone.[20] As in the case of PMPS or HO−PDMS−OH, we identified two relaxation processes in the dielectric spectra of the examined polymer. The faster one was attributed to the segmental process, while the origin of the slower (α') mode was discussed in the context of either motion occurring within supramolecular self-assemblies or the sub-Rouse process. The origin of the observed α'-process was impossible to distinguish. Therefore, to investigate further this issue and solve the mentioned problem, herein, we have examined the dynamics of PMMS at high pressure. Surprisingly, our data demonstrate that irrespective of the applied thermodynamic conditions (T, p), there is a superposition of the segmental and slow (α') modes for the loss spectra characterized by the same segmental relaxation times. This finding clearly indicates that the α'-relaxation process observed in PMMS is rather the sub-Rouse mode, not the Debye relaxation related to the motions occurring within supramolecular self-assemblies. However, to finally verify this hypothesis further studies are required.

2. MATERIALS AND METHODS

2.1. Materials. PMMS homopolymer (75−150 cSt) was purchased from Gelest and used as received (molecular weight, M_{nSEC} = 2400 g/mol, dispersity, $Đ$ = 1.26 determined by Viscotek TDA 305 triple detection, and Tetrahydrofuran as the eluent). The studied PMMS is a water-like thin liquid with the glass transition temperature T_g = 178 K. Note that no trace of crystallization was observed on both cooling and heating calorimetric scans.

2.2. Broadband Dielectric Spectroscopy. Complex dielectric permittivity, $\varepsilon^*(\omega) = \varepsilon'(\omega) - i\varepsilon''(\omega)$, values at ambient pressure were measured using the impedance analyzer (Novocontrol Alpha) over a frequency range from 1×10^{-1} to 3×10^6 Hz. The samples were placed between two stainless-steel electrodes (diameter: 10 mm; gap: 0.05 mm) and mounted inside a cryostat. During the measurement, each sample was maintained under dry nitrogen gas flow. The temperature was controlled by a Quatro Cryosystem using a nitrogen gas cryostat, with stability better than 0.1 K. The temperature-dependent dielectric measurements were performed in the range from 173 to 303 K. The obtained dielectric loss spectra were analyzed by the superposition of one or two Havriliak−Negami (HN) functions with an additional term related to the dc conductivity[21]

$$\varepsilon(\varpi)'' = \frac{\sigma_{dc}}{\varepsilon_0 \varpi} + \mathrm{Im}\sum_{i=1}^{2}\left(\varepsilon_\infty + \frac{\Delta\varepsilon_i}{[1 + (i\varpi\tau_i)^{\alpha_i}]^{\beta_i}}\right) \quad (1)$$

where α and β are the shape parameters related to the symmetric and asymmetric broadening of relaxation peaks, $\Delta\varepsilon$ is related to the dielectric strength, τ_{HN} is the HN relaxation time, ε_0 is the vacuum permittivity, and ϖ is the angular frequency, where $\varpi = 2\pi f$. It should be added that in order to minimize the number of fitting parameters, we fixed α_{HN} = 1 and β_{HN} = 0.7 in the case of the slow mode. Such a procedure was proposed to fit the normal mode in dielectric loss spectra for the low-molecular-weight samples.[22] Details concerning the fitting analysis, fits' quality together with the temperature dependences of HN shape parameters are shown in the Supporting Information file.

For dielectric measurements at elevated pressure, we used a high-pressure system developed at the Institute of High-Pressure Physics of the Polish Academy of Science in Warsaw—UNIPRESS. Thin Teflon spacers were applied to maintain a fixed distance between the plates. The sample capacitor was sealed and mounted inside a Teflon capsule to separate it from the silicon liquid used as a pressure-transmitting

https://doi.org/10.1021/acs.macromol.2c00378
Macromolecules 2022, 55, 5581−5590

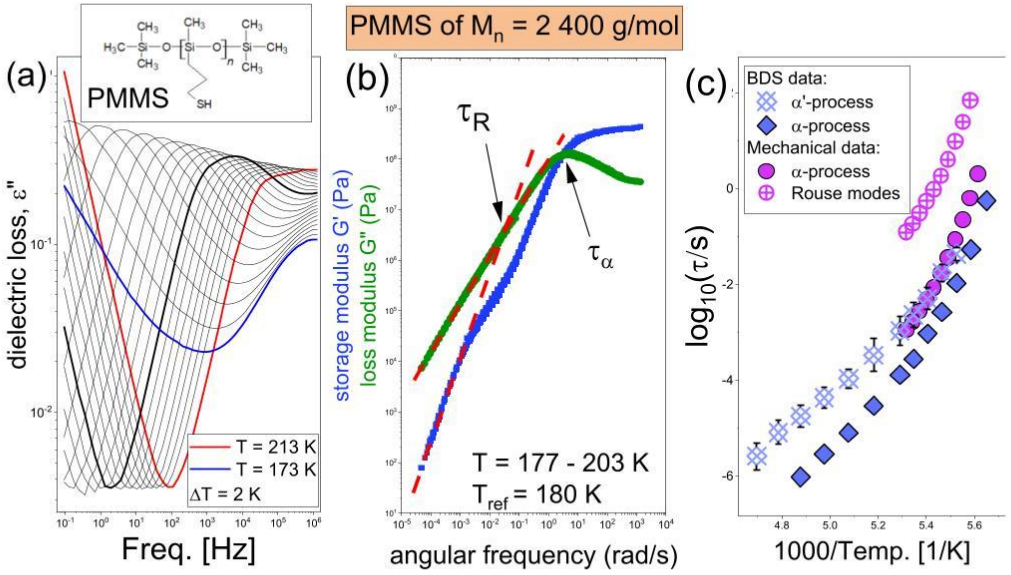

Figure 1. (a) Dielectric loss spectra of examined PMMS recorded as a function of temperature at ambient pressure; (b) master curves of measured storage, G', and loss G'', modulus, (c) temperature dependences of relaxation times obtained from dielectric and mechanical measurements. As the inset in panel (a), the chemical structure of examined PMMS is shown.

medium. The temperature was adjusted with a precision of 0.5 K by means of a refrigerating and heating circulator. Complex dielectric permittivity was measured within the same frequency range as in the case of measurements carried out at ambient pressure.

2.3. DFT Calculations. Density functional theory (DFT) calculations were carried out on Gaussian 09[23] package program using the B3LYP functional method, 6-31G(d) basis set. The structure and dipole moments (according to the CHelp scheme) of isotactic and syndiotactic PMMS and PMPS polymers have been calculated for molecules with four units in the trans backbone configuration. The structures of the molecules are shown in Figure S10. The value of dipole moment and its components depends on the conformation of the polymer, see Table S2. However, the performed calculations show a significantly smaller PMPS dipole moment and a large value of the dipole moment component parallel to the axis of the PMMS main chain.

3. RESULTS AND DISCUSSION

In Figure 1a, we presented dielectric loss spectra measured for PMMS at different temperatures (T). As can be seen, at higher T, the loss peaks are enormously broad-bimodal, suggesting that there are in fact two relaxation processes underlying the dielectric response of this polymer above the glass transition temperature (T_g). This supposition can be easily proved by fitting the experimental data to the one or superposition of the two HN functions (for details see ref 20 and Figures S1−S6 in the Supporting Information file). It is evident that the first approach yields a fit of poor quality with unreliable parameters describing the shape of this mode, while in the case of the latter procedure, one can obtain an accurate description of the obtained loss peaks. As temperature decreases, the width of the main loss peak becomes narrower. Consequently, in the vicinity of T_g, it can be well described by the single HN function. For details please see ref 20. This observation indicates that the two relaxation processes contributing to the measured loss peak merge upon approaching the vitrification point. For the purpose of this paper, the slow and the faster mode will be labeled as α' and α, respectively. Therefore, a question arises. What is the molecular origin of both processes observed in dielectric loss spectra of the investigated polysiloxane? As already outlined in the introduction, the faster one should be the segmental (α) mode, responsible for the liquid−glass transition, while the slower might be a manifestation of the chain-related dynamics (possibly the sub-Rouse mode), or bearing in mind thiol moieties in pendant alkyl side groups in PMMS, it could be assigned to the reorientation occurring within nanoassociates, as was discussed in the case of HO−PDMS−OH.[19] One can recall that, alternatively, the observed slower α'-process could be also a manifestation of additional movements related to the formation of mesophase in the studied polysiloxane. Herein, it should be noted that poly(diethylsiloxane) and poly(dipropylsiloxane) are capable to form local ordering characteristics for liquid crystals.[24] However, differential scanning calorimetry measurements performed did not show the presence of any additional phase transitions besides T_g. Therefore, we exclude this scenario from further considerations. Additionally, one can also recall that the presence of the additional slow mode not related to the terminal relaxation has been also reported for polypeptides,[25] which was assigned to the molecular motion of "α-helical peptide secondary motif". Interestingly, a similar behavior was also shown for polystyrene.[26] However, in this particular case, the presence of the slow mode and spatial organization of this polymer was induced by solvent treatment.[26] Herein, one can also recall our very recent molecular dynamics simulations on the model

https://doi.org/10.1021/acs.macromol.2c00378
Macromolecules 2022, 55, 5581−5590

oligomer with a similar structure to PMMS. It was found that due to H-bonds, most likely some kind of ordering, similar to the nematic one, is present in this system.[27] Finally, it should be mentioned that very recent studies on a series of thin polymer films demonstrated that the presence of the relaxation process, slower than the α-mode, could be a general feature of glassy dynamics and, therefore, does not originate from any kind of polymeric features.[28]

To gain insight into this problem, we have carried out additional mechanical measurements. Master curves of measured storage, G', and loss, G'', modulus of PMMS are shown in Figure 1b. Herein, it should be noted that this plot was constructed from the frequency dependencies of G' and G'' measured in the 0.1−100 rad^{-1} range at different temperatures, which were further shifted horizontally by the shift factor, αT, to superimpose at the reference temperature, T_{ref} = 180 K. As can be seen, at a higher frequency, the storage and loss modulus cross each other, in the vicinity of the maximum of the segmental relaxation process. On the other hand, at a lower frequency, a clear change in the mechanical response is noted in G', suggesting the existence of an additional mode. Considering the slopes of $G'' \sim \omega^1$ and $G' \sim \omega^2$, we can certify that it is a terminal relaxation, observed for polymers. Note that the important feature of the terminal process is that it depends on M_n and the entanglement point of a given macromolecule.

The master curve presented in Figure 1b clearly shows that there is more than two decades in timescale separation between the segmental and terminal relaxation in PMMS. This separation is clearly larger than the difference in the relaxation times determined from dielectric measurement. To quantify those differences, we compared the relaxation times of the slow and fast relaxation processes obtained from the dielectric investigation with the ones determined from the mechanical data. However, to do that properly, one should keep in mind that dielectric data must be converted to the modulus representation (for details, see the Supporting Information file). The application of this procedure is crucial to make a reliable comparison between the relaxation times of the slow and fast modes determined from dielectric data with the ones estimated from the analysis of the storage and loss modulus. After simple recalculations, the loss modulus was fitted to the superposition of the two (high-temperature region) or three (vicinity of T_g) HN functions with an additional term describing the charge transport, where the third fitting component was used to describe the secondary mode appearing in the experimental window upon approaching T_g. To estimate segmental and terminal relaxation times from the mechanical data, the procedures described in refs 20 and 29 were adopted. Afterward, determined relaxation times were plotted versus reciprocal temperature in Figure 1c. Presented data show that there is a notable discrepancy between the temperature evolution of the slow dielectric process and terminal modes detected in PMMS. Although in ref 30, it was shown that the relaxation processes of the same molecular origin may have different times scales in dielectric and mechanical response functions, our data clearly indicates that α' should not be assigned as the normal mode. To support this thesis, one can remind that according to the Stockmayer classification, polysiloxanes are identified as *type-B* polymers.[31] It means that these polymers have no component of dipole moment parallel to the main backbone. Consequently, the chain global dynamics cannot be detected by broadband dielectric spectroscopy (BDS) in this material.

Having this discussion in mind, we decided to digitalize the data reported in the literature for other polysiloxanes, where a part of the segmental relaxation type, also slower modes were detected in dielectric spectra, to gain further insight into the molecular origin of α'observed in PMMS. To simplify the comparison and make some credible conclusions, all temperature evolutions of the segmental and slow modes in PMMS, PMPS, and hydroxyl-terminated HO−PDMS−OH of low M_n (indicated in the figure caption) were rescaled versus T_g and plotted in Figure 2. As can be seen, $\tau_\alpha(T_g/T)$ collapses more or

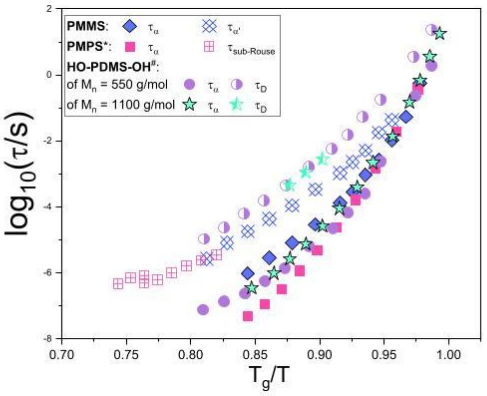

Figure 2. Comparison of the temperature evolution of the segmental and slow mode relaxation times obtained for PMPS, HO−PDMS−OH, and PMMS rescaled with respect to the T_g. *Data for PMPS were taken from ref 11. #Data for HO−PDMS−OH were taken from ref 19.

less onto one master curve for all polymers, while in the case of analogous dependencies for the slow mode, the situation is quite different. It is well seen that there is a very good agreement between $\tau_{sub\text{-}Rouse}(T_g/T)$ and $\tau_{\alpha'}(T_g/T)$ dependencies for the slow modes found in PMPS and PMMS, respectively (see Figure 2). On the other hand, the temperature evolution of the Debye relaxation times (τ_D) versus T_g/T in HO−PDMS−OH reveals different pattern of behavior. This experimental finding suggests that, most likely, the α'-relaxation process detected in dielectric spectra measured for PMMS is the sub-Rouse mode, reflecting motions of the (sub)chain units, and is not related to the mobility within nanoassociates. Nevertheless, to verify this hypothesis, further high-pressure BDS measurements on PMMS were carried out.

In Figure 3a,b, we presented dielectric loss spectra measured for this polymer at isothermal (T = 233 K) and isobaric (p = 505 MPa) conditions. As can be seen, during cooling or compression, the maximum of the observed bimodal loss peak moves toward a lower frequency. Moreover, similar to the data obtained at ambient p, as the maximum of this process shifts to a higher frequency (shorter relaxation times), it becomes broader. This pattern of behavior clearly indicates a bimodal character of this mode even at very high pressure (p = 505 MPa, Figure 3b). To visualize this effect in a better way and illustrate the impact of the compression on the dynamics of the

https://doi.org/10.1021/acs.macromol.2c00378
Macromolecules 2022, 55, 5581−5590

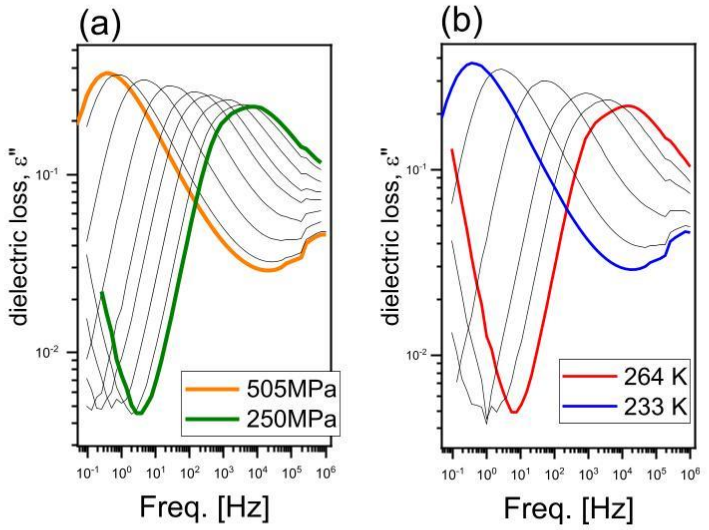

Figure 3. Dielectric loss spectra measured for PMMS at (a) isothermal (T = 233 K) and (b) isobaric (p = 505 MPa) conditions.

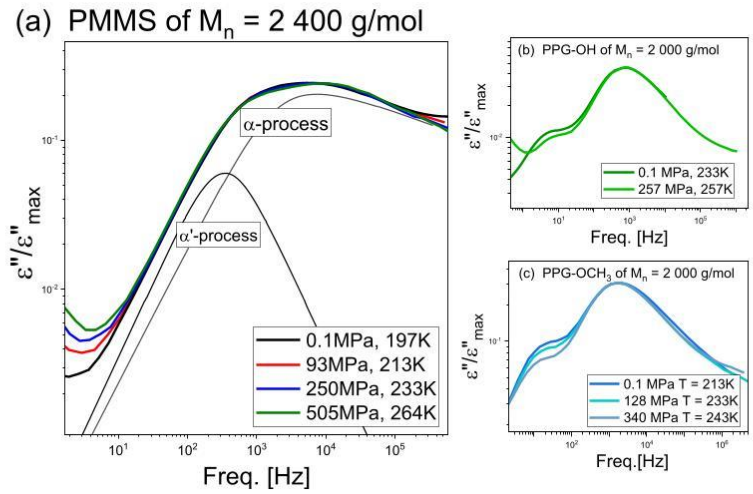

Figure 4. (a) Comparison of the loss spectra (a) obtained for examined PMMS at various thermodynamic conditions that were characterized by the same τ_α. The solid black lines represent the two HN functions used to fit recorded dielectric data. (b,c) Superposition of dielectric loss spectra shown for PPG−OH (b) and PPG−OCH_3 (c) of molecular weight M_n = 2000 g/mol at different thermodynamic conditions. Data for various PPGs were taken from ref 32.

slow and segmental relaxations in PMMS, we compared the loss spectra obtained at various T and p conditions that were characterized by the same τ_α (see Figure 4a).

Herein, it should be noted that usually such a comparison is done for the data collected in the vicinity of T_g. However, this time, we performed it at temperatures much above T_g because the contribution of the α'-process to the loss spectra was detectable only for a data characterized by short segmental relaxation times, τ_α. As can be seen in Figure 4a, dielectric spectra that were measured at many different thermodynamic conditions almost perfectly collapse onto each other. This suggests that (i) the time−temperature−pressure rule, stating that the shape of the loss peak is governed by the structural/segmental relaxation time, is satisfied, and (ii) there is a perfect superposition of the slow and segmental process in PMMS. It means that the timescale separation of both modes is well preserved and does not depend on the thermodynamic conditions. This supposition is also confirmed by fitting the

https://doi.org/10.1021/acs.macromol.2c00378
Macromolecules 2022, 55, 5581−5590

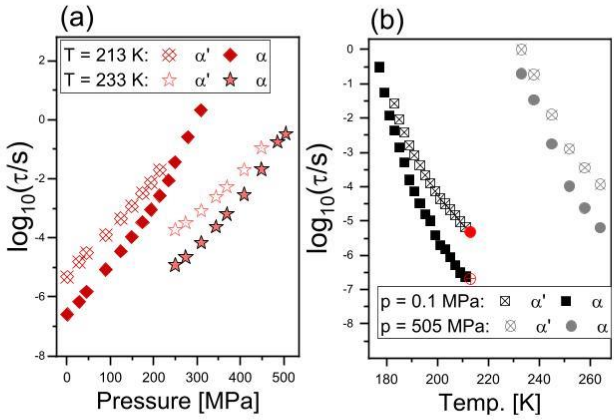

Figure 5. Temperature and pressure dependences of $\tau_{\alpha'}$ and τ_{α} obtained during isothermal (a) and isobaric (b) measurements for PMMS of M_n = 2400 g/mol.

data to the superposition of the two HN functions (see Figure 4a). Herein, it should be noted that a similar finding has been reported for the normal mode and segmental process in poly(propylene glycol) (PPG) or *cis*-1,4-polyisoprene classified as *type-A* polymers.[32,33]

In Figure 4b,c, we presented dielectric loss spectra measured for various PPGs of M_n = 2000 g/mol with hydroxyl and methyl terminated units labeled as PPG−OH and PPG−OCH_3, respectively. As demonstrated, apart from the variation in the amplitude of the normal mode, there is a perfect agreement between the loss spectra measured for both PPGs at various thermodynamic conditions. Therefore, the time scale difference between the chain and segmental dynamics is well preserved upon compression. Thus, high-pressure experiments revealed notable similarities in the behavior of the slow mode in PMMS to the normal mode detected in *type-A* polymers. It might suggest that, most likely, the α'-process might reflect the (sub)chain motions and could be classified as the sub-Rouse mode. Herein, one can stress that even if we had assumed that the α'-relaxation is a manifestation of the motions occurring within nanoassociates, as was done for HO−PDMS−OH, we would have expected a much different dielectric response of this mode with respect to the segmental process at high p. It is commonly accepted that densification changes the strength of H-bonds or even the molecular architecture of self-assemblies. Consequently, the dynamics of the relaxation process, connected to the reorientation of the supramolecular structures with respect to that of the segmental mode, should be modified at varying thermodynamic conditions, as was reported for the low-molecular-weight monohydroxy alcohols.[34] In other words, in such a situation, it is highly anticipated that there will be no superposition of the segmental and slow modes at elevated p, which obviously is not the case. Based on the abovementioned argumentation, we can certify that although PMMS forms supramolecular structures and molecules organize themselves into a nematic-like order, a process driven by thiol moieties (deduced from MD simulations), the slow mode is not a manifestation of the motions within nanoassociates. Contrarily, the presented data suggest that the α'-process reflects the motions of the chain and could be considered the sub-Rouse mode.

In the next step, we analyzed dielectric data obtained at varying T and p conditions to gain insight into the dynamics of segmental and sub-Rouse modes in PMMS. In Figure 5, the pressure and temperature evolution of τ_{α} and $\tau_{\text{sub-Rouse}}(\tau_{\alpha'})$ are shown. At first glance, it is found that both modes tend to merge upon approaching T_g. This clearly indicates that the relaxation times of the sub-Rouse mode have much weaker pressure and temperature sensitivity with respect to the segmental process. Interestingly, a similar pattern of behavior was noted, when we compared the dynamics of the normal mode and α-process in *type-A* polymers.[32]

Further, we decided to calculate the pressure coefficient of the glass transition temperature (dT_g/dp), as well as the activation volume (ΔV)—useful parameters characterizing the dynamics of the investigated systems that have strong physical grounds. To do that, we applied the Avramov model that can be used to parametrize the temperature and pressure dependence of the segmental and sub-Rouse relaxations times and further predict their evolution at given thermodynamic conditions. Herein, one can briefly mention that the following equation was used to fit the data[35]

$$\tau_{\alpha} = \tau_{\infty}\ \exp\left[\ln(\tau_g/\tau_{\infty})\left(\frac{T_r}{T}\right)^{\alpha_0\left(1-\frac{C}{C_{P_0}}\ln\left(1+\frac{p}{\Pi}\right)\right)}\left(1+\frac{p}{\Pi}\right)^{\beta}\right] \tag{2}$$

where τ_{∞} is a relaxation time at extremely high T, $\tau_g = \tau(T_g)$, T_r is a reference temperature lying close to the T_g, Π is a constant with the dimension of pressure, α_0 and β are exponential parameters, which are linked to the thermodynamic quantities via the following relations

$$\alpha_0 = \frac{2C_{P_0}}{ZR} \tag{3}$$

$$\beta = \frac{2\alpha_p V_m}{ZR}\Pi \tag{4}$$

https://doi.org/10.1021/acs.macromol.2c00378
Macromolecules 2022, 55, 5581−5590

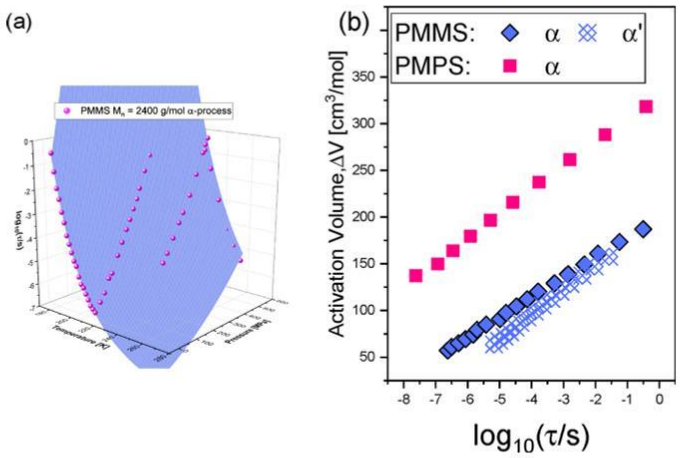

Figure 6. (a) Segmental relaxation times plotted vs temperature and pressure for PMMS. Violet areas represent surface fits to the modified Avramov equation (eq 2). (b) Activation volume (ΔV) obtained for the segmental, and the sub-Rouse mode plotted vs τ_α for PMMS and PMPS.

where C_{p_0} is a specific heat capacity, Z represents the degeneracy of the system, α_p is a volume expansion coefficient at ambient p, and V_m is a molar volume. The results of fitting $\tau_\alpha(T, p)$ and $\tau_{\text{sub-Rouse}}(T, p)$ dependencies to the Avramov equation are presented in Figures 6a and S8. It should be noted that the obtained fits are of very high quality because $R^2 \approx 0.998$ for τ_α and $R^2 \approx 0.993$ for $\tau_{\text{sub-Rouse}}$ in both cases (see Table S1 in the Supporting Information presenting the parameters of eq 2 determined from the global numerical fitting).

Having done the fitting procedure, we calculated T_g at varying pressures as well as the pressure coefficient of the glass transition temperature in the limit of ambient pressure using the pressure derivative of the following Avramov equation[36]

$$T_g(p) = T_g(p_0)\left(1 + \frac{p}{\Pi}\right)^{\beta/\alpha(p)} \tag{5}$$

where

$$\alpha(p) = \alpha_0\left(1 - \frac{C}{C_{p_0}}\left(\ln\left(1 + \frac{p}{\Pi}\right)\right)\right) \tag{6}$$

It was obtained that dT_g/dp for PMMS is equal to dT_g/dp = 156 K/GPa. It seems that this value is, unexpectedly, really low, considering that polysiloxanes are quite flexible polymers, for which the pressure coefficient of the glass transition temperature should be rather high. Herein, it should be noted that silyl derivatives of low-molecular-weight glass formers are characterized by the highest dT_g/dp of all liquids. Just to remind silyl derivative of glucose and trehalose, for which this parameter reaches 412 and 453 K/GPa, respectively.[37,38] Moreover, one can compare the obtained result to the dT_g/dp determined for other polymers. Note that for some representative vinyl macromolecules, including 1,2-PBD,[39] polyethylene,[40] poly(vinyl acetate),[41] and poly(vinyl methyl ether),[42] $dT_g/dp \sim 180-250$ K/GPa. What is more, dT_g/dp for polystyrene varied from 306 to 294 K/Gpa, depending on the molecular weight. One can also mention that PPGs have different terminal units. In these polymers, dT_g/dp changes from ~150 to ~200 K/GPa. To make this discussion even more credible and informative, we decided to perform additional high-pressure dielectric experiments on PMPS of nearly the same molecular weight, which has a similar backbone to PMMS, but a different pendant group (phenyl moiety). Obtained data were analyzed in the analogous way as it was done in the case of PMMS. It was found that dT_g/dp obtained for PMPS, which equals 250 K/GPa, is nearly twice higher than that determined for the investigated macromolecule. Hence, one can claim that such a low value of dT_g/dp in PMMS with respect to the majority of the investigated polymers, including other polysiloxanes having a similar backbone, is strictly related to the presence of thiol moieties, which are capable of forming H-bonds. Although specific interactions created by −SH units are regarded as one of the weakest, they have a tremendous impact on the dynamics of the segmental process and pressure coefficient of the glass transition temperature in PMMS.

Further, we calculated the activation volume in the limit of ambient pressure for segmental and sub-Rouse modes in a wide range of temperatures and compare them to the values determined for PMPS. Herein, it should be stressed that according to transition state theory, ΔV is a measure of a different volume in the activated and standard states. It can be calculated according to the definition

$$\Delta V_x = RT\ \ln(10)\left(\frac{d\log_{10}\tau_x}{dp}\right)_T,\ x = \alpha, \alpha' \tag{7}$$

One can mention that to estimate the activation volume at different thermodynamic conditions, we utilized the parameters obtained from the Avramov fits to the $\tau_\alpha(T, p)$ and $\tau_{\alpha',\text{sub-Rouse}}(T, p)$ evolution in PMMS and PMPS (listed in Table S1 in the Supporting Information). Next, the determined values of ΔV have been plotted versus segmental relaxation times, as shown in Figure 6b. The activation volume for the segmental process is slightly higher, within the limit of uncertainty, with respect to ΔV of the sub-Rouse mode.

https://doi.org/10.1021/acs.macromol.2c00378
Macromolecules 2022, 55, 5581−5590

Interestingly, a similar observation has been reported in previous papers, where it was shown that values of ΔV of the normal mode, reflecting motions of the whole chain, are comparable to ΔV of the shorter distance segmental mobility.[43] At first sight, this finding seems to be controversial because segmental motions obey few reorienting segments, while the sub-Rouse or normal mode is a result of longer distance chain motions. Nevertheless, it was argued that ΔV is not a volume required for the cooperative reorientations of the whole chain but a volume required for the reorientation of the chain ends. Therefore, this is the main reason why the activation volume is so similar in the case of segmental and normal modes in the *type-A* polymer. Hence again we found a similarity in the dynamical behavior of the slow process in PMMS to the normal mode in type A polymer. This finding can be another important clue for identifying the α'-process in the investigated oligomer to the sub-Rouse motions. Herein, it should also be commented that the activation volume determined for the segmental relaxation process in PMPS is more than twice as high as that of PMMS. This result was expected considering both (i) a notable difference in the pressure evolution of T_g and (ii) the size of the pendant phenyl units, which is much larger with respect to the isopropyl alkyl unit. In literature, we can find numerous examples, where the authors demonstrated that ΔV changes with the size of the pendant moiety.[43]

Having analyzed the high-pressure data, one can state that the dynamical behavior of α'-process strongly mimics characteristic features of the normal mode in *type-A* polymers. This suggests that the slow mode must reflect some kind of motions of the chain and could be considered as the sub-Rouse mode found in many polymers including other polysiloxanes characterized by a similar chemical backbone to PMMS. In this context, it should be stressed that although one can consider other molecular motions underlying this mode, they are less probable. To justify this thesis, it should be reminded that in contrast to the α'-mode observed in PMMS, the slow processes assigned to the helical conformations detected in polystyrene (treated with various solvents) show an Arrhenius-like behavior and do not merge with the segmental relaxation.[26] The same pattern of behavior applies to the slow mode detected in the series of thin films, which was supposed to be a universal feature of glass-forming materials.[28] Finally, our last molecular dynamics simulations indicated that although PMMS molecules tend to arrange themselves in a nematic-like order, this process is clearly driven by the H bonds formed by the thiol moiety.[27] On the other hand, it is highly anticipated that due to compression, there should be a clear change in the H-bond pattern and molecular arrangement, which must be reflected in the dynamics of the slow mode as reported repeatedly in numerous monohydroxy alcohols.[34,44,45]

As a final point of this paper, we decided to examine, why there is such a strong variation in the amplitude of the sub-Rouse mode in PMMS and PMPS. This difference is well illustrated in the loss spectra of both polymers measured much above T_g, see Figure S9 in the Supporting Information. For that purpose, additional DFT calculations on the distribution of the dipole moment along the main chain for the monomers as well as oligomers consisting of a few (up to 4) repeated units were performed. The value of the dipole moment and its components depends on the conformation of the polymer, as shown in Table S2. As presented in Figure S10, it was found that both the parallel ($\mu_{\parallel}$) and perpendicular ($\mu_{\perp}$) components of the dipole moment along the main chain in PMMS ($\mu_{\parallel} \sim 1.9-2.8$ and $\mu_{\perp} \sim 1.4-2.3$) are much higher than that in PMPS ($\mu_{\parallel} \sim 0.1$ and $\mu_{\perp} \sim 0.3-0.6$, see Table S2). It should be highlighted that the determined dipole moment's components are solely generated by the presence of the polymer side groups. As shown, these computations clearly indicated that the presence of highly polar moiety in the pendant unit group gives rise to a significant parallel component of dipole moment in PMMS. We are convinced that this is the main source of the difference in the amplitudes of the sub-Rouse modes in both polymers.

4. CONCLUSIONS

In this work, we have investigated the molecular dynamics of PMMS at high pressure. These experiments allowed us to find out that the additional (α') relaxation process, slower than the segmental mode detected in dielectric loss spectra of this polymer, mimics the behavior of the normal mode at varying thermodynamic conditions. Herein, one can list a few similarities, such as a constant time scale separation between τ_{α} and $\tau_{\alpha'}$ during compression, as well as activation volumes comparable to those determined for the segmental motions. Obtained results, together with earlier mechanical data, suggested that the α'-process in PMMS might be the sub-Rouse mode. Herein, it should be mentioned that we have also considered other possible molecular motions that could be responsible for the slow mode in PMMS. However, it seems that although at the moment they cannot be completely rejected, they are less probable. Therefore, apart from PMPS, this polymer is a second polysiloxane, for which such kind of mobility was identified in dielectric loss spectra. Further DFT computations revealed that it was possible due to a high parallel component of dipole moment along the main backbone, which resulted from the presence of the polar thiol moiety in the pendant unit. Moreover, we also found that the pressure coefficient of the glass transition temperaure determined for PMMS is much smaller than PMPS of similar M_n and other polymers investigated in the literature. This outcome, although quite surprising considering the flexible nature of the Si−O connections, is surely connected to the presence of thiol moiety in side groups attached to each monomer. Even though specific interactions formed by this moiety are regarded as one of the weakest of all known, they have a strong impact on the dynamics of segmental and sub-Rouse mode in PMMS. The data presented in this paper clearly emphasize the important role of high-pressure experiments in the elucidation of the most probable nature of additional motions detected in the loss spectra. Furthermore, they seem to be a key element to identify the sub-Rouse mode, which provides information about larger distance chain motions.

■ ASSOCIATED CONTENT

Supporting Information

The Supporting Information is available free of charge at https://pubs.acs.org/doi/10.1021/acs.macromol.2c00378.

Experimental details and additional figures including details on the calculation of modulus, M^*; representation of dielectric data; comparison of the data fitting with the use of two and one HN function for dielectric loss spectra; comparison of the data fitting with the use

https://doi.org/10.1021/acs.macromol.2c00378
Macromolecules 2022, 55, 5581−5590

of two HN functions characterized by different relaxation times; temperature dependences of HN shape parameters; temperature and pressure dependences of τ_α of PMPS; fit together with the fit parameters of the modified Avramov of τ_α and $\tau_{\text{sub-Rouse}}$ for PMMS and PMPS; value of the dipole moment and its components depends on the conformation of the polymer; and structure of 4-units isotactic and syndiotactic PMMS and PMPS (PDF)

AUTHOR INFORMATION

Corresponding Author

Magdalena Tarnacka − *Institute of Physics, University of Silesia in Katowice, 41-500 Chorzów, Poland;* orcid.org/0000-0002-9444-3114; Email: magdalena.tarnacka@us.edu.pl, magdalena.tarnacka@smcebi.edu.pl

Authors

Sara Zimny − *Institute of Chemistry, University of Silesia in Katowice, 40-006 Katowice, Poland;* orcid.org/0000-0003-3812-1353

Ewa Kamińska − *Department of Pharmacognosy and Phytochemistry, Faculty of Pharmaceutical Sciences in Sosnowiec, Medical University of Silesia in Katowice, 41-200 Sosnowiec, Poland;* orcid.org/0000-0001-9725-8654

Roman Wrzalik − *Institute of Physics, University of Silesia in Katowice, 41-500 Chorzów, Poland*

Karolina Adrjanowicz − *Institute of Physics, University of Silesia in Katowice, 41-500 Chorzów, Poland;* orcid.org/0000-0003-0212-5010

Marian Paluch − *Institute of Physics, University of Silesia in Katowice, 41-500 Chorzów, Poland;* orcid.org/0000-0002-7280-8557

Kamil Kamiński − *Institute of Physics, University of Silesia in Katowice, 41-500 Chorzów, Poland;* orcid.org/0000-0002-5871-0203

Complete contact information is available at: https://pubs.acs.org/10.1021/acs.macromol.2c00378

Notes

The authors declare no competing financial interest.

ACKNOWLEDGMENTS

M.T. and K.K. are thankful for financial support from the Polish National Science Centre with the OPUS project (Dec. no. 2019/33/B/ST3/00500).

REFERENCES

(1) Rahimi, A.; Shokrolahi, P. Application of Inorganic Polymeric Materials. I. Polysiloxanes. *Int. J. Inorg. Mater.* **2001**, *3*, 843−847.

(2) Abbasi, F.; Mirzadeh, H.; Katbab, A.-A. Modification of Polysiloxane Polymers for Biomedical Applications: A Review. *Polym. Int.* **2001**, *50*, 1279−1287.

(3) Bischoff, R.; Cray, S. E. Polysiloxanes in Macromolecular Architecture. *Prog. Polym. Sci.* **1999**, *24*, 185−219.

(4) Yi, B.; Liu, P.; Hou, C.; Cao, C.; Zhang, J.; Sun, H.; Yao, X. Dual-Cross-Linked Supramolecular Polysiloxanes for Mechanically Tunable, Damage-Healable and Oil-Repellent Polymeric Coatings. *ACS Appl. Mater. Interfaces* **2019**, *11*, 47382−47389.

(5) Mojsiewicz-Pieńkowska, K.; Jamrógiewicz, M.; Szymkowska, K.; Krenczkowska, D. Direct Human Contact with Siloxanes (Silicones)—Safety or Risk Part 1. Characteristics of Siloxanes (Silicones). *Front. Pharmacol.* **2016**, *7*, 1−8.

(6) Aliyar, H.; Schalau, G. Recent Developments in Silicones for Topical and Transdermal Drug Delivery. *Ther. Delivery* **2015**, *6*, 827−839.

(7) Plazek, D. J.; Bero, C. A.; Neumeister, S.; Floudas, G.; Fytas, G.; Ngai, K. L. Viscoelastic Properties of Amorphous Polymers 3: Low Molecular Weight Poly(Methylphenylsiloxane). *Colloid Polym. Sci.* **1994**, *272*, 1430−1438.

(8) Boese, D.; Momper, B.; Meier, G.; Kremer, F.; Hagenah, J. U.; Fischer, E. W. Molecular Dynamics in Poly(Methylphenylsiloxane) As Studied by Dielectric Relaxation Spectroscopy and Quasielastic Light Scattering. *Macromolecules* **1989**, *22*, 4416−4421.

(9) Adrjanowicz, K.; Winkler, R.; Chat, K.; Duarte, D. M.; Tu, W.; Unni, A. B.; Paluch, M.; Ngai, K. L. Study of Increasing Pressure and Nanopore Confinement Effect on the Segmental, Chain, and Secondary Dynamics of Poly(Methylphenylsiloxane). *Macromolecules* **2019**, *52*, 3763−3774.

(10) Winkler, R.; Tu, W.; Dulski, M.; Laskowski, L.; Adrjanowicz, K. Effect of the Surface Polarity, through Employing Nonpolar Spacer Groups, on the Glass-Transition Dynamics of Poly(Phenyl Methylsiloxane) Confined in Alumina Nanopores. *Macromolecules* **2021**, *54*, 10951−10968.

(11) Tu, W.; Ngai, K. L.; Paluch, M.; Adrjanowicz, K. Dielectric Study on the Well-Resolved Sub-Rouse and JG β-Relaxations of Poly(Methylphenylsiloxane) at Ambient and Elevated Pressures. *Macromolecules* **2020**, *53*, 1706−1715.

(12) Plazek, D. J.; Chay, I.-C.; Ngai, K. L.; Roland, C. M. Viscoelastic Properties of Polymers. 4. Thermorheological Complexity of the Softening Dispersion in Polyisobutylene. *Macromolecules* **1995**, *28*, 6432−6436.

(13) Ngai, K. L.; Plazek, D. J. Identification of Different Modes of Molecular Motion in Polymers That Cause Thermorheological Complexity. *Rubber Chem. Technol.* **1995**, *68*, 376−434.

(14) Ngai, K. L.; Plazek, D. J.; Rizos, A. K. Viscoelastic Properties of Amorphous Polymers. 5. A Coupling Model Analysis of the Thermorheological Complexity of Polyisobutylene in the Glass-Rubber Softening Dispersion. *J. Polym. Sci., Part B: Polym. Phys.* **1997**, *35*, 599−614.

(15) Rizos, A. K.; Jian, T.; Ngai, K. L. Determination of the Coupling Parameter of Local Segmental Motion in Poly(Isobutylene) by Photon Correlation Spectroscopy. *Macromolecules* **1995**, *28*, 517−521.

(16) Santangelo, P. G.; Ngai, K. L.; Roland, C. M. Distinctive Manifestations of Segmental Motion in Amorphous Poly-(Tetrahydrofuran) and Polyisobutylene. *Macromolecules* **1993**, *26*, 2682−2687.

(17) Plazek, D. J.; Ngai, K. L. Resolving the Sub-Rouse Modes by Creep Compliance Measurements in Poly(Methyl- Para-Tolyl-Siloxane). *Macromolecules* **2020**, *53*, 3940−3945.

(18) Patkowski, A.; Gapinski, J.; Pakula, T.; Meier, G. Physical Nature of Complex Structural Relaxation in Polysiloxane—PMpTS: α and α' Relaxations. *Polymer* **2006**, *47*, 7231−7240.

(19) Xing, K.; Chatterjee, S.; Saito, T.; Gainaru, C.; Sokolov, A. P. Impact of Hydrogen Bonding on Dynamics of Hydroxyl-Terminated Polydimethylsiloxane. *Macromolecules* **2016**, *49*, 3138−3147.

(20) Tarnacka, M.; Jurkiewicz, K.; Hachuła, B.; Wojnarowska, Z.; Wrzalik, R.; Bielas, R.; Talik, A.; Maksym, P.; Kaminski, K.; Paluch, M. Correlation between Locally Ordered (Hydrogen-Bonded) Nanodomains and Puzzling Dynamics of Polymethysiloxane Derivative. *Macromolecules* **2020**, *53*, 10225−10233.

(21) Havriliak, S.; Negami, S. A Complex Plane Analysis of α-Dispersions in Some Polymer Systems. *J. Polym. Sci., Part C: Polym. Symp.* **2007**, *14*, 99−117.

(22) *Broadband Dielectric Spectroscopy*; Kremer, F., Schönhals, A., Eds.; Springer-Verlag: Berlin, 2002.

(23) Stockmayer, W. H. Dielectric Dispersion in Solutions of Flexible Polymers. *Pure Appl. Chem.* **1967**, *15*, 539−554.

(24) Godovsky, Y. K.; Papkov, V. S. Thermotropic Mesophases in Linear Polysiloxanes. *Makromol. Chem., Macromol. Symp.* **1986**, *4*, 71−87.

(25) Floudas, G.; Spiess, H. W. Self-Assembly and Dynamics of Polypeptides. *Macromol. Rapid Commun.* **2009**, *30*, 278−298.
(26) Lupaşcu, V.; Picken, S. J.; Wübbenhorst, M. Dynamics of T2G2 Helices in Atactic and Syndiotactic Polystyrene: New Evidence from Dielectric Spectroscopy and FTIR. *Macromolecules* **2006**, *39*, 5152−5158.
(27) Paturej, J.; Koperwas, K.; Tarnacka, M.; Jurkiewicz, K.; Maksym, P.; Grelska, J.; Paluch, M.; Kamiński, K. Supramolecular Structure of Self-Assembled Oligomers under Confinement. *Soft Matter* **2022**, DOI: 10.1039/D2SM00343K.
(28) Song, Z.; Rodríguez-Tinoco, C.; Mathew, A.; Napolitano, S. Fast Equilibration Mechanisms in Disordered Materials Mediated by Slow Liquid Dynamics. *Sci. Adv.* **2022**, *8*, 1−8.
(29) Graessley, W. W. The Entanglement Concept in Polymer Rheology. In *The Entanglement Concept in Polymer Rheology*; Springer-Verlag: Berlin/Heidelberg, 1974; pp 1−179.
(30) McCrum, N. G.; Read, B. E.; Williams, G. *Anelastic and Dielectric Effects in Polymeric Solids*, 1st ed.; John Wiley: New York, NY, 1967.
(31) Schwartz, G. A.; Bergman, R.; Swenson, J. Relaxation Dynamics of a Polymer in a 2D Confinement. *J. Chem. Phys.* **2004**, *120*, 5736−5744.
(32) Talik, A.; Tarnacka, M.; Dzienia, A.; Kaminska, E.; Kaminski, K.; Paluch, M. High-Pressure Studies on the Chain and Segmental Dynamics of a Series of Poly(Propylene Glycol) Derivatives. *Macromolecules* **2019**, *52*, 5658−5669.
(33) Politidis, C.; Alexandris, S.; Sakellariou, G.; Steinhart, M.; Floudas, G. Dynamics of Entangled Cis-1,4-Polyisoprene Confined to Nanoporous Alumina. *Macromolecules* **2019**, *52*, 4185−4195.
(34) Pawlus, S.; Paluch, M.; Dzida, M. Molecular Dynamics Changes Induced by Hydrostatic Pressure in a Supercooled Primary Alcohol. *J. Phys. Chem. Lett.* **2010**, *1*, 3249−3253.
(35) Avramov, I. Pressure Dependence of Viscosity of Glassforming Melts. *J. Non-Cryst. Solids* **2000**, *262*, 258−263.
(36) Avramov, I. Pressure and Temperature Dependence of Viscosity of Glassforming and of Geoscientifically Relevant Systems. *J. Volcanol. Geotherm. Res.* **2007**, *160*, 165−174.
(37) Minecka, A.; Kamińska, E.; Tarnacka, M.; Dzienia, A.; Madejczyk, O.; Waliłko, P.; Kasprzycka, A.; Kamiński, K.; Paluch, M. High Pressure Studies on Structural and Secondary Relaxation Dynamics in Silyl Derivative of D-Glucose. *J. Chem. Phys.* **2017**, *147*, 064502.
(38) Heczko, D.; Grelska, J.; Jurkiewicz, K.; Spychalska, P.; Kasprzycka, A.; Kamiński, K.; Paluch, M.; Kamińska, E. Anomalous Narrowing of the Shape of the Structural Process in Derivatives of Trehalose at High Pressure. The Role of the Internal Structure. *J. Mol. Liq.* **2021**, *336*, 116321.
(39) Roland, C. M.; Casalini, R.; Santangelo, P.; Sekula, M.; Ziolo, J.; Paluch, M. Chemical Structure and Local Segmental Dynamics in 1,2-Polybutadiene. *Macromolecules* **2003**, *36*, 4954−4959.
(40) Ngai, K. L.; Roland, C. M. Chemical Structure and Intermolecular Cooperativity: Dielectric Relaxation Results. *Macromolecules* **1993**, *26*, 6824−6830.
(41) Roland, C. M.; Casalini, R. Temperature and Volume Effects on Local Segmental Relaxation in Poly(Vinyl Acetate). *Macromolecules* **2003**, *36*, 1361−1367.
(42) Casalini, R.; Roland, C. M. Dynamic Properties of Polyvinylmethylether near the Glass Transition. *J. Chem. Phys.* **2003**, *119*, 4052−4059.
(43) Floudas, G.; Paluch, M.; Grzybowski, A.; Ngai, K. *Molecular Dynamics of Glass-Forming Systems*; Advances in Dielectrics; Springer Berlin Heidelberg: Berlin, Heidelberg, 2011; Vol. *1*.
(44) Pawlus, S.; Wikarek, M.; Gainaru, C.; Paluch, M.; Böhmer, R. How Do High Pressures Change the Debye Process of 4-Methyl-3-Heptanol? *J. Chem. Phys.* **2013**, *139*, 064501.
(45) Gainaru, C.; Wikarek, M.; Pawlus, S.; Paluch, M.; Figuli, R.; Wilhelm, M.; Hecksher, T.; Jakobsen, B.; Dyre, J. C.; Böhmer, R. Oscillatory Shear and High-Pressure Dielectric Study of 5-Methyl-3-Heptanol. *Colloid Polym. Sci.* **2014**, *292*, 1913−1921.

A2. Impact of the Graft' Structure on the Behavior of PMMS-Based Brushes. High pressure studies.

AUTORZY: S. Zimny, M. Tarnacka, Ż. Wojnarowska, D. Heczko, P. Maksym, M. Paluch, K. Kamiński.

REFERENCJA: Polymer, 2023, 271, 125790.

DOI: 10.1016/j.polymer.2023.125790

Impact Factor czasopisma z roku opublikowania: 4.1

Liczba punktów ministerialnych MNiSW czasopisma (2023): 100

Mój udział w pracy polegał na przygotowaniu próbek, wykonaniu pomiarów dielektrycznych i analizie otrzymanych wyników, współtworzeniu manuskryptu (przeprowadzenie przeglądu literaturowego, przygotowanie tekstu manuskryptu i rysunków, opis wyników i sformułowanie wniosków), formułowaniu odpowiedzi na uwagi recenzentów oraz korekcie manuskryptu po otrzymanych recenzjach.

Polymer 271 (2023) 125790

Contents lists available at ScienceDirect

Polymer

journal homepage: www.elsevier.com/locate/polymer

Impact of the graft' structure on the behavior of PMMS-based brushes. High pressure studies

Sara Zimny [a], Magdalena Tarnacka [b,*], Zaneta Wojnarowska [b], Dawid Heczko [c], Paulina Maksym [d], Marian Paluch [b], Kamil Kamiński [b]

[a] Institute of Chemistry, University of Silesia in Katowice, Szkolna 9, 40-006, Katowice, Poland
[b] Institute of Physics, University of Silesia in Katowice, 75 Pułku Piechoty 1, 41-500, Chorzów, Poland
[c] Department of Statistics, Department of Instrumental Analysis, Faculty of Pharmaceutical Sciences in Sosnowiec, Medical University of Silesia in Katowice, Ostrogórska 30, 41-200, Sosnowiec, Poland
[d] Institute of Material Science, University of Silesia in Katowice, 75 Pułku Piechoty 1A, 41-500, Chorzów, Poland

A B S T R A C T

In this paper, we have investigated dielectric response at ambient and elevated pressure of poly(mercaptopropyl)methylsiloxane (PMMS) based oligomeric brushes, where the thiol moiety was substituted by various butyl acrylate isomers (*n*-butyl acrylate (nBA), *iso*-butyl acrylate (isoBA), *tert*-butyl acrylate (tertBA)). It was found that the glass transition temperature, T_g, of PMMS is much lower with respect to the other systems despite its ability to form weak hydrogen (H) bonds. What is more, the length scale of cooperativity was the highest in homopolymer and scaled with the steric hindrance of the graft. We also demonstrated that in the examined grafted copolymers, there is one broad relaxation process in dielectric spectra which is wider than that recorded in mechanical response. That probably means that similarly to PMMS, there are two relaxation processes above T_g in grafted copolymers. However, due to similar timescale, they cannot be separated. Further, high-pressure experiments revealed that pressure coefficient of the glass transition temperature, dT_g/dp, as well as the activation volume, ΔV, calculated for the segmental process surprisingly does not scale with either the size of monomer nor steric hindrance. This unexpected result must be related to the specific structure adopted by the studied grafted oligomers. Presented herein data expand our understanding on the impact of topology on the dynamics of polymers at ambient and high pressure.

1. Introduction

Grafted copolymers (polymer brushes, molecular brushes) [1–4] are "macromolecules of two or more different chemical chains in which a chain (named backbone) has multiple branches (grafts) formed from macromolecular chains with a chemical composition different from that of the backbone" [5]. Consequently, the topology of grafted copolymers resembles a comb/brush, which can be moderated by three major parameters: backbone degree of polymerization (N_{bb}), side-chain degree of polymerization (N_{sc}) and grafting density (z). Therefore, the polymer brushes are a very diverse group as those systems can be composed of varying number of (chemically) different branches, introducing additional intra- and intermolecular interactions within those materials. Accordingly, grafted copolymers are often stimuli-responsive materials, sensitive to the variation in temperature, solvents, light, electro-magnetic fields, pH [6–8]. Moreover, one can also mentioned that, interestingly, recent studies on various grafted oligomeric poli (ionic liquids) showed that those materials exhibit enhanced ionic conductivity when compared to their linear counterparts [9,10].

Despite of the high importance of molecular brushes, their molecular dynamics studies especially with the use of dielectric spectroscopy are limited [11–14]. Note that the vast majority of papers devoted to polymer brushes focused on both the probing of mechanical (flow) properties in these materials [7,15–19]. As for oligomeric materials, recent studies on associating poly((mercaptopropyl)methylsiloxane, PMMS) shown that it undergoes the self-association into nanoaggregates [20], which surprisingly, also prevails under confinement [21]. Note that the dielectric studies on various linear telechelic poly(dimethylsiloxane, PDMS) clearly show that the impact of hydrogen bonding end groups of their behavior is dominant only in the low molecular weight range [22–24]. On the other hand, in the case of polymeric bottle brushes, one can recall work by Jakobi et al. [11] on the segmental dynamics of PDMS-based bottlebrushes (PDMS-*g*-PDMS) as a function of their side-chain degree of polymerization ($N_{sc} = 4$–155). Interestingly, it was observed that an increase in N_{sc} between examined PDMS-*g*-PDMS results in longer segmental relaxation times, τ_α, when compared to the "respective single side chains" [11]. Surprisingly, the greatest difference in τ_α was observed in the case of lowest $N_{sc} = 4$. One can mention that

* Corresponding author.
E-mail address: magdalena.tarnacka@us.edu.pl (M. Tarnacka).

https://doi.org/10.1016/j.polymer.2023.125790
Received 28 September 2022; Received in revised form 16 February 2023; Accepted 17 February 2023
Available online 18 February 2023
0032-3861/

also in the case of poly(2-bromoisobutyryloxyethyl methacrylate) (PBiBEM) backbone grafted with poli(*n*-butyl acrylate, PBA) [13], the dynamics were altered when compared to their homopolymer counterparts. However, it should be highlighted that those systems become "dynamically more homogeneous" due to the architectural design.

It is also important to stress that another aspect lacking in our understanding of non-linear polymers (including polymer brushes) is their high-pressure (HP) behavior. This is quite large deficiency since HP experiments deliver important information about the impact of density fluctuation on the segmental dynamics. It should be mentioned that especially recent studies emphasized the role of free volume related to the molecular packing in controlling segmental dynamics of different kind of polymers [25–27]. Moreover, it was clearly demonstrated that the high-pressure data are also crucial to predict behavior of polymers under nanospatial confinement and understand vitrification process in these systems [28–30]. Up to now, the investigations on the compressed linear polymers allowed to elucidate the role of temperature and volume in controlling segmental dynamics and furthermore viscous flow [31, 32], which can be extremely helpful upon manufacturing of these materials. Moreover, previous high-pressure studies on the various kind of polymers characterized by purely van der Waals interactions or other specific intermolecular forces clearly indicated that pressure coefficient of the glass transition, dT_g/dp, strongly depends on the specific intermolecular interactions while not so much on the molecular weight [33]. Additionally, it was found that the variation in the structure of side groups attached to the linear poli(methacrylate methyl) derivatives has a strong impact on their high pressure response [34]. It was found that together with the increasing steric hindrance of the side unit, $dT_g/\ dp$ as well as activation volume, ΔV, varied significantly pointing different role of density in controlling segmental dynamics in these materials. As all available HP data focus on linear polymer, the question arises how bottle brushes (both oligomeric and polymeric) would behave under elevated pressure conditions?

Taking into account that a simple chemical modification of the small side group attached to the backbone of linear polymers has so strong impact on the properties of the macromolecules, we would like to know how the varying steric hindrance of graft affects the behavior of polymer brushes. Therefore, in this paper, we have studied a series of oligomeric PMMS backbone grafted with the different butyl acrylate isomers (BA, see Fig. 1) by means of dielectric spectroscopy measurements performed at both ambient and high-pressure conditions (up to $p > 500\ MPa$). We believe that studies on the oligomeric systems (which physicochemical properties often rapidly change with their molecular weight in the narrow range of M_n) might help us to gain detail knowledge allowing to design (polymeric) material according to our desired purpose. It should be highlighted that all examined grafted copolymers were produced by one of "*grafting to*" techniques (so kind of "click reactions"), in which commercially supplied PMMS backbone functionalized with –SH groups was coupled with acrylates. Note that the thiol-ene coupling photopolymerization is commonly used method characterized by high yield that allows for production of macromolecules of varied composition and topology. For "*grafting to*" technique the average number of branches were determined by degree of polymerization of homopolymer backbone (N_{bb} ~12), whereas the grafts have a length of one monomer unit ($N_{sc} = 1$). The NMR analysis showed the lack of –SH groups confirming the completed thiol-ene coupling (the grafting density, $z = 100\%$, see Figs. S1–S4 in the Supporting Information (SI) file).

2. Materials and methods

Materials. Poly(mercaptopropyl)methylsiloxane homopolymer (PMMS, 75–150 cSt) was purchased from Gelest and used as received (molecular weight, $M_{n,SEC} = 2400$ g/mol, dispersity, $Đ = 1.26$ determined by Viscotek TDA 305 triple detection calibrated with a narrow polystyrene standard, THF as eluent). *n*-butyl acrylate (nBA), *tert*-butyl acrylate (tertBA), *iso*-butyl acrylate (isoBA), 2,2-Dimethoxy-2-phenylacetophenone (DMPA), DMSO-d_6 were purchased from Sigma-Aldrich. Before the polymerization all monomers were purified by passing through a neutral alumina column to remove inhibitors.

Thiol-ene coupling photopolymerization. Example of the synthesis of PMMS-*g*-nBA. PMMS (degree of polymerization, $DP_{PMMS} = 12$; 0.25 g, 0.05 mmol), nBA (0.5 g, 3.90 mmol) and DMPA (0.09 g, 0.36 mmol) were dissolved in THF (2 mL). The solution was purged under nitrogen and purified by one freeze-pump-thaw cycle. Next, the flask was stirred for 160 min under UV irradiation ($\lambda = 365\ nm$), and then THF was evaporated under vacuum. The polymer was purified by washing many times first in methanol/water mixture and then methanol. The purified sample was dried to a constant mass under reduced pressure.

The structure of all grafted oligomers was confirmed by ^{1}H and ^{13}C NMR analysis. Note that NMR spectra were recorded on using 500 MHz spectrometer (Bruker) for samples in commercially available DMSO-d_6. Signals from the respective groups of atoms for PMMS-*g*-nBA, PMMS-*g*-isoBA, and PMMS-*g*-tertBA are shown in Figs. S1–S4. The total disappearance of the thiol signal at 2.08 ppm initially present in the ^{1}H NMR spectra of PMMS and peaks coming from incorporated acrylate units indicate a quantitative thiol-ene ligations (see representative spectrum of PMMS-*g*-isoBA in Fig. S1). Similar observations were noted in the previous papers concerning PMMS-based polymers [9,10]. As can be seen, all spectra present purified products without the presence of unreacted PMMS or monomers.

Differential Scanning Calorimetry (DSC). Calorimetric measurements of PMMS were carried out by Mettler-Toledo DSC apparatus equipped with a liquid nitrogen cooling accessory and an HSS8 ceramic sensor (heat flux sensor with 120 thermocouples). Temperature and enthalpy calibrations were performed by using indium and zinc standards. The sample was prepared in an open aluminum crucible (40 μL) outside the DSC apparatus and measured on heating from 150 K to 298 K at a constant heating rate of 10 K/min. Additionally, each sample was cooled at different cooling rates (50, 20, 5, 1 K/min), an than heated with a standard heating scan at 20 K/min. This procedure allows to determine the fragility parameter from calorimetric measurements

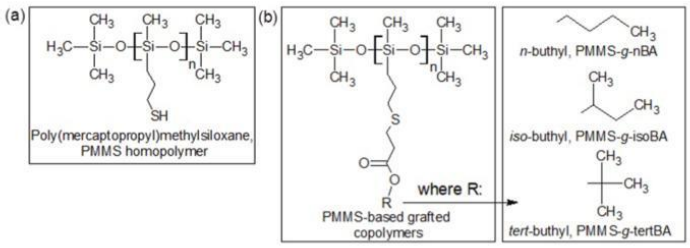

Fig. 1. The chemical structure of poly(mercaptopropyl)methylsiloxane, labeled as PMMS, (a) and its examined grafted derivatives (b).

according to the procedure reported in Refs. [35–38].

Temperature-modulated Differential Scanning Calorimetry (TMDSC). Using a stochastic TMDSC technique implemented by Mettler-Toledo TOPEM ®, the dynamic behavior of PMMS has been analyzed in the frequency range from 1 to 20 mHz in one single measurement at a heating rate of 0.5 K/min. In the experiment, the temperature amplitude of the pulses of 0.5 K was selected with a switching time range with minimum and maximum values of 15 and 30 s, respectively. The calorimetric structural relaxation times, $\tau_\alpha = 1/2\pi f$, were determined from the temperature dependences of the real part of the complex heat capacity, $C_p'(T)$, obtained at different frequencies in the glass transition region. The glass transition temperature T_g was determined for each frequency as the temperature of the half step height of $C_p'(T)$.

Broadband Dielectric Spectroscopy (BDS). Complex dielectric permittivity, $\varepsilon*(\omega) = \varepsilon'(\omega) - i\varepsilon''(\omega)$, values at ambient pressure were measured using the impendance analyzer (Novocontrol Alpha) over a frequency range from 1×10^{-1} to 3×10^{6} Hz. The samples were placed between two stainless-steel electrodes (diameter: 10 mm; gap: 0.05 mm) and mounted inside a cryostat. During the measurement, each sample was maintained under dry nitrogen gas flow. The temperature was controlled by a Quatro Cryosystem using a nitrogen gas cryostat, with stability better than 0.1 K. The temperature-dependent dielectric measurements were performed in the range from 173 to 303 K.

For dielectric measurements at elevated pressure, we used a high-pressure system developed at the Institute of High Pressure Physics of the Polish Academy of Science in Warsaw – UNIPRESS. Thin Teflon spacers were applied to maintain a fixed distance between the plates. The sample capacitor was sealed and mounted inside a Teflon capsule to separate it from the silicon liquid used as a pressure-transmitting medium. The temperature was adjusted with a precision of 0.5 K by means of refrigerated and heating circulator. Complex dielectric permittivity was measured within the same frequency range as in the case of measurements carried out at ambient pressure.

Shear Rheology. The viscosity of PMMS-*g*-nBA and PMMS-*g*-tertBA was determined by means of an ARES G2 Rheometer. The viscosity measurement in the vicinity of liquid-glass transition was performed by means of aluminum parallel plates geometry (diameter = 4 mm). For the oscillation-frequency rheological experiments, the investigated sample was tested in the frequency range from 0.1 to 100 rad/s (12 points per decade) and over the temperature range from $T = 177$–203 K. The frequency dependencies of G'' measured for studied graft and star-graft copolymers are shown in Fig. S11. In the temperature range, where the G'' peaks are not visible, the time-temperature superposition (TTS) rule can be applied to determine the segmental relaxation times, τ_α. According to this criterion, G' and G'' spectra collected at various temperature conditions form the master curve when shifted horizontally by the shift factor, a_T, to superimpose at the chosen reference temperature, see Fig. 6. Therefore, τ_α is determined according to the following equation, $log(\tau_\alpha(T)) = log(\tau(T_{ref})) + log(a_T)$. Note that $\tau(T_{ref})$ indicates the segmental relaxation time calculated by the following equation, $\tau = 1/(2\pi f)$, where f is a frequency of $G''(\omega)$ maximum at chosen T_{ref}. On the other hand, the relaxation time of the slower terminal relaxation, τ_{Rouse}, can be estimated from the crossover of the two straight lines, representing the dependences of $log(G') \approx 2\, log(\omega)$ and $log(G'') \approx log(\omega)$ in the low frequency regime of the master curve (constructed due the time−temperature superposition) by as proposed by Graessley [39].

3. Results and discussion

DSC thermograms recorded for all examined PMMS-based polymer brushes are shown in Fig. 2. As can be seen, aside of the one heat capacity jump (assigned to the glass transition), examined materials undergo no additional phase transitions in the studied range of temperatures. Interestingly, the glass transition temperatures, T_g s,

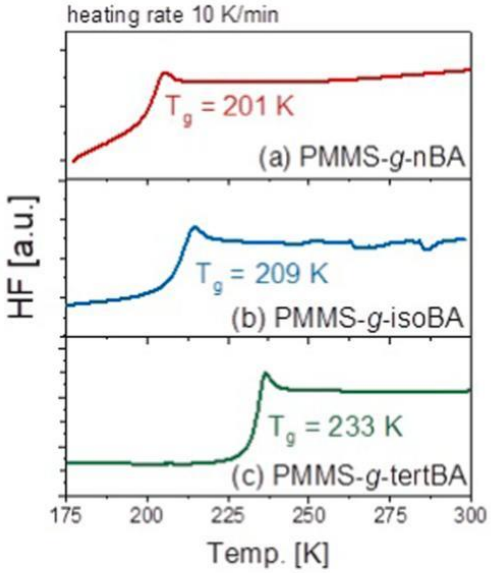

Fig. 2. DSC thermograms of all studied grafted PMMS.

change significantly according to the increased steric hindrance of grafts. Note that T_g increase from $T_g = 201$ K to $T_g = 233$ K for PMMS-*g*-nBA and PMMS-*g*-tertBA, respectively. Values of T_g determined from the calorimetric investigations are listed in Fig. 2 and Table 1. Interestingly, the more hindered branches, the higher glass transition of the polymer. Moreover, it is also worthwhile to comment that all examined grafted systems are characterized by higher T_g with respect to PMMS homopolymer ($T_g = 178$ K [20]). It is quite surprising taking into account that usually associating materials are characterized by higher values of various the phase transitions temperatures when compared to their van der Waals counterparts [40]. Note that homopolymer is capable to form weak *H*-bonds (by thiol moieties); while in the grafted polymers these specific interactions are completely eliminated. Thus, it seems that our data are in contrast to what can be expected. However, in this context, one can refer to the studies on poly(tert-butoxystyrene (PtBOS) polymacromonomers [41], where non-associating materials showed a much higher glass transition temperature ($\Delta T_g = 10$ K), when compared to their macromonomers [41]. The authors attributed an increasing T_g of the grafted polymers to their more constrained structure, which prevents the mobility of grafts. Additionally, also in the case of PDMS-*g*-PDMS, the grafting process was observed to increase T_g [11]. Although this pattern of behavior is not the general rule, as for poly (atactic polypropylene terminated norbornenyl) poly(aPP-NB), T_g is within 3K of that measured for atactic linear polypropylene. Dalsin et al. [15], also concluded that the glass transition temperature of bottle-brushes is, in fact, governed by grafts and not backbone, chemistry nor their molecular weight, M_n. In this context, one can assume that the observed increase in the T_g of the grafted copolymers with respect to the PMMS homopolymer is a result on both (i) the elongation on the graft and (ii) their hindrance, especially considering that thiol units form very weak *H* bonds.

In addition, we also determined the length scale of cooperativity, ζ, and the number of particles involved in correlated motion, N_c. One can recall that in terms of the Adam-Gibbs theory [42], the observed

Table 1
Glass transition temperatures (T_g), the length scale of cooperativity (ξ), the number of particles involved in correlated motion, (N_c), fragility estimated from BDS (m_p) and DSC (m) data, activation energy of γ-process (E_a) and the pressure coefficient of the glass transition temperature (dT_g/dp) determined for all examined materials.

sample	T_g, *DSC* [K]	ζ [nm]	N_c	$T_{g,BDS}$ [K] for $\tau = 100s$	m_p	m	γ-process	dT_g/dp
							E_a [kJ/mol]	
PMMS	178	0.76	107	171	91	113	28	156
PMMS-*g*-nBA	201	0.54	22	197	70	64	46	173
PMMS-*g*-isoBA	209	0.49	17	208	69	55	30	–
PMMS-*g*-tertBA	233	0.59	31	226	76	74	30	233

significant slowing down of supercooled liquid dynamics undergoing the glass transition is connected to the increasing length scale of cooperatively rearranging regions (labeled as ζ) upon cooling. We would like to know how both parameters would change dependently on the graft structure. Taking into account the thermodynamic fluctuation theory, ζ and N_c can be estimated in the glass transition region using Donth equation [43,44]:

$$\zeta^3 = \frac{k_B T_g^2 \Delta\left(C_v^{-1}\right)}{\rho(\delta T)^2} \tag{1}$$

$$N_c = \frac{R T_g^2 \Delta\left(C_v^{-1}\right)}{M(\delta T)^2} \tag{2}$$

where k_B is Bolztman constant, δT is the mean temperature fluctuation, C_v is the isochoric heat capacity, ρ is density, R is molar gas constant and M is molecular mass. Determined values of both parameters are listed in Table 1. As illustrated, the highest values of ζ and N_c were obtained for PMMS homopolymer which most likely result from the formation of hydrogen bonding structure [20,21]. Interestingly, both parameters decrease significantly in the case of examined grafted copolymers. This might confirm the dominant impact of hydrogen bonding on the behavior of PMMS homopolymer, as their removal in the case of grafted copolymers leads to a totally different behavior. One can also add that interestingly, in the case of PMMS-*g*-tertBA, ζ and N_c are slightly higher when compared to the other examined brushes. As one can expect that the presence of *tert*-butyl acrytale (tertBA) group leads to a higher value of the length scale of cooperativity due to an increase steric hindrance.

Subsequently, we have carried out dielectric measurements in a wide temperature range to characterize the molecular dynamics of grafted copolymers at ambient pressure. Fig. 3 presents dielectric loss spectra of PMMS-*g*-nBA and PMMS-*g*-tertBA measured above and below the glass transition temperature T_g, respectively. The reference dielectric loss spectra for PMMS are also shown in the inset to Fig. 3(b). As can be seen for homopolymer, there is a bimodal loss peak consisted of the two relaxation processes (segmental and sub-Rouse) that tend to merge upon approaching the glass transition temperature [20,45]. This fact is well-illustrated in Fig. S5 in the Supporting Information (SI) file, where experimentally measured loss peaks were described using both one and two Havriliak-Negami (HN) functions with an additional term related to the dc conductivity [46]:

$$\varepsilon(\varpi)'' = \frac{\sigma_{dc}}{\varepsilon_0 \varpi} + Im \sum_{i=1}^{2} \left(\varepsilon_\infty + \frac{\Delta\varepsilon_i}{\left[1 + (i\varpi\tau_i)^{\alpha_{HN}}\right]^{\beta_{HN}}} \right) \tag{3}$$

where α_{HN} and β_{HN} are the HN shape parameters related to the sym-

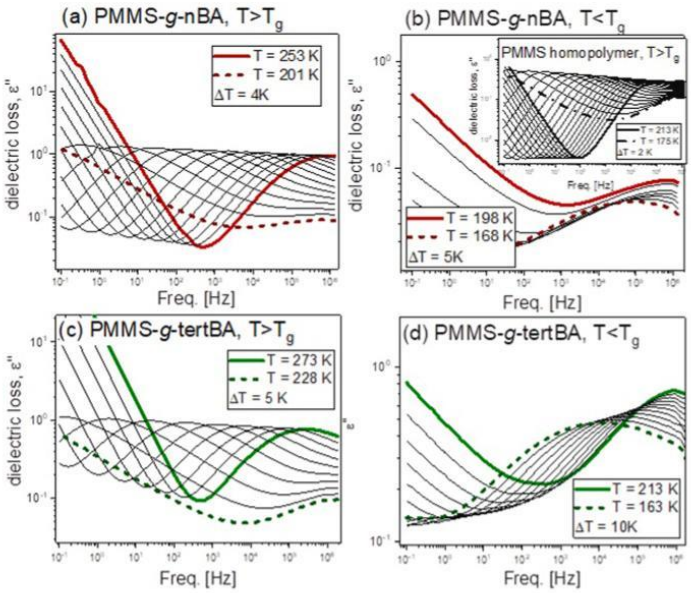

Fig. 3. Dielectric spectra of PMMS-*g*-nBA (a,b) and PMMS-*g*-tertBA (c,d) collected above and below their glass transition temperature. As the inset of panel (a), the dielectric spectra of homopolymer PMMS are presented. Data for PMMS were taken from Ref. [20].

metric and asymmetric broadening of relaxation peaks, $\Delta\varepsilon$ is related to the dielectric strength, τ_{HN} is the HN relaxation time, ε_0 is the vacuum permittivity and ϖ is an angular frequency, where $\varpi = 2\pi f$. As shown, single HN function poorly describes experimental data collected at high temperature regime for PMMS homopolymer indicating the presence of additional relaxation process, see Figs S5(a and c). On the other hand for the all examined grafted copolymers, we can observe a single loss peak above the glass transition temperature, see Fig. 3(a,c).

In Fig. 4, we compared directly the loss peaks characterized by the same segmental relaxation times for the grafted copolymers together with PMMS. This simple comparison clearly indicated that (i) the relaxation processes of examined polymer brushes are monomodal (although quite broad) in contrast to PMMS and interestingly, (ii) the width of the α-loss peaks varies with the change in the steric hindrance of the graft (where the broadest peak can be observed for PMMS-*g*-tertBA (see Fig. 4(b)). Therefore, we assigned the relaxation process recorded for graft copolymers solely to the α-process. Although, it should be mentioned that the width of the loss peaks unexpectedly decreases with lowering temperature, see Flg. S10. Note that the dielectric loss spectra measured at different temperatures, were shifted horizontally to coincide at the maximum. This might suggest that, in fact, the loss peaks of polymer brushes, similarly to PMMS, is consisted of the two relaxation processes whose time scale separation is too small to make it possible to detect them as separated loss peaks. Consequently, similarly to PMMS narrowing of the loss peak might be due to decreasing difference in their relaxation times upon approaching T_g. To find out whether this explanation is correct, we performed additional fitting of the loss peak recorded for the grafted polymers to the single and superposition of the two HN functions, see Figs. S6–S8. Interestingly the quality of the fits in both cases was very good. That means that most likely broad segmental relaxation process of grafted polymers may be inherent feature of these material. Although, we cannot completely reject the possibility of a presence of two processes of similar times scale. Nevertheless, due to very good description of the data with the use of single HN function in this paper, we will present results of this analysis. Additionally, it should be mentioned that all samples reveal the presence of one secondary relaxation, denoted with Greek letter γ, appearing at high frequencies region upon cooling, see Fig. 3(b,d).

To get better insight into the molecular dynamics of the grafted polymers, we further analyzed the temperature evolution of the relaxation times, τ, for the all observed processes. Both τ_α and τ_γ were estimated from the fitting loss spectra obtained above and below T_g to the HN function (Eq. (3)). Determined values of α- and γ-relaxation times plotted as a function of $1/T$ for all the investigated sample are presented in Fig. 5(a). In addition, we also carried out a series of temperature-modulated TM-DSC measurements to determine the value of τ_α near T_g. As found, the dielectric relaxation times agree well with the relaxation times from TM-DSC measurements suggesting that τ_α is the segmental relaxation associated with the glass transition. Due to a pronounced differences in T_g s between examined materials, additionally, all determined relaxation times were plotted versus T_g/T to visualize potential difference in their temperature evolutions, see Fig. 5(b). Note that the glass transition temperature, T_g, was defined as the temperature at which $\tau_\alpha = 100$s. As illustrated, one can see some differences in both τ_α and τ_γ between all examined materials. To quantify the difference in the steepness of $\tau_\alpha(T_g/T)$, we calculated the fragility parameter, m_p, defining sensitivity of the structural/segmental relaxation times upon cooling:

$$m_p = \left[\frac{d\log\tau_\alpha}{d(T_g/T)}\right]_{T=T_g} \tag{4}$$

Note that the fragility parameter typically changes in the range $m_p = 16 - 200$ for various materials, whereas those characterized by low and high m_p are considered as strong and fragile systems, respectively. Interestingly, m_p determined for grafted copolymers are very similar and varies between 69 and 72 (Table 1), which indicates that the examined materials might be categorized as strong. One can add that similar values of the fragility were determined from calorimetric data, m, which also change in the range 55–74 (Table 1). Note that the m parameter was estimated according to the procedure reported in Refs. [35–38].

Furthermore, in the case of the temperature evolution of the γ-relaxation times, one can see that although, $\tau_\gamma(T_g/T)$ of PMMS and PMMS-*g*-isoBA collapses almost perfectly onto each other; while, some notable discrepancies can be found for the other two systems. That means that variation in the steric hindrance of the side group has quite significant impact on the dynamics of this local mobility. Therefore, we calculated the activation barrier, E_a, from the fitting of τ_γ $(1/T)$ to the Arrhenius equation:

$$\tau = \tau_\infty \exp\left(\frac{E_a}{k_B T}\right) \tag{5}$$

where τ_∞ is the high temperature limit of the relaxation rate. Values of calculated E_a are listed in Table 1. All examined systems are characterized by comparable values of the activation barrier; however, one can see that the highest E_a of the local motions was determined for the least constrained graft copolymer, PMMS-*g*-nBA (see Table 1).

Complementary, we have performed also rheological measurements. Master curves of the measured storage, G', and loss, G'', modulus of examined PMMS-*g*-nBA and PMMS-*g*-tertBA are shown in Fig. 6. Note that as the inset in Fig. 6(a), we shown the mechanical data for PMMS homopolymer. The presented master curve was constructed from the

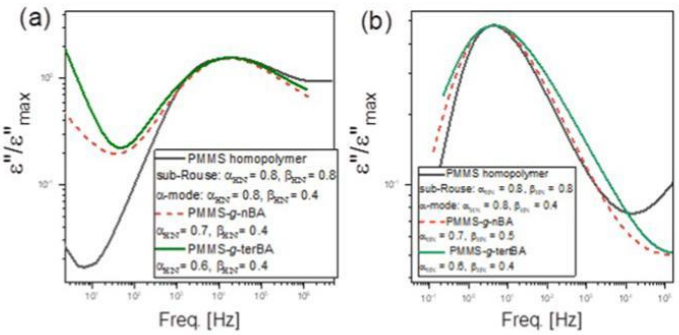

Fig. 4. Comparison of the distribution of relaxation times obtained at constant τ_α for all examined materials.

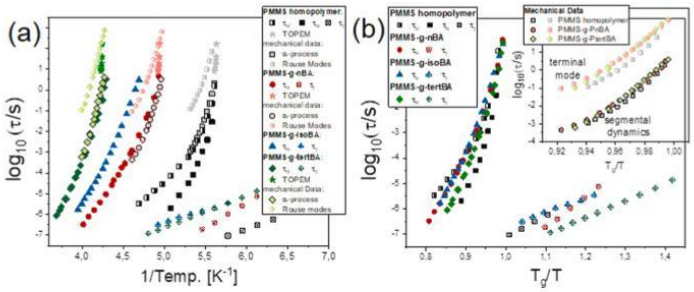

Fig. 5. Relaxation Times plotted as a function of $1/T$ (a) and T_g/T (b). As the inset in panel (b), segmental, τ_α, and terminal, τ_{Rouse}, relaxation times determined from the mechanical measurements are plotted as a function of T_g/T.

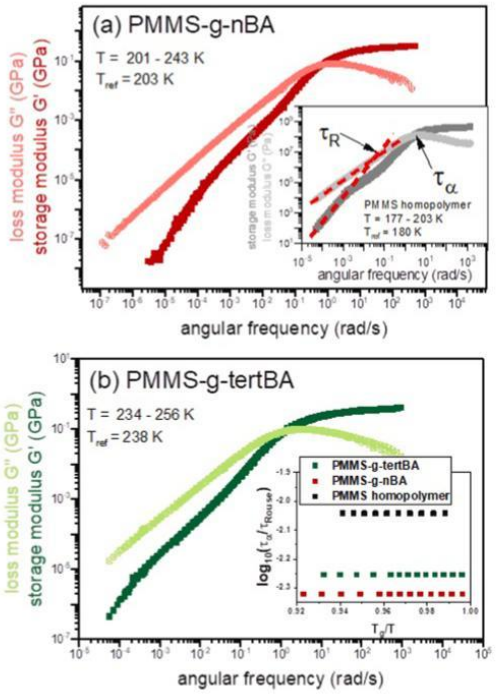

Fig. 6. Master curves of measured storage, G', and loss, G'', modulus of examined (a) PMMS-*g*-nBA and (b) PMMS-*g*-tertBA. As the inset in panel (a), master curves of G' and G'' of PMMS homopolymer is shown. In panel (b), the log $(\tau_\alpha/\tau_{Rouse})$ vs. T_g/T is presented.

frequency dependence of G' and G'' measured in the range 0.1–100 rad/s at different temperatures (see Fig. S10), which were shifted horizontally by the shift factor, α_T, to superimpose measured spectra with one obtained at the chosen reference temperatures, T_{ref}. As can be seen, two processes can be detected, attributed to (i) segmental motion (manifested as maximum at higher frequency), and (ii) terminal relaxation motion (Rouse mode; manifested as a shoulder at lower frequency), respectively. Both of them are separated by ~2 orders of magnitude on the time scale for all examined systems. One can recall that similar rheological results were reported for both linear homopolymers [22,47] and a series of bottlebrushes, i.e., PBiBEM-g-PBA [13] and polybutadiene-based multiarms star polymers [48]. Note that often for heavily grafted copolymers, an additional process appears at the intermediate frequency regime reflecting the relaxation of grafts [15,17–19,49]. In case of our study, we do not see such a process most likely due to low molecular weight of examined materials.

The obtained values of segmental, τ_α, and Rouse, τ_{Rouse}, relaxation times were added to Fig. 5. Details regarding the determination of τ_α and τ_{Rouse} are given in the **Experimental section**. It can be clearly seen that τ_α determined by mechanical studies agree with the values obtained with previously applied techniques. This behavior supports the previous analysis of the dielectric loss spectra with the use of one HN function (see Figs. S6–S8) and confirms that the broad segmental relaxation process of grafted copolymers might be inherent feature of these materials. In contrast, the Rouse mode are shifted by ~2 orders towards lower frequencies for all examined samples. Although, one can see that the difference in the timescale between segmental and Rouse mode is higher for graft copolymers when compared to PMMS homopolymer, see the inset in Fig. 5(b). Moreover, when we compare the loss modulus, G'', spectra with the dielectric loss, ε'', near T_g, one can see that the α-peak recorded in mechanical measurements has much different shape (narrower) than the one detected in dielectric spectra (Fig. S12). Note that the difference between both relaxations increases with a steric hindrance of the graft, as for PMMS-*g*-tertBA, the dielectric α-mode is significantly broader than mechanical one when compared to PMMS-*g*-PnBA. This might imply that indeed, there is an additional process present in examined grafted copolymers as previously reported for PMMS homopolymer, although both of those processes have similar times scale.

Finally, we have carried out high-pressure dielectric measurements at various thermodynamic (T,p) conditions. In Fig. 7(a, c, e), we presented the representative dielectric loss spectra of homopolymer PMMS, PMMS-*g*-nBA and PMMS-*g*-tertBA, collected at various isobaric and isothermal conditions. As can be seen for all materials, the loss peak shifts towards a lower frequency upon both compression and cooling. Note that as the performed dielectric and calorimetric measurements shows the greatest differences between PMMS-g-nBA and PMMS-g-tertBA, further studies focused solely on those two materials in comparison to the homopolymer. The high-pressure data for PMMS homopolymer were taken from Ref. [45]. Moreover, similarly to the data obtained at ambient pressure, the bimodal loss peak observed form PMMS merge when approaching T_g also at the elevated pressures. This indicates a similar sensitivity of both processes (α and sub-Rouse) to the variation in temperature and pressure. Interestingly, we found that the distribution of the relaxation times of the segmental process remains constant with compression for all examined materials (Fig. 7(b, d, f)). Note that the high-pressure dielectric spectra measured at various

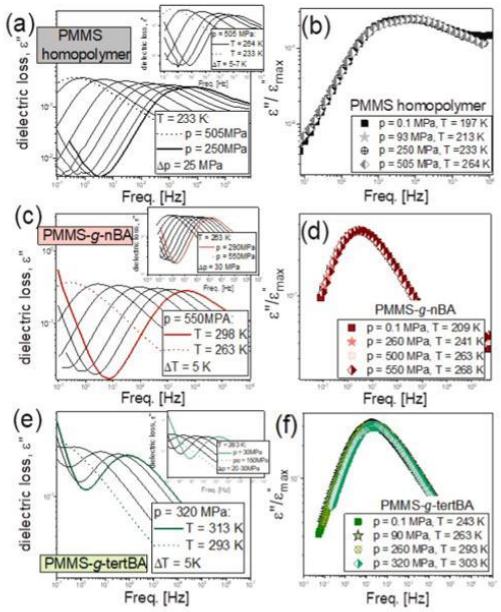

Fig. 7. (a, c, e) Dielectric loss spectra measured at various isobaric conditions. At the insets, dielectric loss spectra measured different isothermal conditions are shown. (b, d, f) Comparison the loss spectra obtained at various thermodynamic conditions that were characterized by the same τ_α.

thermodynamic conditions were shifted vertically to superpose at constant τ_α. This suggests that the shape of the α-loss peak depends on the structural/segmental relaxation time and are not affected by varying T and p conditions, fulfilling the Time-Temperature-Pressure (TPS) rule independently to the chemical structure of grafted copolymers. Similar observation was made for other polymers [50].

Fig. 8 shows the temperature and pressure evolution of τ_α. Note that, the dielectric data obtained at high-pressure conditions were analyzed in the same manner as those recorded at ambient pressure. Furthermore, we calculated the pressure coefficient of the glass transition temperature, d T_g/dp, to parametrize pressure sensitivity of the glass transition temperature examined grafted copolymers. For this purpose, the Avramov model [51] was used to describe the pressure and temperature dependence of the segmental relaxation times. Details regarding the analysis are presented in **the SI file**. The results of fitting $\tau_\alpha(T,p)$ dependencies to the Avramov equation are depicted in Fig. 9, whereas the fit parameters are listed in Table S1. It should be noted that the obtained fits are of very high quality since $R^2 \sim 0.999$ and $R^2 \sim 0.988$ for PMMS-*g*-nBA and PMMS-*g*-tertBA, respectively. After fitting of $\tau_\alpha(T,p)$ shown in Fig. 9, T_g was calculated at different pressures, and consequently the pressure coefficient of the glass transition in the limit of ambient pressure was determined using the pressure derivative of the following equation [52]:

$$T_g(p) = T_g(p_0)\left(1+\frac{p}{\Pi}\right)^{\beta/\alpha(p)} \tag{6}$$

and

$$\alpha(p) = \alpha_0\left(1-\frac{C}{C_{p_0}}\left(\ln\left(1+\frac{p}{\Pi}\right)\right)\right) \tag{7}$$

where Π is a constant with the dimension of pressure, C_{p_0} is a specific heat capacity, α_p is a volume expansion coefficient at ambient p, α_0 and β are exponential parameters (details in **the SI file**). Finally, we obtained that the pressure coefficient of the glass transition temperature, dT_g/dp, is equal to 173.16 K/GPa and 233.48 K/GPa for PMMS-*g*-nBA and PMMS-*g*-tertBA, respectively (see Table 1 and Fig. 10(a)). These values are significantly higher than the one determined for the PMMS homopolymer ($dT_g/dp = 155.97$ K/GPa). Note that for the homopolymer, this value was assumed to be closely related to the presence of thiol molecules capable of forming hydrogen bonds, which had a great impact on the dynamics of the segmental process and dT_g/dp. In grafted polymers, due to the attachment of more and more branched substituents to the

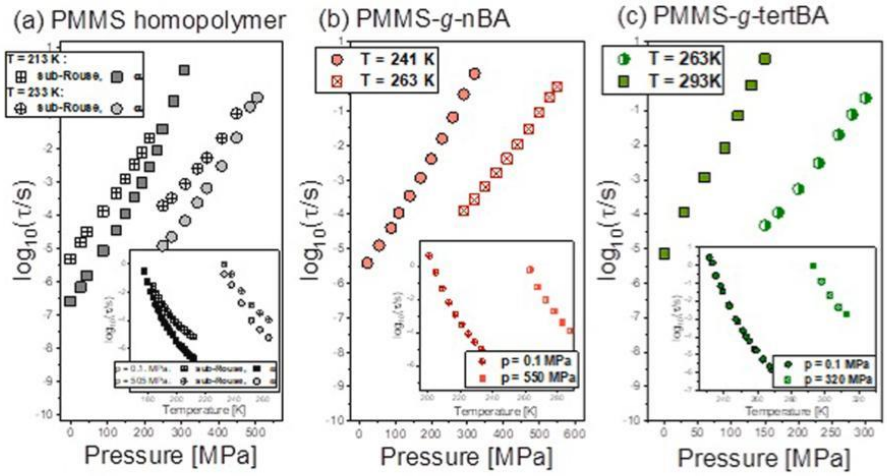

Fig. 8. Temperature and pressure dependences of τ_α obtained during isobaric and isothermal measurements for PMMS and examined grafted copolymers. Note that data for $\tau_{sub-Rouse}$ of PMMS homopolymer were taken from Ref. [45].

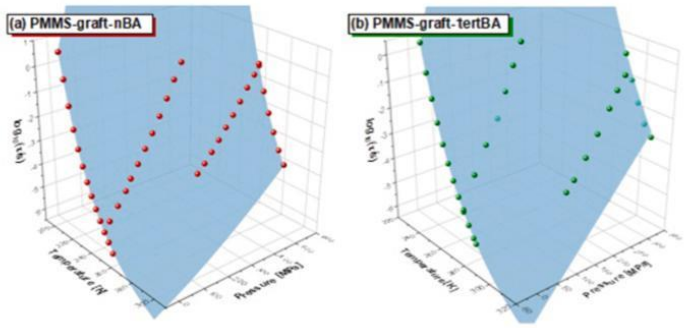

Fig. 9. Segmental relaxation times plotted versus temperature and pressure for PMMS-*g*-nBA and PMMS-*g*-tertBA. Blue areas represent surface fits to the modified Avramov equation (Eq. (S1)). (For interpretation of the references to colour in this figure legend, the reader is referred to the Web version of this article.)

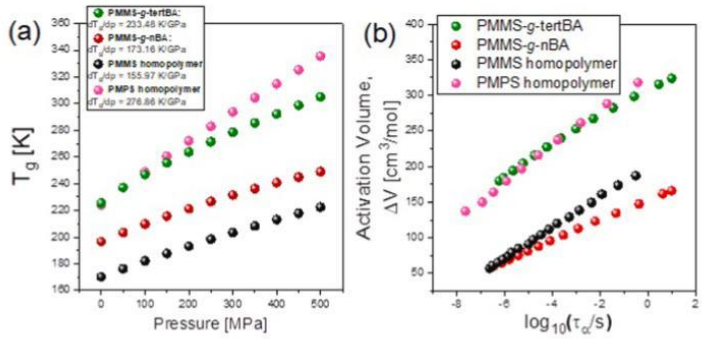

Fig. 10. (a) The pressure dependence of the glass transition temperature determined from the Avramow equation (eq. (5)) for indicated materials. (b) The activation volume (ΔV) obtained for the segmental mode plotted versus τ_α for PMMS, PMPS and two examined grafted copolymers.

side chain (as in the case of PMMS-*g*-tertBA) leading to the elimination of the *H* bonds the values of dT_g/dp are much higher than in the case of homopolymer. However, the values are still low compared to silyl derivatives of low-molecular-weight vitreous substances, which have the highest dT_g/dp of all liquids. It is worth noting that also the $dT_g/\ dp$ for polystyrene was 306–294 K/GPa [50,53,54], depending on the molecular weight. On the other hand, for PMPS homopolymer, $dT_g/\ dp = 250$ K/GPa, similarly to the one determined for the polymer grafted with tertBA groups. Therefore, the pressure coefficient of T_g in the examined herein grafted polymers seems to be very low with respect to that determined for the other polymers.

Furthermore, the activation volume, ΔV, in the ambient pressure limit for the segmental process was calculated and compared with the values determined for PMMS and PMPS homopolymers. In terms of the transition state theory, ΔV is a difference of volume between activated and standard state, and is calculated according to the following definition:

$$\Delta V = RT\ ln(10)\left(\frac{d\ log_{10}\tau_\alpha}{dp}\right)_T, \tag{8}$$

Note that to estimate ΔV under different thermodynamic conditions, the Avramow fit parameters were used (Table S1). The determined activation volumes plotted as a function of the segmental relaxation times are shown in Fig. 10(b). As illustrated, ΔV of PMMS-*g*-tertBA is much larger when compared to the one of PMMS homopolymer and, interestingly, is similar to the activation volume of PMPS. In contrast, for PMMS-*g*-nBA, ΔV is only slightly larger than the ΔV of PMMS. The results are quite unexpected since we did not see any regularity in the variation of this parameter with the size of the monomer/graft etc. In this context, it should be mentioned that generally there is correlation between activation volume and the size of the segment for the investigated polymer [11]. One can suppose that the this behaviour could be connected to the chemical structure of grafts (especially their an increasing steric hindrance) in the examined copolymers. However, this issue must be verified in the future.

4. Conclusion

In the present work, we investigated the molecular dynamics of three different PMMS-based oligomeric brushes under various thermodynamic conditions. Interestingly, it was shown that the glass transition temperature and the length scale of cooperativity rearranging regions are strongly affected by a graft structure. Dielectric studies combined with results from mechanical tests confirm that the broad segmental relaxation process of grafted copolymers may be an inherent feature of these materials. Pressure tests showed that the distribution of relaxation times of the segmental process remains constant with pressure for all materials tested. In addition, it was found that the pressure coefficient of

the glass transition determined for grafted polymers are significantly higher than for the homopolymer, due to the increasing steric hindrance coming from the grafted side groups, which limit the ability to form hydrogen bonds. The data presented in this paper clearly highlight the important role of high-pressure experiments in elucidating the effect of graft structure on the behavior of local mobility dynamics. We believe that the presented herein data allow better understanding of the impact of topology on the dynamics of polymers and further developing the correlation between the structure, architecture and properties of great importance in the context of further development of new generation of polymeric materials.

Notes

The authors declare no competing financial interests.

CRediT authorship contribution statement

Sara Zimny: Investigation, Formal analysis, Visualization, Writing – original draft. **Magdalena Tarnacka:** Formal analysis, Writing – review & editing, Funding acquisition. **Zaneta Wojnarowska:** Investigation. **Dawid Heczko:** Investigation, Funding acquisition. **Paulina Maksym:** Investigation. **Marian Paluch:** Supervision. **Kamil Kamiński:** Conceptualization, Methodology, Supervision, Writing – review & editing.

Declaration of competing interest

The authors declare the following financial interests/personal relationships which may be considered as potential competing interests: Magdalena Tarnacka reports financial support was provided by Polish National Science Centre.

Data availability

Data will be made available on request.

Acknowledgment

M.T. and K.K. are thankful for financial support from the Polish National Science Centre within the OPUS project (Dec. no 2019/33/B/ST3/00500). D. H. is thankful for financial support from Medical University of Silesia within Research for Young Scientists (Contract No. PCN-2-059/N/0/F).

Appendix A. Supplementary data

Supplementary data to this article can be found online at https://doi.org/10.1016/j.polymer.2023.125790.

References

[1] Z. Li, M. Tang, S. Liang, M. Zhang, G.M. Biesold, Y. He, S.M. Hao, W. Choi, Y. Liu, J. Peng, Z. Lin, Bottlebrush polymers: from controlled synthesis, self-assembly, properties to applications, Prog Polym Sci 116 (2021), 101387, https://doi.org/10.1016/j.progpolymsci.2021.101387.
[2] M. Müllner, Molecular polymer brushes in nanomedicine, Macromol Chem Phys 217 (2016) 2209–2222, https://doi.org/10.1002/macp.201600086.
[3] T.A. Saleh, Polymer science and polymerization methods toward hybrid materials, in: Polymer Hybrid Materials and Nanocomposites, William Andrew Publishing, 2021, pp. 59–103, https://doi.org/10.1016/b978-0-12-813294-4.00004-2.
[4] D. Neugebauer, Two decades of molecular brushes by ATRP, Polymer (Guildf) 72 (2015) 413–421, https://doi.org/10.1016/j.polymer.2015.02.054.
[5] C. Hagiopol, Copolymers, in: Reference Module in Materials Science and Materials Engineering, Elsevier, 2016, https://doi.org/10.1016/B978-0-12-803581-8.01126-7.
[6] H. Lee, J. Pietrasik, S.S. Sheiko, K. Matyjaszewski, Stimuli-responsive molecular brushes, Prog Polym Sci 35 (2010) 24–44, https://doi.org/10.1016/j.progpolymsci.2009.11.002.
[7] M. Abbasi, L. Faust, M. Wilhelm, Comb and bottlebrush polymers with superior rheological and mechanical properties, Advanced Materials 31 (2019), 1806484, https://doi.org/10.1002/adma.201806484.
[8] S.S. Sheiko, B.S. Sumerlin, K. Matyjaszewski, Cylindrical molecular brushes: synthesis, characterization, and properties, Prog Polym Sci 33 (2008) 759–785, https://doi.org/10.1016/j.progpolymsci.2008.05.001.
[9] A. Jourdain, A. Serghei, E. Drockenmuller, Enhanced ionic conductivity of a 1,2,3-triazolium-based poly(siloxane ionic liquid) homopolymer, ACS Macro Lett 5 (2016) 1283–1286, https://doi.org/10.1021/acsmacrolett.6b00761.
[10] P. Maksym, M. Tarnacka, R. Bielas, B. Hachuła, A. Zajac, A. Szpecht, M. Smiglak, K. Kaminski, M. Paluch, Structure-property relationships of tailored imidazolium- and pyrrolidinium-based poly(ionic liquid)s. Solid-like vs. gel-like systems, Polymer (Guildf) 192 (2020), 122262, https://doi.org/10.1016/j.polymer.2020.122262.
[11] B. Jakobi, K.J. Bichler, A. Sokolova, G.J. Schneider, Dynamics of PDMS- g -PDMS bottlebrush polymers by broadband dielectric spectroscopy, Macromolecules 53 (2020) 8450–8458, https://doi.org/10.1021/acs.macromol.0c01277.
[12] M. Staropoli, A. Raba, C.H. Hövelmann, M.-S. Appavou, J. Allgaier, M. Krutyeva, W. Pyckhout-Hintzen, A. Wischnewski, D. Richter, Melt dynamics of supramolecular comb polymers: viscoelastic and dielectric response, J Rheol (N Y N Y). 61 (2017) 1185–1196, https://doi.org/10.1122/1.5001059.
[13] C. Grigoriadis, A. Nese, K. Matyjaszewski, T. Pakula, H.-J. Butt, G. Floudas, Dynamic homogeneity by architectural design - bottlebrush polymers, Macromol Chem Phys 213 (2012) 1311–1320, https://doi.org/10.1002/macp.201200064.
[14] C. Nikovia, L. Theodoridis, S. Alexandris, P. Bilalis, N. Hadjichristidis, G. Floudas, M. Pitsikalis, Macromolecular brushes by combination of ring-opening and ring-opening metathesis polymerization. Synthesis, self-assembly, thermodynamics, and dynamics, Macromolecules 51 (2018) 8940–8955, https://doi.org/10.1021/acs.macromol.8b01905.
[15] S.J. Dalsin, M.A. Hillmyer, F.S. Bates, Molecular weight dependence of zero-shear viscosity in atactic polypropylene bottlebrush polymers, ACS Macro Lett 3 (2014) 423–427, https://doi.org/10.1021/mz500082h.
[16] M. Abbasi, L. Faust, K. Riazi, M. Wilhelm, Linear and extensional rheology of model branched polystyrenes: from loosely grafted combs to bottlebrushes, Macromolecules 50 (2017) 5964–5977, https://doi.org/10.1021/acs.macromol.7b01034.
[17] I.N. Haugan, M.J. Maher, A.B. Chang, T.P. Lin, R.H. Grubbs, M.A. Hillmyer, F. S. Bates, Consequences of grafting density on the linear viscoelastic behavior of graft polymers, ACS Macro Lett 7 (2018) 525–530, https://doi.org/10.1021/acsmacrolett.8b00116.
[18] M. Kempf, D. Ahirwal, M. Cziep, M. Wilhelm, Synthesis and linear and nonlinear melt rheology of well-defined comb architectures of PS and PpMS with a low and controlled degree of long-chain branching, Macromolecules 46 (2013) 4978–4994, https://doi.org/10.1021/ma302033g.
[19] M. Hu, Y. Xia, G.B. McKenna, J.A. Kornfield, R.H. Grubbs, Linear rheological response of a series of densely branched brush polymers, Macromolecules 44 (2011) 6935–6943, https://doi.org/10.1021/ma2009673.
[20] M. Tarnacka, K. Jurkiewicz, B. Hachuła, Z. Wojnarowska, R. Wrzalik, R. Bielas, A. Talik, P. Maksym, K. Kaminski, M. Paluch, Correlation between locally ordered (hydrogen-bonded) nanodomains and puzzling dynamics of polymethysiloxane derivative, Macromolecules 53 (2020) 10225–10233, https://doi.org/10.1021/acs.macromol.0c01289.
[21] J. Paturej, K. Koperwas, M. Tarnacka, K. Jurkiewicz, P. Maksym, J. Grelska, M. Paluch, K. Kamiński, Supramolecular structures of self-assembled oligomers under confinement, Soft Matter 18 (2022) 4930–4936, https://doi.org/10.1039/D2SM00343K.
[22] K. Xing, M. Tress, P. Cao, S. Cheng, T. Saito, V.N. Novikov, A.P. Sokolov, Hydrogen-bond strength changes network dynamics in associating telechelic PDMS, Soft Matter 14 (2018) 1235–1246, https://doi.org/10.1039/c7sm01805c.
[23] M. Tress, K. Xing, S. Ge, P. Cao, T. Saito, A. Sokolov, What dielectric spectroscopy can tell us about supramolecular networks, European Physical Journal E 42 (2019), https://doi.org/10.1140/epje/i2019-11897-4.
[24] S. Ge, M. Tress, K. Xing, P.-F. Cao, T. Saito, A.P. Sokolov, Viscoelasticity in associating oligomers and polymers: experimental test of the bond lifetime renormalization model, Soft Matter 16 (2020) 390–401, https://doi.org/10.1039/C9SM01930H.
[25] R.P. White, J.E.G. Lipson, Explaining the T , V -dependent dynamics of glass forming liquids: the cooperative free volume model tested against new simulation results, J Chem Phys 147 (2017), 184503, https://doi.org/10.1063/1.5001714.
[26] R.P. White, J.E.G. Lipson, The cooperative free volume rate model for segmental dynamics: application to glass-forming liquids and connections with the density scaling approach, The European Physical Journal E 42 (2019) 100, https://doi.org/10.1140/epje/i2019-11862-3.
[27] R.P. White, J.E.G. Lipson, Connecting pressure-dependent dynamics to dynamics under confinement: the cooperative free volume model applied to poly(4-chlorostyrene) bulk and thin films, Macromolecules 51 (2018) 7924–7941, https://doi.org/10.1021/acs.macromol.8b01392.
[28] K. Adrjanowicz, K. Kaminski, K. Koperwas, M. Paluch, Negative pressure vitrification of the isochorically confined liquid in nanopores, Phys Rev Lett 115 (2015) 1–5, https://doi.org/10.1103/PhysRevLett.115.265702.
[29] K. Adrjanowicz, K. Kaminski, M. Tarnacka, G. Szklarz, M. Paluch, Predicting nanoscale dynamics of a glass-forming liquid from its macroscopic bulk behavior and vice versa, J Phys Chem Lett 8 (2017) 696–702, https://doi.org/10.1021/acs.jpclett.6b02974.
[30] A. Talik, M. Tarnacka, M. Geppert-Rybczynska, A. Minecka, E. Kaminska, K. Kaminski, M. Paluch, Impact of the interfacial energy and density fluctuations

on the shift of the glass-transition temperature of liquids confined in pores, The Journal of Physical Chemistry C 123 (2019) 5549–5556, https://doi.org/10.1021/acs.jpcc.8b12551.
[31] R. Casalini, C.M. Roland, Thermodynamical scaling of the glass transition dynamics, Phys Rev E 69 (2004), 062501, https://doi.org/10.1103/PhysRevE.69.062501.
[32] M. Naoki, H. Endou, K. Matsumoto, Pressure effects on dielectric relaxation of supercooled o-terphenyl, Journal of Physical Chemistry 91 (1987) 4169–4174, https://doi.org/10.1021/j100299a044.
[33] C.M. Roland, R. Casalini, P. Santangelo, M. Sekula, J. Ziolo, M. Paluch, Chemical structure and local segmental dynamics in 1,2-polybutadiene, Macromolecules 36 (2003) 4954–4959, https://doi.org/10.1021/ma034416j.
[34] D.M. Duarte, W. Tu, A. Dzienia, K. Adrjanowicz, Study on the effect of side-chain group on the segmental dynamics of selected methacrylate polymers at ambient and high pressures, Polymer (Guildf) 183 (2019), 121860, https://doi.org/10.1016/j.polymer.2019.121860.
[35] S. Gao, Y.P. Koh, S.L. Simon, Calorimetric glass transition of single polystyrene ultrathin films, Macromolecules 46 (2013) 562–570, https://doi.org/10.1021/ma3020036.
[36] P. Badrinarayanan, S.L. Simon, Origin of the divergence of the timescales for volume and enthalpy recovery, Polymer (Guildf) 48 (2007) 1464–1470, https://doi.org/10.1016/j.polymer.2007.01.064.
[37] J. Shen, E. Yildirim, S. Li, Y. Caydamli, M.A. Pasquinelli, A.E. Tonelli, Role of local polymer conformations on the diverging glass transition temperatures and dynamic fragilities of isotactic-, syndiotactic-, and atactic-poly(methyl methacrylate)s, Macromolecules (2019), https://doi.org/10.1021/acs.macromol.9b00434.
[38] L.M. Wang, V. Velikov, C.A. Angell, Direct determination of kinetic fragility indices of glassforming liquids by differential scanning calorimetry: kinetic versus thermodynamic fragilities, Journal of Chemical Physics 117 (2002) 10184–10192, https://doi.org/10.1063/1.1517607.
[39] W.W. Graessley, The entanglement concept in polymer rheology, in: The Entanglement Concept in Polymer Rheology, Springer-Verlag, Berlin/Heidelberg, n.d.: pp. 1–179. https://doi.org/10.1007/BFb0031037.
[40] C.L. Lewis, K. Stewart, M. Anthamatten, The influence of hydrogen bonding side-groups on viscoelastic behavior of linear and network polymers, Macromolecules 47 (2014) 729–740, https://doi.org/10.1021/ma402368s.
[41] G.v. Theodosopoulos, S.-L. Bitsi, M. Pitsikalis, Complex brush-like macromolecular architectures via anionic and ring opening metathesis polymerization: synthesis, characterization, and thermal properties, Macromol Chem Phys 219 (2018), 1700253, https://doi.org/10.1002/macp.201700253.
[42] J.H. Gibbs, G. Adam, On the temperature dependence of cooperative relaxation properties in glass-forming liquids, J Chem Phys 43 (1965) 139–146.
[43] E. Donth, Characteristic length of the glass transition, J Polym Sci B Polym Phys 34 (1996) 2881–2892, https://doi.org/10.1002/(SICI)1099-0488(199612)34:17<2881::AID-POLB3>3.0.CO;2-U.
[44] E.-J. Donth, The Glass Transition, Springer Berlin Heidelberg, Berlin, Heidelberg, 2001, https://doi.org/10.1007/978-3-662-04365-3.
[45] S. Zimny, M. Tarnacka, E. Kamińska, R. Wrzalik, K. Adrjanowicz, M. Paluch, K. Kamiński, Studies on the molecular dynamics at high pressures as a key to identify the sub-rouse mode in PMMS, Macromolecules 55 (2022) 5581–5590, https://doi.org/10.1021/acs.macromol.2c00378.
[46] S. Havriliak, S. Negami, A complex plane representation of dielectric and mechanical relaxation processes in some polymers, Polymer (Guildf) 8 (1967) 161–210, https://doi.org/10.1016/0032-3861(67)90021-3.
[47] K. Xing, S. Chatterjee, T. Saito, C. Gainaru, A.P. Sokolov, Impact of hydrogen bonding on dynamics of hydroxyl-terminated polydimethylsiloxane, Macromolecules 49 (2016) 3138–3147, https://doi.org/10.1021/acs.macromol.6b00262.
[48] T. Pakula, D. Vlassopoulos, G. Fytas, J. Roovers, Structure and dynamics of melts of multiarm polymer stars, Macromolecules 31 (1998) 8931–8940, https://doi.org/10.1021/ma981043r.
[49] F. Abbasi, H. Mirzadeh, A.A. Katbab, Modification of polysiloxane polymers for biomedical applications: a review, Polym Int 50 (2001) 1279–1287, https://doi.org/10.1002/pi.783.
[50] C.M. Roland, S. Hensel-Bielowka, M. Paluch, R. Casalini, Supercooled dynamics of glass-forming liquids and polymers under hydrostatic pressure, Reports on Progress in Physics 68 (2005) 1405–1478, https://doi.org/10.1088/0034-4885/68/6/R03.
[51] I. Avramov, Pressure dependence of viscosity of glassforming melts, J Non Cryst Solids 262 (2000) 258–263, https://doi.org/10.1016/S0022-3093(99)00712-7.
[52] I. Avramov, Pressure and temperature dependence of viscosity of glassforming and of geoscientifically relevant systems, Journal of Volcanology and Geothermal Research 160 (2007) 165–174, https://doi.org/10.1016/j.jvolgeores.2006.09.006.
[53] G.A. Schwartz, J. Colmenero, Á. Alegría, Dielectric study of the segmental relaxation of low and high molecular weight polystyrenes under hydrostatic pressure, J Non Cryst Solids 353 (2007) 4298–4302, https://doi.org/10.1016/j.jnoncrysol.2007.02.070.
[54] V.A. Harmandaris, G. Floudas, K. Kremer, Temperature and pressure dependence of polystyrene dynamics through molecular dynamics simulations and experiments, Macromolecules 44 (2011) 393–402, https://doi.org/10.1021/ma102179b.

A3. Influence of Graft Rigidity on the Dynamical Behavior of PMMS-Based Polymer Brushes at Ambient and High Pressure.

AUTORZY: S. Zimny, M. Tarnacka, P. Maksym, Ż. Wojnarowska, M. Paluch, K. Kamiński.

REFERENCJA: Macromolecules, 2024, 57 (22), 10754-10766.

DOI: 10.1021/acs.macromol.4c01779

Impact Factor czasopisma z roku opublikowania: 5.1

Liczba punktów ministerialnych MNiSW czasopisma (2024): 140

Mój udział w pracy polegał na przygotowaniu próbek, wykonaniu pomiarów dielektrycznych i analizie otrzymanych wyników, współtworzeniu manuskryptu (przeprowadzenie przeglądu literaturowego, przygotowanie tekstu manuskryptu i rysunków, opis wyników i sformułowanie wniosków), formułowaniu odpowiedzi na uwagi recenzentów oraz korekcie manuskryptu po otrzymanych recenzjach.

Macromolecules

pubs.acs.org/Macromolecules Article

The Influence of Graft Rigidity on the Dynamical Behavior of PMMS-Based Polymer Brushes at Ambient and High Pressures

Sara Zimny, Magdalena Tarnacka,* Paulina Maksym, Żaneta Wojnarowska, Marian Paluch, and Kamil Kamiński

Cite This: *Macromolecules* 2024, 57, 10754−10766 Read Online

ACCESS | Metrics & More | Article Recommendations | Supporting Information

ABSTRACT: In this paper, we investigated the molecular dynamics of polymer brushes based on poly(mercaptopropyl)-methylsiloxane (PMMS), in which the thiol group was grafted with different homologous flexible acrylates (acrylate-based PMMS copolymers) and more rigid methacrylate (methacrylate-based PMMS copolymers) monomers of varying lengths of alkyl chain under ambient and elevated pressure conditions. It was found that the glass transition temperature, T_g, of PMMS homopolymer is significantly lower compared to the other systems. Moreover, surprisingly, in the methacrylate-grafted copolymers, there are two relaxation processes (α and α'), while in the systems grafted with various acrylates, only a single process is present in the supercooled phase. Complementary rheological investigations indicated that the faster α process comes from the segmental motions, while α' is not detected in the mechanical response. Further high-pressure experiments showed that there is a superposition between segmental and α' modes irrespective of applied pressure, p, in methacrylate-based PMMS copolymers. This result suggests that the latter process might be considered as a sub-Rouse mode, or alternatively, it may originate from the dielectric active relaxation of the rigid polar side chain (grafts). Moreover, analysis of the high-pressure data allowed us to estimate the pressure coefficient of the glass transition temperature, dT_g/dp, which was much higher for polymer brushes with respect to the PMMS homopolymer. Interestingly, the values of dT_g/dp for methacrylate-grafted copolymers are slightly higher compared to acrylate-based PMMS copolymers, which may be due to the different flexibility/rigidity of both groups of materials as all examined materials have the same degree of polymerization of homopolymer backbone ($N_{bb} \sim 12$) and side chain ($N_{sc} = 1$). However, for both groups of studied systems, dT_g/dp values did not scale with chain length. This unexpected result must be related to the structure of the studied grafted copolymers and the character of grafts, derivatives of acrylates/methacrylates. The data presented here extend our knowledge of the influence of the architecture of different molecules on the dynamics of polymers at ambient and high pressures.

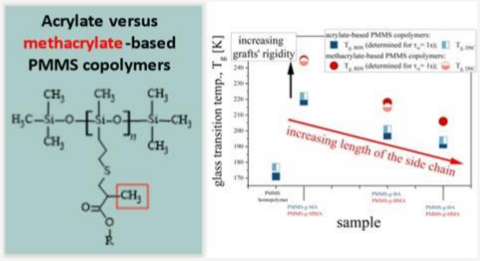

I. INTRODUCTION

Today, polymers constitute a significant group of compounds that are finding an increasing number of applications in many different fields, replacing traditional materials. They are used as lubricants,[1] solvent-free elastomers,[2] surface modifiers,[3] in photonic crystals,[4] as membranes for batteries,[5] in lithography,[6] or as drug delivery agents.[7,8] This substantial expansion takes its source from their properties, which can be easily controlled and modified by varying the molecular weight, density, dispersity, chemical composition, and topology. It is worthwhile to mention that the recent development of the reversible deactivation radical polymerization methods (especially atom transfer radical polymerization, ATRP),[9−15] has enabled access to a variety of advanced materials (i.e., polymeric responsive systems) characterized by desired and controlled macromolecular architectures, such as molecular brushes, star-shaped, dendrimeric, or hyperbranched structures.[16,17] This expansion of (often) complex polymeric structure clearly suggests that the latter factor, topology, might significantly influence the properties and applications of these materials. Hence, growing attention has been focused on studying the fundamental relationship between the spatial organization of chains and their properties. For example, in the molecular brushes, their physical properties are assumed to be governed by the grafted polymer side chains.[18] Thus, when rigid grafts are attached to the flexible main chain, they might act as "stiffeners" to the backbone affecting strongly macro-

Received: July 26, 2024
Revised: October 22, 2024
Accepted: October 22, 2024
Published: November 15, 2024

https://doi.org/10.1021/acs.macromol.4c01779
Macromolecules 2024, 57, 10754−10766

Scheme 1. Chemical Structure of Poly(mercaptopropyl)methylsiloxane, Labeled as PMMS, (a) and Its Examined Grafted Derivatives, (b)

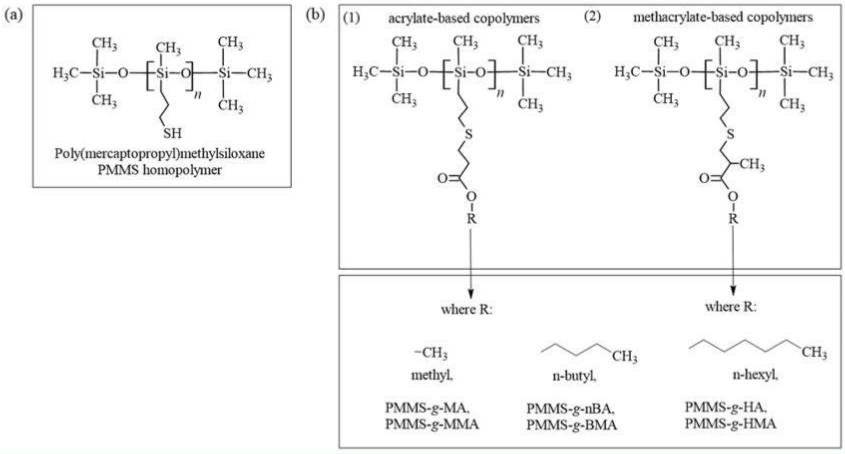

molecules conformation. However, in the opposite scenario ("flexible" grafts attached to the rigid backbone), they will have an unnoticeable effect on the conformation and physical properties of the entire molecule.[19,20] Moreover, it should also be mentioned that an increasing degree of side-chain polymerization, N_{sc}, and graft density, z, helps to reduce the entanglement plateau modulus in molten bottlebrushes and polymer brushes.[3,21−24] Just to mention work focused on poly(2-ethyl-2-oxazoline, PEOXA)-based molecular brushes (differentiated as linear grafts, "loop" and cyclic brushes)[25] has shown that the physicochemical properties of all examined systems significantly vary depending on their topology. As found, the cyclic and "loop" brushes were characterized by better lubricating properties or reduced viscoelasticity compared with the linear ones. Additionally, it was pointed out that for PEOXA-based "loop" brushes, the presence of "loops" itself increased the steric stability of the particle, whereas the cyclic structure provided the most increased steric stability for the macromolecule.

Dielectric studies on poly(dimethylsiloxane, PDMS) grafted polymers (PDMS-*g*-PDMS)[26] revealed changes in the dynamics of examined systems, i.e., a strong deviation in the segmental relaxation times, τ_α, with increasing side chain length. The observed effect was attributed to the grafting process and was found to be independent of the grafting density.

For bottlebrush polymer consisting of poly(2-bromoisobutyryloxyethyl methacrylate, PBiBEM) grafted with poly(*n*-butyl acrylate, PBA),[27] it was shown that the dynamics of the side chains is slowed down compared to homopolymers, due to the constraints imposed by the main chain and the strong interactions of the disordered side chains. Meanwhile, the backbone dynamics became plasticized by the PBA chains, which further stiffened the polymer backbone. Although, PBiBEM retains some conformational freedom. In a separate study on bottlebrushes with a polyisoprene backbone (PI) grafted with polystyrene side chains (PS),[28] dielectric and rheo-optical studies revealed global (main) chain relaxation, which reflects the fluctuation of the end-to-end vector in the examined samples. The intensity of this relaxation was much higher than expected for linear PI, indicating that the PI backbone is locally stiffened and stretched. Additionally, PI-*g*-PS showed lower main chain stiffness compared to PS-*g*-PS, which was attributed to differences in branching density along the main chain.

In this context, one can also recall previous investigations on a series of poly(mercaptopropyl)methylsiloxane (PMMS) oligomeric brushes grafted with various butyl acrylate (BA) isomers (with increased steric hindrance, PMMS-*g*-*x*BA),[29] which revealed that the glass transition temperature, T_g, and its pressure coefficient, dT_g/dp, of PMMS-*g*-*x*BA polymers were significantly higher compared to the homopolymer. This increase was due to increased steric hindrance from the grafted side groups. Inspired by these results, we aim to expand our knowledge of this group of materials by exploring the impact of the grafts' stiffness/flexibility on the molecular dynamics of a series of oligomeric PMMS grafted with a various acrylate (acrylate-based PMMS copolymers—considered as more flexible grafts) and methacrylates (methacrylate-based PMMS copolymers, marked as more rigid ones) homologous monomers (methyl, butyl and hexyl) by means of dielectric spectroscopy measurements under various thermodynamic conditions (where temperature, T = 193−303 K, and pressure, p = 0.1−450 MPa). The chemical structures of the chosen systems are listed in Scheme 1. It should be highlighted that studied materials were obtained by the "grafting to" technique, where the -SH present within PMMS homopolymer was substituted by either acrylates or methacrylate-based monomer of varying length of alkyl chain. Thus, all examined grafted copolymers were characterized by the same degree of polymerization of homopolymer backbone ($N_{bb} \sim 12$), whereas the grafts have a length of one monomer unit (N_{sc} = 1) of varying alkyl chain. The NMR analysis of synthesized PMMS-based copolymers (confirming the grafting density, z = 100%) is shown in Figures S1−S6 in the Supporting Information (SI).

https://doi.org/10.1021/acs.macromol.4c01779
Macromolecules 2024, 57, 10754−10766

II. MATERIALS AND METHODS

II.I. Materials. Poly(mercaptopropyl)methylsiloxane homopolymer (PMMS, 75−150 cSt) was purchased from Gelest and used as received (molecular weight, $M_{n,SEC}$ = 2400 g/mol, dispersity, $Đ$ = 1.26 determined by Viscotek TDA 305 triple detection calibrated with a narrow polystyrene standard, tetrahydrofuran (THF) as eluent). Methyl acrylate (MA), *n*-butyl acrylate (*n*BA), hexyl acrylate (HA), methyl methacrylate (MMA), butyl methacrylate (BMA), hexyl methacrylate (HMA), 2,2-Dimethoxy-2-phenylacetophenone (DMPA), and DMSO-d_6 were purchased from Sigma-Aldrich.

All copolymers were synthesized by one of the "grafting to" techniques, in which commercially supplied PMMS backbone functionalized with − SH groups was coupled with either acrylates or methacrylates. For "grafting to" technique, the average number of branches was determined by the degree of polymerization of homopolymer backbone (N_{bb} ∼ 12), whereas the side-chain degree of polymerization, N_{sc} = 1, and the grafting density, z = 100%. The chemical structures of the chosen systems are shown in Scheme 1. Before the polymerization, all monomers were purified by passing through a neutral alumina column to remove inhibitors.

II.II. Thiol−Ene Coupling Photopolymerization: Example of the Synthesis of PMMS-*g*-HMA. PMMS (0.25 g, 0.05 mmol), HMA (0.5 g, 2.94 mmol), and DMPA (0.09 g, 0.36 mmol) were dissolved in THF (2 mL). The solution was purged under nitrogen and purified by one freeze−pump−thaw cycle. Next, the flask was stirred for 160 min under ultraviolet (UV) irradiation, and then, THF was evaporated under vacuum. The polymer was purified by washing it many times, first in a methanol/water mixture and then in methanol. The purified sample was dried to a constant mass under reduced pressure.

The structure of all grafted oligomers was confirmed by ^{1}H and ^{13}C NMR analysis. Note that NMR spectra were recorded using a 500 MHz spectrometer (Bruker) for samples in commercially available DMSO-d_6. Signals from the respective groups of atoms for all examined copolymers are shown in Figures S1−S6. The total disappearance of the thiol signal at 2.08 ppm initially present in the ^{1}H NMR spectra of PMMS, and peaks coming from incorporated acrylate and methacrylate units, indicate quantitative thiol−ene ligations. Previous papers noted similar observations concerning PMMS-based polymers.[30,31] As can be seen, all spectra present purified products in the absence of unreacted PMMS or monomers. The molecular weights, M_w, of the oligomers were determined using SEC-LALLS (triple detection, THF). As previously demonstrated,[29] for the "grafting to" technique, the average number of branches was determined by the degree of polymerization of the homopolymer backbone (N_{bb} ∼ 12), while the grafts consist of a single monomer unit (N_{sc} = 1). The final theoretical polymer M_w is determined by the number of PMMS initiating centers. Considering that NMR analysis showed the absence of −SH groups, this confirms the completion of the thiol−ene coupling (Figures S1−S6). Significant differences in M_w are not expected, as the monomers chosen for the photopolymerization process have very similar molecular weights. Taking into account the N_{bb} of PMMS and the molecular weights of the monomers, the theoretical molecular weights should fall within a narrow range of 3400−4700 Da.

II.III. Differential Scanning Calorimetry (DSC). Calorimetric measurements of PMMS were carried out by a Mettler-Toledo DSC apparatus equipped with a liquid nitrogen cooling accessory and an HSS8 ceramic sensor (heat flux sensor with 120 thermocouples). Temperature and enthalpy calibrations were performed using indium and zinc standards. All samples were prepared in an open aluminum crucible (40 μL) outside the DSC apparatus and measured on heating from 150 to 298 K at a constant heating rate of 10 K/min.

II.IV. Broadband Dielectric Spectroscopy (BDS). Complex dielectric permittivity, $\varepsilon^*(\omega) = \varepsilon'(\omega) - i\varepsilon''(\omega)$, values at ambient pressure were measured using the impedance analyzer (Novocontrol α) over a frequency range from 1×10^{-1} to 3×10^6 Hz. The samples were placed between two stainless-steel electrodes (diameter: 10 mm; Teflon spacer: 0.05 mm) and mounted inside a cryostat. During the measurement, each sample was maintained under a dry nitrogen gas flow. The temperature was controlled by a Quatro Cryosystem using a nitrogen gas cryostat with stability better than 0.1 K. The temperature-dependent dielectric measurements were performed in the range from 173 to 303 K.

For dielectric measurements at elevated pressure, we used a high-pressure system developed at the Institute of High-Pressure Physics of the Polish Academy of Science in Warsaw, UNIPRESS. Thin Teflon spacers were applied to maintain a fixed distance between the plates. The sample capacitor was sealed and mounted inside a Teflon capsule to separate it from the silicon liquid used as a pressure-transmitting medium. The temperature was adjusted with a precision of 0.5 K by means of a refrigerated and heating circulator. Complex dielectric permittivity was measured within the same frequency range as that in the case of measurements carried out at ambient pressure.

II.V. Shear Rheology. The viscosity of the examined polymer brushes was determined by means of an ARES G2 Rheometer. The viscosity measurement in the vicinity of the liquid-glass transition was performed by means of an aluminum parallel plate geometry (diameter of 4 mm). For the oscillation-frequency rheological experiments, the investigated sample was tested in the frequency range from 0.1 to 100 rad/s (12 points per decade) and over the temperature range from T = 177−303 K. In the temperature range, where the G'' peaks are not visible, the time−temperature superposition (TTS) rule can be applied to determine the segmental relaxation times, τ_α. According to this criterion, G' and G'' spectra collected at various temperature conditions form the master curve when shifted horizontally by the shift factor, α_T, to superimpose at the chosen reference temperature, see Figure 4.

III. RESULTS AND DISCUSSION

III.I. Ambient Pressure Studies. As a first step, we performed the calorimetric measurements. Representative thermograms are displayed in Figure 1. For all samples, only a prominent step in the recorded heat capacity, related to the glass transition, can be seen. Values of the determined calorimetric glass transition temperatures, $T_{g,DSC}$, are shown

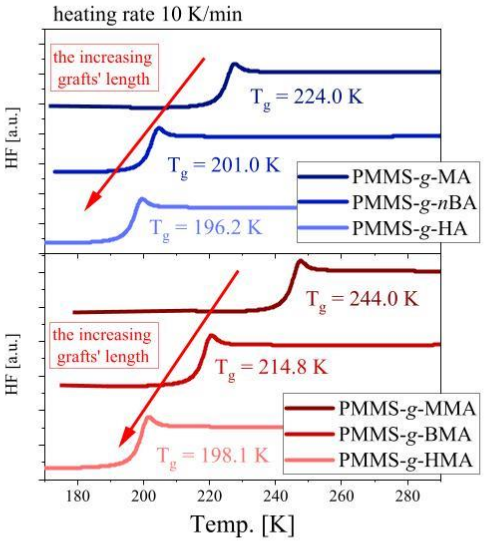

Figure 1. DSC thermograms recorded for all examined graft copolymers..

https://doi.org/10.1021/acs.macromol.4c01779
Macromolecules 2024, 57, 10754−10766

in Figure 2 and listed in Table 1. It should be highlighted that $T_{g,DSC}$s of all explored graft systems are much higher compared

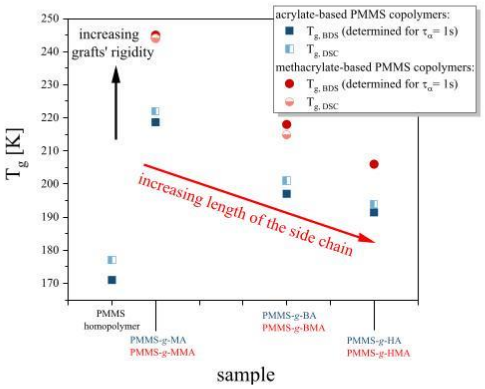

Figure 2. Glass transition temperatures, T_g, determined by different experimental techniques plotted versus the length of the graft.

Table 1. Molecular Weights (M_w) and Glass Transition Temperature (T_g) Molecules Obtained from Both Calorimetric and Dielectric Measurements (with an Experimental Error of ±2 K)

sample	M_w [g/mol]	$T_{g,BDS}$ [K] for τ_α = 1 s	$T_{g,DSC}$ [K]
PMMS homopolymer	2400	177.0	178.0
PMPS	2500	230.0	230.0
Acrylate-based PMMS Copolymers			
PMMS-*g*-MA	3400	231.0	224.0
PMMS-*g*-*n*BA	4100	204.0	201.0
PMMS-*g*-HA	4600	198.0	196.2
Methacrylate-based PMMS Copolymers			
PMMS-*g*-MMA	3600	244.0	244.0
PMMS-*g*-BMA	4100	218.0	214.8
PMMS-*g*-HMA	4700	206.0	198.1

to the associating PMMS homopolymer (which can form specific interactions via thiol moiety but of relatively weak strength), characterized by $T_{g,DSC}$ = 178 K.[32] This result agrees with our previous studies carried out for PMMS-based oligomeric brushes grafted with various butyl acrylate isomers (PMMS-*g*-*x*BA),[29] where a similar trend was observed. Moreover, one can see that the glass transition shifts toward lower temperatures with the elongation of the grafts. Additionally, methacrylate-based PMMS copolymers are characterized by the higher $T_{g,DSC}$ compared to their acrylates counterparts, as seen in Figure 2. This implies that the increased steric hindrance caused by both the grafts' elongation and stiffness leads to a pronounced variation in the glass transition temperatures. However, it seems that the latter factor, stiffness, seems to have a higher impact, as the observed effects intensify in the case of methacrylate-based PMMS copolymers. Note that taking into account the chemical structure of the studied PMMS-based copolymers, they are all characterized by the same degree of polymerization of homopolymer backbone ($N_{bb} \sim 12$), and grafting density (z = 100%). The only differences between them are the stiffness of the grafts and the length of the alkyl chain; see the chemical structures shown in Scheme 1. Similarly, in the case of PMMS-*g*-*x*BA, it was clearly observed that the more hindered the grafts, the higher the T_g.[29] In this context, it is also worthwhile to stress that increased glass transition temperatures were reported for the bottlebrush polymers PDMS-*g*-PDMS, which was attributed to the grafting process.[26] Similar results were reported for poly(*tert*-butoxystyrene, PtBOS) polymacromonomers, which were characterized by a higher T_g compared to the macromonomer. The effect of increasing glass transition temperature was attributed to the restrictive structure of the grafted polymer, which prevented the mobility of the grafted side chains.[33] Dalsin et al. pointed out that the glass transition temperature of brush polymers depends on the grafted side chains and does not depend on the molar weight, M_n, chemical structure, or skeleton length.[24]

Furthermore, we performed dielectric measurements over a wide temperature range to characterize the molecular dynamics of the studied systems. Figure 3 shows the representative dielectric loss spectra of chosen acrylate-based PMMS copolymers and their methacrylate counterparts measured above T_g. Data obtained for the PMMS homopolymer, taken from ref 32, are shown as the inset in Figure 3a. For acrylate-based PMMS copolymers, we can distinguish: (i) dc-conductivity associated with the charge transport of ions (at lower frequencies) and (ii) a single (monomodal) segmental α-relaxation process, which shifts toward lower frequencies as the temperature decreases. However, surprisingly, in the case of the methacrylate-grafted copolymers, the dominant relaxation process appearing at high frequencies seems to be clearly bimodal. Upon lowering the temperature, this bimodal character is lost, and around T_g, only a single broad relaxation process is detected. For a better representation of what is mentioned above, dielectric loss peaks measured for acrylate-based PMMS copolymers and their methacrylate counterparts were compared in Figure S7. For this purpose, we have chosen spectra recorded at various temperatures that coincide at the maximum of the peak. As displayed, the main relaxation mode of methacrylate-based PMMS copolymers clearly exhibits a bimodal nature, indicating the presence of additional mobility within those systems, which cannot be observed in the case of acrylate-based PMMS copolymers. Note that all acrylate-grafted PMMS reveals a similar monomodal mode, as shown in Figure S8. It should be highlighted that this agrees with previous studies on PMMS-*g*-xBA, which reported the presence of only one broad relaxation process in which shape remains constant under varying thermodynamic conditions.[29]

Interestingly, dielectric studies allowed us to observe pronounced differences between PMMS-based copolymers grafted with either acrylate or methacrylate monomers. The former systems, acrylate-based PMMS copolymers, exhibited a single α-relaxation mode. On the other hand, methacrylate-based PMMS copolymers showed a bimodal relaxation process, similar to that observed in the case of PMMS homopolymer. A bimodal loss peak in this material (see the inset in Figure 3a)[32] was discussed as due to a superposition of the two processes reflecting different mobility. Originally, it was assumed that the (additional) slower relaxation mode (assigned as α'-process) resulted from either "the association–dissociation phenomenon within lamellar-like self-assemblies or the sub-Rouse mode"; whereas the faster process reflects the segmental dynamics.[32] Nevertheless, the performed dielectric high-pressure experiments clearly supported the latter (sub-

https://doi.org/10.1021/acs.macromol.4c01779
Macromolecules 2024, 57, 10754−10766

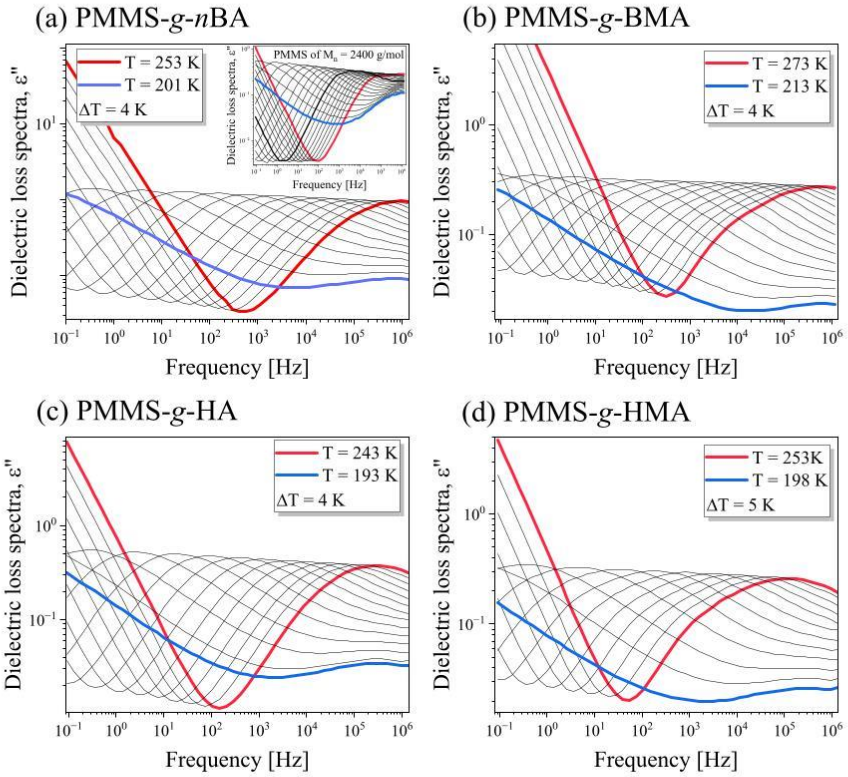

Figure 3. Dielectric spectra of (a) PMMS-g-nBA and (c) PMMS-g-HA, as well as their methacrylate (b, d) counterparts collected above their glass transition temperature. As the inset of panel (a), the dielectric spectra of homopolymer PMMS are presented. Data for PMMS were taken from ref 32.

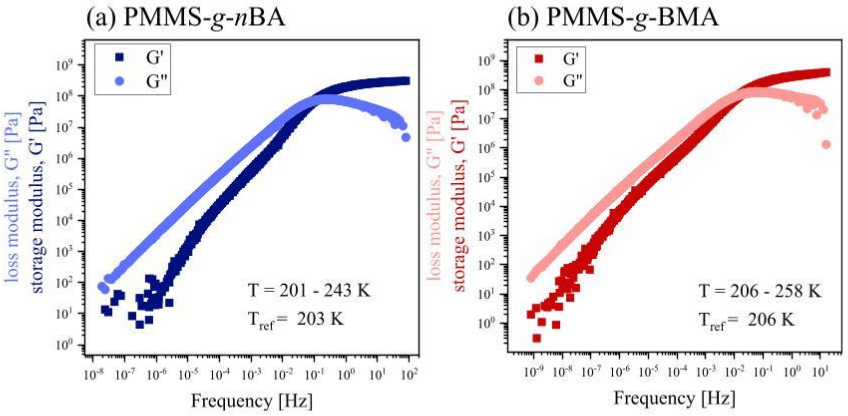

Figure 4. Master curves of measured storage, G', and loss, G'', modulus of examined (a) PMMS-g-nBA and (b) PMMS-g-BMA. These plots were constructed from the frequency dependences of G' and G'' measured in the range 0.1−100 rad/s at different temperatures, which were then shifted horizontally by a shift factor, a_T, in order to superimpose the measured spectra at a selected reference temperature, T_{ref}.

https://doi.org/10.1021/acs.macromol.4c01779
Macromolecules 2024, 57, 10754−10766

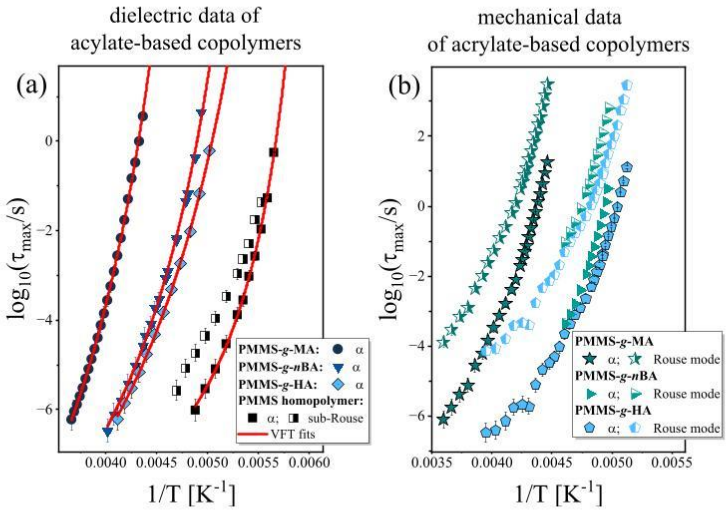

Figure 5. (a) Temperature dependences of dielectric relaxation times, τ_{α}, of acrylate-based PMMS copolymers. (b) Temperature dependences of mechanical segmental, τ_{α}, and terminal, τ_{Rouse}, relaxation times determined for acrylate-based PMMS copolymers..

Rouse) supposition.[34] However, note that the systems studied herein are grafted copolymers. Therefore, additional processes may be directly related to the presence of grafts in their structure. Recent studies on grafted molecular brushes, poly(poly(dimethylsiloxane methacrylate)) (polyPDMSMA) and their three-armed star counterparts revealed multiple relaxation processes in their dielectric loss spectra, including the chain and segmental modes, as well as a process related to graft relaxation and/or star arm relaxation.[35] One would expect that copolymers grafted with acrylate/methacrylate monomers would exhibit similar behavior, i.e., an additional graft relaxation process. However, it should be noted that the grafted polyPDMSMAs had significantly higher molecular weights compared with the grafted copolymers investigated herein. Thus, the question remains: what kinds of mobility did we observe dielectrically (sub-Rouse or graft relaxation)? And why is it so different for both examined types of grafted copolymers? Is stiffness the major factor responsible for the observed differences?

To further investigate the PMMS-based brushes, a rheological study was conducted. The master curves of storage modulus G' and loss modulus G'' for PMMS-*g*-*n*BA and PMMS-*g*-BMA are presented in Figure 4, with additional data included in Figure S9. As observed, two processes can be detected: (i) the segmental process visible at a higher frequency (where both moduli cross each other near the maximum) and (ii) the Rouse mode at a lower frequency, where a clear change in the mechanical response is observed (where $G'(f) \sim f^2$ and $G''(f) \sim f$). This agrees with our previous mechanical results collected for PMMS-*g*-*x*BA.[29] One can recall that similar data were also reported for PBiBEM[27] or polyolefin-based[24] polymer brushes. However, it should be highlighted that there is no presence of the additional (intermediate) process related to the graft relaxation,[36−39] which might be due to the relatively small molecular weight of examined materials. Nevertheless, comparing the loss modulus spectra G'' with the $\varepsilon''(f)$ near T_g for methacrylate- or acrylate-based PMMS copolymers (Figure S10), it can be seen that the peak recorded in the mechanical studies has a significantly different shape, being narrower than the relaxation process observed in the dielectric loss spectra (Figure S10(a)). This difference is clearly visible in both dielectric (Figure S10(c)) and mechanical data obtained for PMMS-*g*-BMA, where the dielectric dominant process is much broader than the mechanical one. In the case of PMMS-*g*-*n*BA the shape of the segmental mode in mechanical and dielectric data is similar. Indeed, this confirms that for the methacrylate-derived graft copolymers under study, there is an additional process, as described earlier, for the PMMS homopolymer. Herein, it should be emphasized that branched brush polymers are expected to exhibit sequential relaxation: the chain segments should relax first, then the side chains, and finally the whole polymer. Therefore, in the mechanical response of such materials, three relaxation processes—segmental, terminal, and those originating from the side chains (graft/arm relaxation)—should be observed. This scenario was found in brush polymers such as polynorbornene-*g*-poly(D,L)-lactide,[40] or the grafted molecular brushes polyPDMSMA.[35] However, herein, only two processes (segmental and Rouse modes) are visible. This apparent inconsistency with the data presented in previous studies[35,40] is related to the low M_n of the studied here systems.

At this point, in order to better characterize the molecular dynamics of the studied systems, we plotted the temperature dependences of the relaxation times, τ, for all observed relaxation processes determined from both dielectric and mechanical measurements, as shown in Figure 5. For dielectric data, the measured dielectric loss peaks are described using one or two Havriliak−Negami (HN) functions with an additional term related to dc-conductivity[41]

https://doi.org/10.1021/acs.macromol.4c01779
Macromolecules 2024, 57, 10754−10766

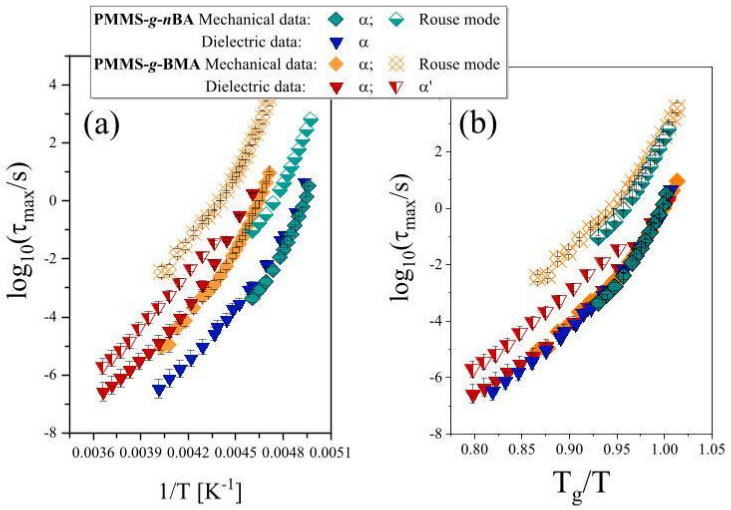

Figure 6. Temperature dependences of dielectric, τ_α, $\tau_{\alpha'}$ as well mechanical segmental, τ_α, and terminal, τ_{Rouse}, relaxation times plotted vs inverse temperature (a) and T_g/T (b) for the two representative copolymers.

$$\varepsilon(\varpi)'' = \frac{\sigma_{dc}}{\varepsilon_0 \varpi} + \text{Im} \sum_{i=1}^{2} \left(\varepsilon_\infty + \frac{\Delta\varepsilon_i}{[1 + (i\varpi\tau_i)^{\alpha_{HNi}}]^{\beta_{HNi}}} \right) \quad (1)$$

where α_{HN} and β_{HN} are the HN shape parameters related to the symmetric and asymmetric broadening of relaxation peaks, $\Delta\varepsilon$ is related to the dielectric strength, τ_{HN} is the HN relaxation time, ε_0 is the vacuum permittivity and ϖ is an angular frequency (where $\varpi = 2\pi f$). It should be highlighted that in the case of acrylate-based PMMS copolymers, we used one HN function (for details, see data for PMMS-*g*-*n*BA shown in Figure S11(a)), whereas for the studied methacrylate-grafted brushes, only the application of two HN functions allows us to describe the experimental data in a satisfactory manner (due to the presence of an additional relaxation process, see data for PMMS-*g*-BMA shown in Figure S11(b)). The determined values of relaxation times were plotted as a function of $1/T$ and are shown in Figure 5a for acrylate-based PMMS copolymers, whereas all collected $\tau_\alpha(T)$ dependences are displayed in Figure S12. Data for the PMMS homopolymer was also added.[32] Note that at this point, we also determined the values of dielectric glass transition temperatures, $T_{g,BDS}$, by fitting the obtained $\tau_\alpha(T)$ − dependences with the Vogel−Fulcher−Tammann (VFT) equation[42−44]

$$\tau_\alpha = \tau_\infty \exp\left(\frac{D_T T_0}{T - T_0}\right) \quad (2)$$

where τ_∞, D_T, and T_0 are the fitting parameters. Estimated values of $T_{g,BDS}$ were added to Figure 2 and Table 1. Note that $T_{g,BDS}$ was defined as the temperature at which segmental relaxation time is equal to $\tau_\alpha = 1$ s for further comparison with the high-pressure data. It should be mentioned that the obtained $T_{g,BDS}$ of all samples are comparable to those estimated from the DSC technique, see Figure 2. Additionally, we also estimated activation barriers, $E_a = R \cdot \mathrm{d}\ln\tau_\alpha/\mathrm{d}T$, for both segmental and α' relaxations at T_g for both kinds of polymer brushes, see Table S1. It was found that there are some notable differences in E_a between acrylate- and methacrylate-based copolymers. Furthermore, the activation barrier for the slow process is much smaller with respect to the segmental relaxation in the latter polymer brushes.

On the other hand, the mechanical relaxation times, τ, were determined according to the following equation

$$\log(\tau(T)) = \log(\tau(T_{ref})) + \log(\alpha_T) \quad (3)$$

where $\tau(T_{ref})$ indicates the corresponding relaxation time determined at the chosen T_{ref}, and α_T is the shift factor. In the case of mechanical τ_α, $\tau_\alpha(T_{ref})$ is calculated at frequency, f, of $G''(f)$ maximum (as $\tau = 1/2\pi f$). On the other hand, the relaxation time of the terminal relaxation, $\tau_{Rouse}(T_{ref})$, was estimated using the Graessley[45] method, from the crossover of the two straight lines, representing the dependences of $\log(G') \approx 2\log(f)$ and $\log(G'') \approx \log(f)$ in the low-frequency regime of the master curve (constructed due the time−temperature superposition). The temperature dependences of mechanical τ_α and τ_{Rouse} obtained for acrylate-based PMMS copolymers are shown in Figure 5b.

In Figure 6a, the relaxation times determined from both mechanical and dielectric measurements are compared for PMMS-*g*-*n*BA (acrylate derivative) and PMMS-*g*-BMA (methacrylate derivative). As can be seen, for the former system, the mechanical τ_α agrees with the values obtained from the dielectric investigations, and the Rouse mode is slower by ∼2 decades. The same agreement in segmental dynamics can also be observed for the second grafted copolymer (PMMS-*g*-BMA). However, interestingly, there is a clear discrepancy in the time scale of the mechanical Rouse mode and the dielectric α'-process observed for this material, as shown in Figure 6b. This discrepancy indicates that the additional dielectric mode is not related to global chain dynamics. One can recall that similar behavior was reported for the PMMS homopolymer, leading to the primary assignment of the observed dielectric

https://doi.org/10.1021/acs.macromol.4c01779
Macromolecules 2024, 57, 10754−10766

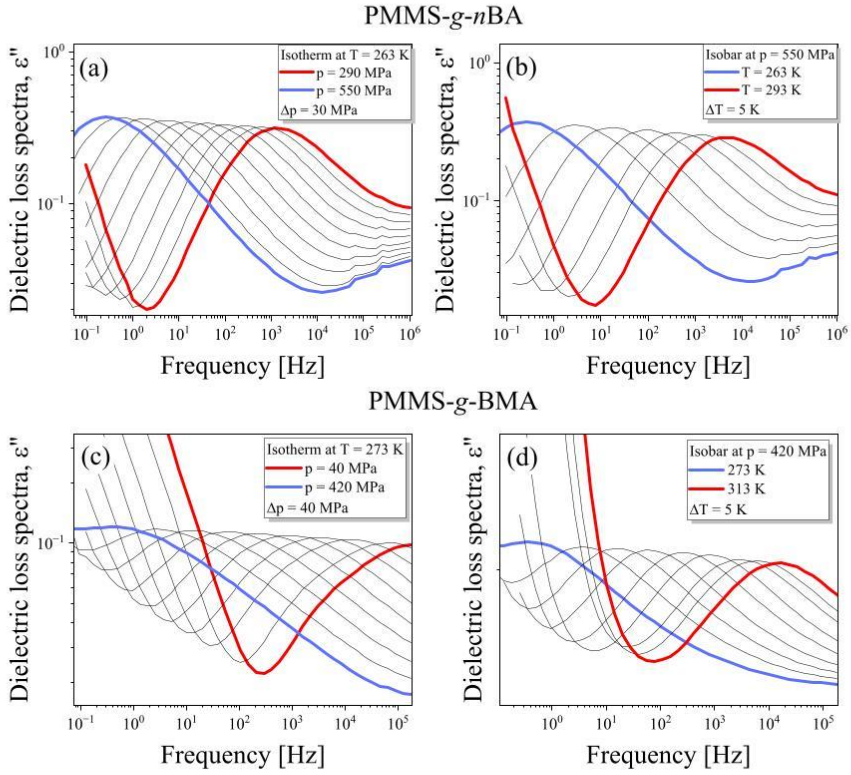

Figure 7. Dielectric loss spectra measured for PMMS-*g*-nBA (a, b) and PMMS-*g*-BMA (c, d) at various temperatures and pressures.

α'-process to either "the association−dissociation phenomenon within lamellar-like self-assemblies or the sub-Rouse mode".[32] However, high-pressure studies suggest that the latter origin (as the sub-Rouse mode) is more likely. Note that our data are in agreement with other studies on various poly(dimethylsiloxane) derivatives, which clearly report the occurrence of the sub-Rouse relaxation characterized by intermediate time and length scale between segmental and Rouse mode relaxation.[46−49] Based on the similarities with the data collected for the PMMS homopolymer, one can assume that the dielectric α'-process distinguished for methacrylate-based PMMS copolymers might also be related to some kind of backbone motions.[34] This claim is even more supported once we consider temperature evolution of the mechanical Rouse and dielectric α' mode that can be easily superimposed within experimental uncertainty (having the same curvature) in the studied range of temperatures as can be deduced from Figure 6b.

In fact, when we shift the data vertically, they collapse almost perfectly onto each other (see Figure S13). Nevertheless, as the α'-process is not observed for their acrylates counterparts, it is supposed that its appearance in the dielectric loss spectra could be related to the grafts' stiffness, which is the only significant difference between both examined groups of oligomeric polymer brushes which have similar molecular weight, graft density, etc. Consequently, there might be different dipole moment distribution in both studied herein systems allowing us to observe additional sub-Rouse chain mobility in methacrylate-based PMMS copolymers.

III.II. High-Pressure Studies. Based on the above-mentioned data, one can conclude that the additional dielectric α'-process has a different time scale than the terminal mode observed in the rheological study. Thus, we have reason to believe that this process may reflect the movements of (sub)chain units of the sub-Rouse mode kind, or alternatively, it may be related to the motions of the grafts (side chains) active in the dielectric measurement due to their stiffness. Having that in mind, further high-pressure BDS measurements were performed under various thermodynamic conditions (temperature, T, and pressure, p) to gain new information on the dynamics of α'-process in methacrylate-based PMMS copolymers. In Figure 7, we present representative dielectric loss spectra obtained under different isothermal and isobaric conditions collected for PMMS-*g*-*n*BA and PMMS-*g*-BMA. Data measured for the other systems are displayed in Figure S14. As can be seen, similarly to the ambient pressure studies of acrylate-based PMMS copolymers, a single (monomodal) relaxation mode is observed, with the maximum shifting toward lower frequencies upon both cooling and compression. Conversely, for PMMS-based copolymers grafted with

https://doi.org/10.1021/acs.macromol.4c01779
Macromolecules 2024, 57, 10754−10766

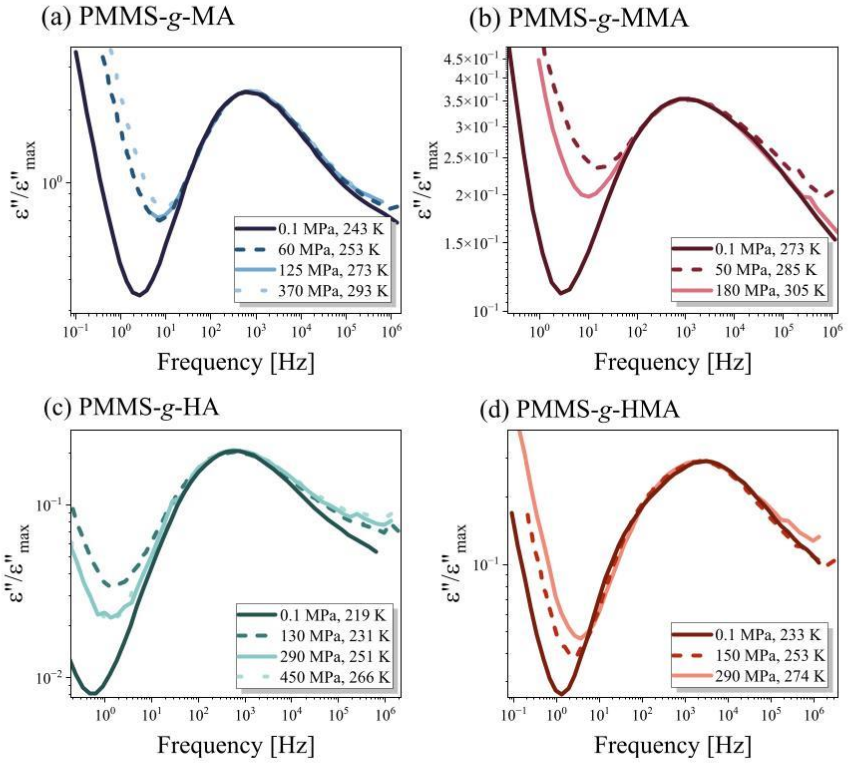

Figure 8. Comparison of the loss spectra obtained at various thermodynamic conditions that were characterized by the same τ_α and $\tau_{\alpha'}$ for PMMS-*g*-MA (a), PMMS-*g*-MMA (b), PMMS-*g*-HA (c), and PMMS-*g*-HMA (d).

methacrylate monomers, a clearly bimodal relaxation process is observed under various isobaric and isothermal conditions. Notably, as seen at ambient pressure data, there is a narrowing of the dielectric loss peak upon both cooling and compression for PMMS-*g*-BMA, see Figure 7c,d. At this point, it should also be highlighted that the recorded dielectric loss spectra superimpose at constant τ_α independently on the thermodynamic conditions, as shown in Figure 8. This indicates that (i) there is a good superposition of the slow and segmental process in copolymers grafted with methacrylate monomers and (ii) time−temperature−pressure (TPS) rule is satisfied for all materials studied herein.[50]

Hence, in the methacrylate-based PMMS copolymers, we have a situation similar to that found in the PMMS, where a superposition of the segmental and slow modes under various thermodynamic conditions was revealed. This suggests that α' in the polymer brushes might rather be related to the sub-Rouse motions. However, we cannot rule out the mobility of the rigid methacrylate-based grafts to be responsible for this additional process in these brushes.

To obtain better insight into the dynamics of graft copolymers at elevated pressure, high-pressure dielectric loss spectra were fitted using either one or two Havriliak−Negami (HN) functions with an additional term related to dc-conductivity in the case of acrylate- and methacrylate-based PMMS copolymers, respectively, in the same manner as for ambient pressure data. The $\tau_\alpha(T, p)$ and $\tau_{\alpha'}(T, p)$ − dependences obtained at various thermodynamic conditions are shown in Figure 9. The glass transition temperatures at different pressures were estimated by fitting temperature and pressure dependences of the segmental relaxation times to the VFT eq (eq 2) and its pressure counterpart (pVFT)[50,51]

$$\tau_\alpha = \tau_\infty \exp\left(\frac{D_p P}{P_0 - P}\right) \tag{4}$$

where P_0 is an estimate of the ideal glass pressure and D_p is the pressure-related fragility strength parameter. It should be added that T_g and p_g were defined as the temperature or pressure at which τ_α = 1 s. From the determined data, we calculated the pressure coefficient of the glass transition temperature, dT_g/dp, which is a parameter that directly informs about the sensitivity of structural or segmental relaxation to compression. It is worth noting that the higher the dT_g/dp value, the greater the expected sensitivity of τ_α to changes in the sample density. For this purpose, this parameter was determined using the empirical Andersson−Andersson equation[52]

https://doi.org/10.1021/acs.macromol.4c01779
Macromolecules 2024, 57, 10754−10766

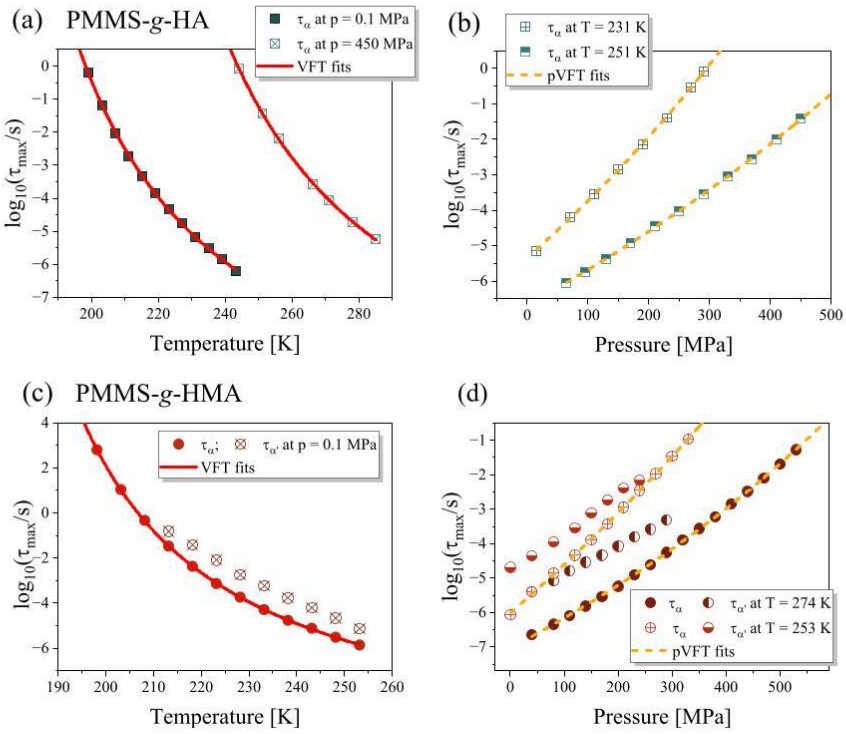

Figure 9. Temperature and pressure dependences of τ_α obtained during isobaric and isothermal measurements for examined grafted copolymers for PMMS-*g*-HA (a, b) and PMMS-*g*-HMA (c, d).

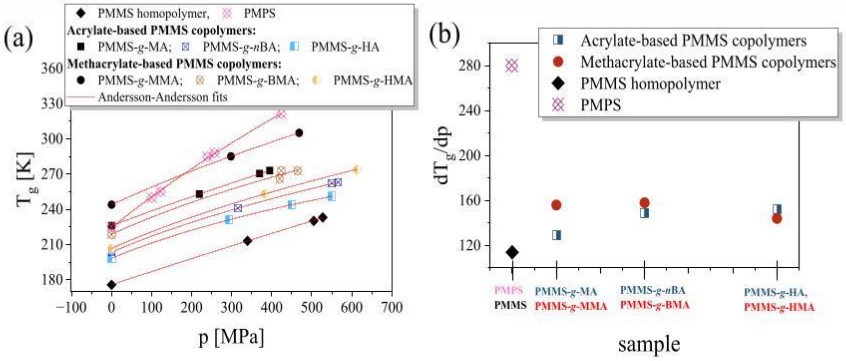

Figure 10. (a) Pressure dependence of the glass transition temperature determined from the Andersson−Andersson equation for indicated materials; (b) dT_g/dp plotted for all examined samples. T_g or p_g are defined as a temperature or pressure for which τ_α = 1 s.

$$T_g = k_1\left(1 + \frac{k_2}{k_3}p\right)^{1/k_2} \quad (5)$$

where k_1, k_2, and k_3 are material constants. The determined dT_g/dp for all tested samples is shown in Figure 10 and summarized in Table S2. It should be noted that the dT_g/dp values of graft copolymers are much higher compared to those of the PMMS homopolymer ($dT_g/dp \sim 114$ K/GPa), for which the segmental relaxation and the dT_g/dp value are probably reflecting the possibility of formation of hydrogen bonds by the thiol group. For acrylate-based PMMS copolymers, the attachment of increasingly longer grafts

https://doi.org/10.1021/acs.macromol.4c01779
Macromolecules 2024, 57, 10754−10766

(from MA to HA) to the PMMS side chain eliminates hydrogen bonding or association ability, leading to the higher dT_g/dp that increases with the chain length. Interestingly, for methacrylate-based PMMS copolymers dT_g/dp remains similar ($dT_g/dp \sim 152-158$ K/GPa) regardless of the grafts' length. This is quite striking. Polysiloxanes are quite flexible polymers, and the dT_g/dp value should be higher. In this context, one can mention that in the case of polymer materials, the pressure coefficient of the glass transition temperature, dT_g/dp, is affected by many factors related to their structure, i.e., molecular weight, the presence of functional, terminal groups, the flexibility and the length of the side chain.[50,53−55] Generally, high-molecular-weight polymers usually have higher dT_g/dp values when compared to those of their low-molecular-weight counterparts. Nevertheless, it should be highlighted that taking into account the chemical structure of the studied PMMS-based copolymers, they are all characterized by the same degree of polymerization of homopolymer backbone ($N_{bb} \sim 12$), and grafting density ($z = 100\%$). The only differences between them is the stiffness of the grafts and the length of their alkyl chain. Thus, we can assume that grafting the polymers with methacrylate and acrylate derivatives promotes chain stiffness, and the chemical structure of the grafts increases steric hindrance in the studied copolymers. Based on the above-mentioned data, it was observed that the acrylate-grafted copolymers showed one distinct segmental α process in their dynamics, while the methacrylate-grafted copolymers showed the presence of two α and α' processes. The former corresponded to the segmental relaxation, and the latter showed similarities to the sub-Rouse mode that occurs in the PMMS homopolymer. These include (i) intermediate time scale of the α'-process that is between segmental and terminal relaxation times, (ii) superposition of the α' and segmental process at varying thermodynamic conditions as found for normal mode and segmental relaxation in type-A polymers such as PPG or polyisoprene.[53−55] Furthermore, one can also remind us that temperature dependences of the terminal (mechanical response) and α' relaxation (dielectric data) have similar curvature, which is highly expected for the sub-Rouse mode in the materials where the time temperature superposition (TTS) rule is satisfied when analyzing the mechanical data.

IV. CONCLUSIONS

In the present work, we investigated the molecular dynamics of oligomeric PMMS-based brushes grafted with acrylate and methacrylate monomers of varying molecular weight under different thermodynamic conditions. The study showed that the glass transition temperature depends on the strain chain length and the steric hindrance used in the grafting process. These effects are enhanced with an increasing strain chain stiffness in the case of methacrylate-based PMMS copolymers. Dielectric studies revealed the presence of two relaxation processes (α and α') in one group of grafted polymers and one broad relaxation process (α) in the other. Moreover, comparing dielectric data with mechanical data allowed us to determine that the faster α relaxation process in both groups of compounds originates from the segmental movements, while the additional slower α'-process is not apparent in the rheological measurements. Further high-pressure experiments on methacrylate-based PMMS copolymers indicated that, similarly to the PMMS homopolymer, there is a superposition between the segmental and α' mode regardless of the applied pressure. This behavior may suggest that the slow mode originates from the movements of (sub)chain units of the sub-Rouse kind. Additional support of this claim comes from the direct comparison of the temperature dependences of the terminal and α' relaxation, which have the same curvature, and after vertical shift, they superimpose very well in the studied range of temperatures. However, we cannot rule out the possibility that it is related to the relaxation of the stiff methacrylate side group. Moreover, the pressure experiments showed that values of dT_g/dp for the oligomeric brushes are much higher than for the homopolymer. It can be related to the increase in chain stiffness and steric hindrance in the examined copolymers, as well as lack of specific interactions. We believe that the data presented in this article clearly emphasize the role of dielectric and mechanical studies in explaining the influence of the structure of grafted polymers on their dynamic properties under ambient and varying thermodynamic conditions. However, more research is needed to further understand the effect of the topology and architecture of the grafts on the molecular dynamics of the polymers and their correlation. All of this is important for understanding the behavior of such materials and for further the development of new polymeric materials.

■ ASSOCIATED CONTENT

Supporting Information

The Supporting Information is available free of charge at https://pubs.acs.org/doi/10.1021/acs.macromol.4c01779.

^{1}H and ^{13}C NMR spectra (Figures S1−S6); comparison of shapes of the loss spectra (Figure S7); comparison of dielectric loss peak shapes (Figure S8); master curves (Figure S9); comparison of normalized shear and dielectric α-peaks (Figure S10); comparison of the data fitting (Figure S11); temperature dependences of relaxation times (Figure S12); activation energies (Table S1); temperature dependences of mechanical terminal and dielectric α'-relaxation processes (Figure S13); dielectric loss spectra (Figure S14); and pressure coefficient of the glass transition temperature (Table S2) (PDF)

■ AUTHOR INFORMATION

Corresponding Author

Magdalena Tarnacka − *Institute of Physics, University of Silesia in Katowice, 41-500 Chorzów, Poland;* orcid.org/0000-0002-9444-3114; Email: magdalena.tarnacka@us.edu.pl

Authors

Sara Zimny − *Institute of Chemistry, University of Silesia in Katowice, 40-006 Katowice, Poland;* orcid.org/0000-0003-3812-1353

Paulina Maksym − *Institute of Material Science, University of Silesia in Katowice, 41-500 Chorzów, Poland;* orcid.org/0000-0002-8506-7102

Żaneta Wojnarowska − *Institute of Physics, University of Silesia in Katowice, 41-500 Chorzów, Poland;* orcid.org/0000-0002-7790-2999

Marian Paluch − *Institute of Physics, University of Silesia in Katowice, 41-500 Chorzów, Poland;* orcid.org/0000-0002-7280-8557

Kamil Kamiński − *Institute of Physics, University of Silesia in Katowice, 41-500 Chorzów, Poland;* orcid.org/0000-0002-5871-0203

Complete contact information is available at: https://pubs.acs.org/10.1021/acs.macromol.4c01779

Funding

The part of this research was funded by National Science Centre, Poland [Dec. no 2022/47/B/ST4/00236]. For the purpose of Open Access, the author has applied a CC-BY public copyright licence to any Author Accepted Manuscript (AAM) version arising from this submission.

Notes

The authors declare no competing financial interest.

REFERENCES

(1) Wang, J.; Li, Z.; Xu, Y.; Hu, W.; Zheng, G.; Zheng, L.; Ren, T. Synthesis and Tribological Behavior of Bridged Bicyclic Polymers as Lubricants. *Ind. Eng. Chem. Res.* **2020**, *59* (47), 20730−20739.

(2) Abbasi, M.; Faust, L.; Wilhelm, M. Comb and Bottlebrush Polymers with Superior Rheological and Mechanical Properties. *Adv. Mater.* **2019**, *31* (26), No. 1806484, DOI: 10.1002/adma.201806484.

(3) Daniel, W. F. M.; Burdyńska, J.; Vatankhah-Varnoosfaderani, M.; Matyjaszewski, K.; Paturej, J.; Rubinstein, M.; Dobrynin, A. V.; Sheiko, S. S. Solvent-Free, Supersoft and Superelastic Bottlebrush Melts and Networks. *Nat. Mater.* **2016**, *15* (2), 183−189.

(4) Miyake, G. M.; Weitekamp, R. A.; Piunova, V. A.; Grubbs, R. H. Synthesis of Isocyanate-Based Brush Block Copolymers and Their Rapid Self-Assembly to Infrared-Reflecting Photonic Crystals. *J. Am. Chem. Soc.* **2012**, *134* (34), 14249−14254.

(5) Bates, C. M.; Chang, A. B.; Momčilović, N.; Jones, S. C.; Grubbs, R. H. ABA Triblock Brush Polymers: Synthesis, Self-Assembly, Conductivity, and Rheological Properties. *Macromolecules* **2015**, *48* (14), 4967−4973.

(6) Verduzco, R.; Li, X.; Pesek, S. L.; Stein, G. E. Structure, Function, Self-Assembly, and Applications of Bottlebrush Copolymers. *Chem. Soc. Rev.* **2015**, *44* (8), 2405−2420.

(7) Pesek, S. L.; Lin, Y. H.; Mah, H. Z.; Kasper, W.; Chen, B.; Rohde, B. J.; Robertson, M. L.; Stein, G. E.; Verduzco, R. Synthesis of Bottlebrush Copolymers Based on Poly(Dimethylsiloxane) for Surface Active Additives. *Polymer* **2016**, *98*, 495−504.

(8) Johnson, J. A.; Lu, Y. Y.; Burts, A. O.; Xia, Y.; Durrell, A. C.; Tirrell, D. A.; Grubbs, R. H. Drug-Loaded, Bivalent-Bottle-Brush Polymers by Graft-through ROMP. *Macromolecules* **2010**, *43* (24), 10326−10335.

(9) Matyjaszewski, K.; Xia, J. Atom Transfer Radical Polymerization. *Chem. Rev.* **2001**, *101* (9), 2921−2990.

(10) Jakubowski, W.; Matyjaszewski, K. Activator Generated by Electron Transfer for Atom Transfer Radical Polymerization. *Macromolecules* **2005**, *38* (10), 4139−4146.

(11) Börner, H. G.; Matyjaszewski, K. Graft Copolymers by Atom Transfer Polymerization. *Macromol. Symp.* **2002**, *177* (1), 1−16.

(12) Sheiko, S. S.; Sumerlin, B. S.; Matyjaszewski, K. Cylindrical Molecular Brushes: Synthesis, Characterization, and Properties. *Prog. Polym. Sci.* **2008**, *33* (7), 759−785.

(13) Lee, H.-i.; Pietrasik, J.; Sheiko, S. S.; Matyjaszewski, K. Stimuli-Responsive Molecular Brushes. *Prog. Polym. Sci.* **2010**, *35* (1−2), 24−44.

(14) Neugebauer, D.; Zhang, Y.; Pakula, T.; Sheiko, S. S.; Matyjaszewski, K. Densely-Grafted and Double-Grafted PEO Brushes via ATRP. A Route to Soft Elastomers. *Macromolecules* **2003**, *36* (18), 6746−6755.

(15) Savin, D. A.; Pyun, J.; Patterson, G. D.; Kowalewski, T.; Matyjaszewski, K. Synthesis and Characterization of Silica-Graft-Polystyrene Hybrid Nanoparticles: Effect of Constraint on the Glass-Transition Temperature of Spherical Polymer Brushes. *J. Polym. Sci., Part B: Polym. Phys.* **2002**, *40* (23), 2667−2676.

(16) Peterson, G. I.; Choi, T. L. The Influence of Polymer Architecture in Polymer Mechanochemistry. *Chem. Commun.* **2021**, *57* (53), 6465−6474.

(17) Bhattacharya, A.; Misra, B. N. Grafting: A Versatile Means to Modify Polymers: Techniques, Factors and Applications. *Prog. Polym. Sci.* **2004**, *29* (8), 767−814.

(18) Wu, Y.; Tang, Q.; Zhang, M.; Li, Z.; Zhu, W.; Liu, Z. Synthesis of Bottlebrush Polymers with V-Shaped Side Chains. *Polymer* **2018**, *143*, 190−199.

(19) Liang, H.; Wang, Z.; Sheiko, S. S.; Dobrynin, A. V. Comb and Bottlebrush Graft Copolymers in a Melt. *Macromolecules* **2019**, *52* (10), 3942−3950.

(20) Mai, X.; Hao, P.; Liu, D.; Ding, M. Conformation of a Comb-like Chain in Solution: Effect of Backbone Rigidity. *ACS Omega* **2023**, *8* (12), 11177−11183.

(21) Hu, M.; Xia, Y.; McKenna, G. B.; Kornfield, J. A.; Grubbs, R. H. Linear Rheological Response of a Series of Densely Branched Brush Polymers. *Macromolecules* **2011**, *44* (17), 6935−6943.

(22) López-Barrón, C. R.; Brant, P.; Eberle, A. P. R.; Crowther, D. J. Linear Rheology and Structure of Molecular Bottlebrushes with Short Side Chains. *J. Rheol.* **2015**, *59* (3), 865−883.

(23) Fetters, L. J.; Lohse, D. J.; García-Franco, C. A.; Brant, P.; Richter, D. Prediction of Melt State Poly(α-Olefin) Rheological Properties: The Unsuspected Role of the Average Molecular Weight per Backbone Bond. *Macromolecules* **2002**, *35* (27), 10096−10101.

(24) Dalsin, S. J.; Hillmyer, M. A.; Bates, F. S. Linear Rheology of Polyolefin-Based Bottlebrush Polymers. *Macromolecules* **2015**, *48* (13), 4680−4691.

(25) Divandari, M.; Morgese, G.; Trachsel, L.; Romio, M.; Dehghani, E. S.; Rosenboom, J.-G.; Paradisi, C.; Zenobi-Wong, M.; Ramakrishna, S. N.; Benetti, E. M. Topology Effects on the Structural and Physicochemical Properties of Polymer Brushes. *Macromolecules* **2017**, *50* (19), 7760−7769.

(26) Jakobi, B.; Bichler, K. J.; Sokolova, A.; Schneider, G. J. Dynamics of PDMS-g-PDMS Bottlebrush Polymers by Broadband Dielectric Spectroscopy. *Macromolecules* **2020**, *53* (19), 8450−8458.

(27) Grigoriadis, C.; Nese, A.; Matyjaszewski, K.; Pakula, T.; Butt, H.-J.; Floudas, G. Dynamic Homogeneity by Architectural Design − Bottlebrush Polymers. *Macromol. Chem. Phys.* **2012**, *213* (13), 1311−1320.

(28) Iwawaki, H.; Urakawa, O.; Inoue, T.; Nakamura, Y.; Matsumiya, Y.; Watanabe, H. Rheo-Optical and Dielectric Study on Dynamics of Bottlebrush-like Polymacromonomer Consisting of a Polyisoprene Main Chain and Polystyrene Side Chains. *Macromolecules* **2020**, *53* (16), 7096−7106.

(29) Zimny, S.; Tarnacka, M.; Wojnarowska, Z.; Heczko, D.; Maksym, P.; Paluch, M.; Kamiński, K. Impact of the Graft' Structure on the Behavior of PMMS-Based Brushes. High Pressure Studies. *Polymer* **2023**, *271*, No. 125790.

(30) Jourdain, A.; Serghei, A.; Drockenmuller, E. Enhanced Ionic Conductivity of a 1,2,3-Triazolium-Based Poly(Siloxane Ionic Liquid) Homopolymer. *ACS Macro Lett.* **2016**, *5* (11), 1283−1286.

(31) Maksym, P.; Tarnacka, M.; Bielas, R.; Hachuła, B.; Zajac, A.; Szpecht, A.; Smiglak, M.; Kaminski, K.; Paluch, M. Structure-Property Relationships of Tailored Imidazolium- and Pyrrolidinium-Based Poly(Ionic Liquid)s. Solid-like vs. Gel-like Systems. *Polymer* **2020**, *192*, No. 122262.

(32) Tarnacka, M.; Jurkiewicz, K.; Hachuła, B.; Wojnarowska, Z.; Wrzalik, R.; Bielas, R.; Talik, A.; Maksym, P.; Kaminski, K.; Paluch, M. Correlation between Locally Ordered (Hydrogen-Bonded) Nanodomains and Puzzling Dynamics of Polymethysiloxane Derivative. *Macromolecules* **2020**, *53* (22), 10225−10233.

(33) Theodosopoulos, G. V.; Bitsi, S. L.; Pitsikalis, M. Complex Brush-Like Macromolecular Architectures via Anionic and Ring Opening Metathesis Polymerization: Synthesis, Characterization, and Thermal Properties. *Macromol. Chem. Phys.* **2018**, *219* (1), No. 1700253.

(34) Zimny, S.; Tarnacka, M.; Kamińska, E.; Wrzalik, R.; Adrjanowicz, K.; Paluch, M.; Kamiński, K. Studies on the Molecular

Dynamics at High Pressures as a Key to Identify the Sub-Rouse Mode in PMMS. *Macromolecules* **2022**, *55* (13), 5581−5590.
(35) Tarnacka, M.; Bielas, R.; V, A. K. S.; Wojnarowska, Z.; Maksym, P.; Neugebauer, D.; Paluch, M.; Kamiński, K. The Impact of Architecture on the Behavior of Siloxane-Grafted Polymethacrylate. *Polymer* **2024**, *297*, No. 126827.
(36) Dalsin, S. J.; Hillmyer, M. A.; Bates, F. S. Molecular Weight Dependence of Zero-Shear Viscosity in Atactic Polypropylene Bottlebrush Polymers. *ACS Macro Lett.* **2014**, *3* (5), 423−427.
(37) Abbasi, F.; Mirzadeh, H.; Katbab, A. A. Modification of Polysiloxane Polymers for Biomedical Applications: A Review. *Polym. Int.* **2001**, *50* (12), 1279−1287.
(38) Kempf, M.; Ahirwal, D.; Cziep, M.; Wilhelm, M. Synthesis and Linear and Nonlinear Melt Rheology of Well-Defined Comb Architectures of PS and PpMS with a Low and Controlled Degree of Long-Chain Branching. *Macromolecules* **2013**, *46* (12), 4978−4994.
(39) Haugan, I. N.; Maher, M. J.; Chang, A. B.; Lin, T. P.; Grubbs, R. H.; Hillmyer, M. A.; Bates, F. S. Consequences of Grafting Density on the Linear Viscoelastic Behavior of Graft Polymers. *ACS Macro Lett.* **2018**, *7* (5), 525−530.
(40) Iwawaki, H.; Urakawa, O.; Inoue, T.; Nakamura, Y. Rheo-Optical Study on Dynamics of Bottlebrush-Like Polymacromonomer Consisting of Polystyrene. II. Side Chain Length Dependence on Dynamical Stiffness of Main Chain. *Macromolecules* **2012**, *45* (11), 4801−4808.
(41) Havriliak, S.; Negami, S. A Complex Plane Representation of Dielectric and Mechanical Relaxation Processes in Some Polymers. *Polymer* **1967**, *8* (C), 161−210.
(42) Vogel, H. Temperatura Bhangigkeitgesetz Der Viskosität von Flüssigkeiten. *J. Phys. Z.* **1921**, *22*, 645−646.
(43) Fulcher, G. S. Analysis of Recent Measurements of the Viscosity of Glasses. *J. Am. Ceram. Soc.* **1925**, *8*, 339−355.
(44) Tammann, G.; Hesse, W. Die Abhängigkeit Der Viscosität von Der Temperatur Bie Unterkühlten Flüssigkeiten. *Z. Anorg. Allg. Chem.* **1926**, *156*, 245−257.
(45) Graessley, W. W. The Entanglement Concept in Polymer Rheology. *The Entanglement Concept in Polymer Rheology*, Springer-Verlag: Berlin/Heidelberg, Vol *16*, pp 1−179.
(46) Ngai, K. L.; Plazek, D. J.; Rizos, A. K. Viscoelastic Properties of Amorphous Polymers. 5. A Coupling Model Analysis of the Thermorheological Complexity of Polyisobutylene in the Glass-Rubber Softening Dispersion. *J. Polym. Sci., Part B: Polym. Phys.* **1997**, *35* (4), 599−614.
(47) Plazek, D. J.; Ngai, K. L. Resolving the Sub-Rouse Modes by Creep Compliance Measurements in Poly(Methyl- Para -Tolyl-Siloxane). *Macromolecules* **2020**, *53* (10), 3940−3945.
(48) Adrjanowicz, K.; Winkler, R.; Chat, K.; Duarte, D. M.; Tu, W.; Unni, A. B.; Paluch, M.; Ngai, K. L. Study of Increasing Pressure and Nanopore Confinement Effect on the Segmental, Chain, and Secondary Dynamics of Poly(Methylphenylsiloxane). *Macromolecules* **2019**, *52* (10), 3763−3774.
(49) Tu, W.; Ngai, K. L.; Paluch, M.; Adrjanowicz, K. Dielectric Study on the Well-Resolved Sub-Rouse and JG β-Relaxations of Poly(Methylphenylsiloxane) at Ambient and Elevated Pressures. *Macromolecules* **2020**, *53* (5), 1706−1715.
(50) Roland, C. M.; Hensel-Bielowka, S.; Paluch, M.; Casalini, R. Supercooled Dynamics of Glass-Forming Liquids and Polymers under Hydrostatic Pressure. *Rep. Prog. Phys.* **2005**, *68* (6), 1405−1478.
(51) Paluch, M.; Grzybowska, K.; Grzybowski, A. Effect of High Pressure on the Relaxation Dynamics of Glass-Forming Liquids. *J. Phys.: Condens. Matter* **2007**, *19* (20), No. 205117.
(52) Andersson, S. P.; Andersson, O. Relaxation Studies of Poly(Propylene Glycol) under High Pressure. *Macromolecules* **1998**, *31* (9), 2999−3006.
(53) Talik, A.; Tarnacka, M.; Dzienia, A.; Kaminska, E.; Kaminski, K.; Paluch, M. High-Pressure Studies on the Chain and Segmental Dynamics of a Series of Poly(Propylene Glycol) Derivatives. *Macromolecules* **2019**, *52* (15), 5658−5669.
(54) Floudas, G.; Gravalides, C.; Reisinger, T.; Wegner, G. Effect of Pressure on the Segmental and Chain Dynamics of Polyisoprene. Molecular Weight Dependence. *J. Chem. Phys.* **1999**, *111* (21), 9847−9852.
(55) Floudas, G.; Reisinger, T. Pressure Dependence of the Local and Global Dynamics of Polyisoprene. *J. Chem. Phys.* **1999**, *111* (11), 5201−5204.

Chorzów, dnia 15.05.2025 r.

Prof. dr hab. Kamil Kamiński
Instytut Fizyki im. A. Chełkowskiego
Wydział Nauk Ścisłych i Technicznych,
Uniwersytet Śląski w Katowicach,
ul. 75. Pułku Piechoty 1,
41-500 Chorzów

OŚWIADCZENIE

Oświadczam, że w pracy:

A1. S. Zimny, M. Tarnacka, E. Kamińska, R. Wrzalik, K. Adrjanowicz, M. Paluch, K. Kamiński. **Studies on the Molecular Dynamics at High Pressures as a Key Identify the Sub-Rouse Mode in PMMS.** *Macromolecules, 2022, 55 (13), 5581-5590.*

Mój udział polegał na nadzorowaniu przeprowadzonych analiz, dyskusji otrzymanych wyników oraz finansowaniu badań w ramach projektu NCN OPUS.

A2. S. Zimny, M. Tarnacka, Ż. Wojnarowska, D. Heczko, P. Maksym, M. Paluch, K. Kamiński. **Impact of the Graft' Structure on the Behavior of PMMS-Based Brushes. High Pressure Studies.** *Polymer, 2023, 271, 125790.*

Mój udział polegał na nadzorowaniu przeprowadzonych analiz, dyskusji otrzymanych wyników oraz finansowaniu badań w ramach projektu NCN OPUS.

A3. S. Zimny, M. Tarnacka, P. Maksym, Ż. Wojnarowska, M. Paluch, K. Kamiński. **The Influence of Graft Rigidity on the Dynamical Behavior of PMMS-Based Polymer Brushes at Ambient and High Pressures.** *Macromolecules, 2024, 57 (22), 10754-10766.*

Mój udział polegał na nadzorowaniu przeprowadzonych analiz, dyskusji otrzymanych wyników oraz finansowaniu badań w ramach projektu NCN OPUS.

.....

Podpis współautora publikacji

Chorzów, dnia 13.05.2025 r.

Dr hab. Magdalena Tarnacka, prof. UŚ
Instytut Fizyki im. A. Chełkowskiego
Wydział Nauk Ścisłych i Technicznych,
Uniwersytet Śląski w Katowicach,
ul. 75. Pułku Piechoty 1,
41-500 Chorzów

OŚWIADCZENIE

Oświadczam, że w pracy:

A1. S. Zimny, M. Tarnacka, E. Kamińska, R. Wrzalik, K. Adrjanowicz, M. Paluch, K. Kamiński. **Studies on the Molecular Dynamics at High Pressures as a Key Identify the Sub-Rouse Mode in PMMS.** *Macromolecules, 2022, 55 (13), 5581-5590.*

Mój udział polegał na wykonaniu pomiarów kalorymetrycznych, ich analizie i interpretacji, dyskusji otrzymanych wyników, współtworzeniu manuskryptu wraz z odpowiedziami na uwagi recenzentów.

A2. S. Zimny, M. Tarnacka, Ż. Wojnarowska, D. Heczko, P. Maksym, M. Paluch, K. Kamiński. **Impact of the Graft' Structure on the Behavior of PMMS-Based Brushes. High Pressure Studies.** *Polymer, 2023, 271, 125790.*

Mój udział polegał na wykonaniu pomiarów kalorymetrycznych, ich analizie i interpretacji, dyskusji otrzymanych wyników, współtworzeniu manuskryptu wraz z odpowiedziami na uwagi recenzentów.

A3. S. Zimny, M. Tarnacka, P. Maksym, Ż. Wojnarowska, M. Paluch, K. Kamiński. **The Influence of Graft Rigidity on the Dynamical Behavior of PMMS-Based Polymer Brushes at Ambient and High Pressures.** *Macromolecules, 2024, 57 (22), 10754-10766.*

Mój udział polegał na wykonaniu pomiarów kalorymetrycznych, ich analizie i interpretacji, dyskusji otrzymanych wyników, współtworzeniu manuskryptu wraz z odpowiedziami na uwagi recenzentów.

Magdalena Tarnacka

.....

Podpis współautora publikacji

Chorzów, dnia 19.05.2025 r.

Prof. dr hab. Marian Paluch
Instytut Fizyki im. A. Chełkowskiego
Wydział Nauk Ścisłych i Technicznych,
Uniwersytet Śląski w Katowicach,
ul. 75. Pułku Piechoty 1,
41-500 Chorzów

OŚWIADCZENIE

Oświadczam, że w pracy:

A1. S. Zimny, M. Tarnacka, E. Kamińska, R. Wrzalik, K. Adrjanowicz, M. Paluch, K. Kamiński. **Studies on the Molecular Dynamics at High Pressures as a Key Identify the Sub-Rouse Mode in PMMS.** *Macromolecules, 2022, 55 (13), 5581-5590.*

Mój udział polegał na udziale w dyskusji otrzymanych wyników.

A2. S. Zimny, M. Tarnacka, Ż. Wojnarowska, D. Heczko, P. Maksym, M. Paluch, K. Kamiński. **Impact of the Graft' Structure on the Behavior of PMMS-Based Brushes. High Pressure Studies.** *Polymer, 2023, 271, 125790.*

Mój udział polegał na udziale w dyskusji otrzymanych wyników.

A3. S. Zimny, M. Tarnacka, P. Maksym, Ż. Wojnarowska, M. Paluch, K. Kamiński. **The Influence of Graft Rigidity on the Dynamical Behavior of PMMS-Based Polymer Brushes at Ambient and High Pressures.** *Macromolecules, 2024, 57 (22), 10754-10766.*

Mój udział polegał na udziale w dyskusji otrzymanych wyników.

.....

Podpis współautora publikacji

Chorzów, dnia 16.05.2025 r.

Prof. dr hab. Żaneta Wojnarowska
Instytut Fizyki im. A. Chełkowskiego
Wydział Nauk Ścisłych i Technicznych,
Uniwersytet Śląski w Katowicach,
ul. 75. Pułku Piechoty 1,
41-500 Chorzów

OŚWIADCZENIE

Oświadczam, że w pracy:

A2. S. Zimny, M. Tarnacka, Ż. Wojnarowska, D. Heczko, P. Maksym, M. Paluch, K. Kamiński. **Impact of the Graft' Structure on the Behavior of PMMS-Based Brushes. High Pressure Studies.** *Polymer, 2023, 271, 125790.*

Mój udział polegał na wykonaniu badań reologicznych. oraz ich analizie i dyskusji wyników.

A3. S. Zimny, M. Tarnacka, P. Maksym, Ż. Wojnarowska, M. Paluch, K. Kamiński. **The Influence of Graft Rigidity on the Dynamical Behavior of PMMS-Based Polymer Brushes at Ambient and High Pressures.** *Macromolecules, 2024, 57 (22), 10754-10766.*

Mój udział polegał na wykonaniu badań reologicznych. oraz ich analizie i dyskusji wyników.

Ż. Wojnarowska
.....
Podpis współautora publikacji

Chorzów, dnia 13.05.2025 r.

Dr inż. Paulina Maksym
Instytut Inżynierii Materiałowej
Wydział Nauk Ścisłych i Technicznych,
Uniwersytet Śląski w Katowicach,
ul. 75. Pułku Piechoty 1,
41-500 Chorzów

OŚWIADCZENIE

Oświadczam, że w pracy:

A2. S. Zimny, M. Tarnacka, Ż. Wojnarowska, D. Heczko, P. Maksym, M. Paluch, K. Kamiński. **Impact of the Graft' Structure on the Behavior of PMMS-Based Brushes. High Pressure Studies.** *Polymer, 2023, 271, 125790.*

Mój udział polegał na wykonaniu syntezy kopolimerów PMMS szczepionych różnymi izomerami akrylanu butylu oraz charakterystyce uzyskanych produktów metodą NMR.

A3. S. Zimny, M. Tarnacka, P. Maksym, Ż. Wojnarowska, M. Paluch, K. Kamiński. **The Influence of Graft Rigidity on the Dynamical Behavior of PMMS-Based Polymer Brushes at Ambient and High Pressures.** *Macromolecules, 2024, 57 (22), 10754-10766.*

Mój udział polegał na wykonaniu syntezy kopolimerów PMMS szczepionych homologicznymi monomerami akrylanów i metakrylanów oraz charakterystyce uzyskanych produktów metodą NMR.

.....

Podpis współautora publikacji

Chorzów, dnia 15.05.2025 r.

Prof. dr hab. n. farm. Ewa Ozimina-Kamińska
Katedra i Zakład Farmakognozji i Fitochemii
Wydział Nauk Farmaceutycznych w Sosnowcu
Śląskiego Uniwersytetu Medycznego w Katowicach
ul. Jagiellońska 4
41-200 Sosnowiec

OŚWIADCZENIE

Oświadczam, że w pracy:

A1. S. Zimny, M. Tarnacka, E. Kamińska, R. Wrzalik, K. Adrjanowicz, M. Paluch, K. Kamiński. **Studies on the Molecular Dynamics at High Pressures as a Key Identify the Sub-Rouse Mode in PMMS.** *Macromolecules, 2022, 55 (13), 5581-5590.*

Mój udział polegał na uczestnictwie w dyskusji otrzymanych wyników.

Ewa Ozimina-Kamińska

Podpis współautora publikacji

Chorzów, dnia 19.05.2025 r.

Dr hab. Roman Wrzalik, prof. UŚ
Instytut Fizyki im. Augusta Chełkowskiego
Wydział Nauk Ścisłych i Technicznych
Uniwersytet Śląski w Katowicach
ul. 75. Pułku Piechoty 1
41-500 Chorzów

OŚWIADCZENIE

Oświadczam, że w pracy:

A1. S. Zimny, M. Tarnacka, E. Kamińska, R. Wrzalik, K. Adrjanowicz, M. Paluch, K. Kamiński. **Studies on the Molecular Dynamics at High Pressures as a Key Identify the Sub-Rouse Mode in PMMS.** *Macromolecules, 2022, 55 (13), 5581-5590.*

Mój udział polegał na przeprowadzeniu obliczeń DFT oraz dyskusji wyników.

.....

Podpis współautora publikacji

Chorzów, dnia 19.05.2025 r.

Prof. dr hab. Karolina Adrjanowicz
Instytut Fizyki im. Augusta Chełkowskiego
Wydział Nauk Ścisłych i Technicznych
Uniwersytet Śląski w Katowicach
ul. 75. Pułku Piechoty 1
41-500 Chorzów

OŚWIADCZENIE

Oświadczam, że w pracy:

A1. S. Zimny, M. Tarnacka, E. Kamińska, R. Wrzalik, K. Adrjanowicz, M. Paluch, K. Kamiński. **Studies on the Molecular Dynamics at High Pressures as a Key Identify the Sub-Rouse Mode in PMMS.** *Macromolecules, 2022, 55 (13), 5581-5590.*

Mój udział polegał na udziale w dyskusji otrzymanych wyników.

.....

Podpis współautora publikacji

Sosnowiec, dnia 16.05.2025 r.

Dr n. farm. Dawid Heczko
Zakład Statystyki Medycznej
Wydział Nauk Farmaceutycznych
Śląskiego Uniwersytetu Medycznego w Katowicach
ul. Ostrogórska 30,
41-200 Sosnowiec

OŚWIADCZENIE

Oświadczam, że w pracy:

A2. S. Zimny, M. Tarnacka, Ż. Wojnarowska, D. Heczko, P. Maksym, M. Paluch, K. Kamiński. **Impact of the Graft' Structure on the Behavior of PMMS-Based Brushes. High Pressure Studies.** *Polymer, 2023, 271, 125790.*

Mój udział polegał na uczestnictwie w dyskusji otrzymanych wyników.

ADIUNKT BADAWCZO-DYDAKTYCZNY
Zakładu Statystyki Medycznej
Śląskiego Uniwersytetu Medycznego w Katowicach

dr n. farm. Dawid Heczko

.....Dawid Heczko.....

Podpis współautora publikacji

V. PODSUMOWANIE I WNIOSKI

Niniejsza rozprawa doktorska składa się ze zbioru trzech artykułów naukowych poświęconych badaniom dynamiki molekularnej polimerów z grupy polisiloksanów – poli(merkaptopropylometylosiloksanu) (PMMS) oraz kopolimerów szczepionych otrzymanych na bazie PMMS, do którego poprzez sfunkcjonalizowaną grupę tiolową przyłączono łańcuchy polimerowe monomerów akrylanów i metakrylanów o różnej długości łańcucha alkilowego. Przedstawione wyniki przeprowadzonych eksperymentów podkreśliły istotną rolę wysokociśnieniowych badań dielektrycznych w wyjaśnianiu natury dodatkowych procesów relaksacyjnych obserwowanych w polisiloksanach, a w przypadku kopolimerów szczepionych pozwoliły na lepsze zrozumienie wpływu topologii i architektury polimeru na ich dynamikę molekularną.

Pierwsza z prac (**A1**), w oparciu o wyniki badań mechanicznych oraz dielektrycznych badań wysokociśnieniowych ujawniła, że dodatkowy proces relaksacyjny α' obserwowany dla PMMS jest relaksacją typu *sub-Rouse*. Co więcej, proces α' naśladuje zachowanie procesu relaksacyjnego *normal-mode* w zmiennych warunkach termodynamicznych (T i p). Podobieństwa te były widoczne jako superpozycja wolniejszego procesu α' i relaksacji segmentalnej α (stała separacja skali czasowej obu procesów) niezależnie od warunków termodynamicznych. Ponadto, wyznaczone objętości aktywacji dla obu relaksacji miały porównywalne wartości. To niezwykłe odkrycie sprawia, że PMMS jest drugim polisiloksanem, dla którego proces *sub-Rouse* został zidentyfikowany na widmach strat dielektrycznych.

W drugiej pracy (**A3**) przeprowadzone badania dla kopolimerów szczepionych wskazały, że na temperaturę zeszklenia mają wpływ zwiększająca się zawada steryczna związana z długością oraz sztywnością przyłączonych łańcuchów bocznych. Z kolei badania dielektryczne wykazały dla kopolimerów PMMS szczepionych homologicznymi monomerami

akrylanów (PMMS-*graft*-MA, PMMS-*graft*-*n*BA, PMMS-*graft*-HA) obecność jednego, szerokiego procesu relaksacyjnego (α), natomiast dla kopolimerów szczepionych monomerami metakrylanów (PMMS-*graft*-MMA, PMMS-*graft*-BMA, PMMS-*graft*-HMA) zaobserwowano dwa procesy relaksacyjne (α i α'). Porównanie danych dielektrycznych z mechanicznymi pozwoliło ustalić, że proces α dla obu grup badanych związków wynika z relaksacji segmentalnej, podczas gdy proces α' nie był widoczny w badaniach reologicznych. Wysokociśnieniowe eksperymenty dielektryczne wykonane na kopolimerach szczepionych monomerami metakrylanów wykazały, że podobnie jak dla homopolimeru PMMS, niezależnie od zastosowanych warunków termodynamicznych, istnieje superpozycja pomiędzy relaksacją α' a relaksacją segmentalną, co sugeruje, że proces α' jest związany z częściowymi ruchami molekularnymi łańcucha polimeru, typu *sub-Rouse*. Nie możemy jednak całkowicie wykluczyć możliwości, że proces α' może być pewnym rodzajem relaksacji pochodzącej od szczepu monomerów metakrylanu w łańcuchu bocznym kopolimeru.

Najważniejszym wnioskiem wysuniętym z trzeciej pracy (**A2**) było pokazanie, że modyfikacja polimeru poprzez szczepienie łańcucha bocznego znacząco wpływa na dynamikę molekularną. Temperatury zeszklenia dla kopolimerów PMMS szczepionych izomerami akrylanu butylu były znacznie wyższe niż T_g homopolimeru, a ich wartość wzrastała z coraz bardziej rozgałęzioną strukturą szczepu. Pomiary dielektryczne i komplementarne badania mechaniczne wykazały, że zaobserwowany szeroki proces relaksacyjny pochodzi od relaksacji segmentalnej α, a szerokość obserwowanego procesu koreluje z zawadą steryczną szczepu. Ponadto stwierdzono, że wartości współczynników ciśnieniowych temperatury przejścia szklistego (dT_g/dp) oraz objętości aktywacji (ΔV) określone dla kopolimerów szczepionych są znacznie wyższe niż dla homopolimeru PMMS ze względu na wzrastającą zawadę steryczną.

Uzyskane wyniki wyraźnie wskazują jak ważne jest zrozumienie wpływu struktury oraz topologii szczepów na dynamikę molekularną polimerów w zmiennych warunkach

termodynamicznych. Dlatego też, w dalszej perspektywie uzasadnione wydają się badania kopolimerów szczepionych PMMS, dla których do głównego łańcucha poprzez sfunkcjonalizowaną grupę -SH zostałyby przyłączone boczne odgałęzienia wybranych polimerów. Badania te mogą wnieść istotny wkład w naukę o polimerach, a co więcej pozwolą na jeszcze lepsze zrozumienie zachowania tego typu materiałów oraz będą kluczem do wytworzenia nowych, unikalnych materiałów polimerowych i ich aplikacyjności w wielu dziedzinach przemysłu.

VI. BIBLIOGRAFIA

(1) Jenkins, A. D.; Stepto, R. F. T.; Kratochvíl, P.; Suter, U. W. Glossary of Basic Terms in Polymer Science (IUPAC Recommendations 1996). *Pure and Applied Chemistry* 1996, *68* (12). https://doi.org/10.1351/pac199668122287.

(2) Wang, J.; Li, Z.; Xu, Y.; Hu, W.; Zheng, G.; Zheng, L.; Ren, T. Synthesis and Tribological Behavior of Bridged Bicyclic Polymers as Lubricants. *Ind Eng Chem Res* 2020, *59* (47), 20730–20739. https://doi.org/10.1021/ACS.IECR.0C04030.

(3) Abbasi, M.; Faust, L.; Wilhelm, M. Comb and Bottlebrush Polymers with Superior Rheological and Mechanical Properties. *Advanced Materials* 2019, *31* (26). https://doi.org/10.1002/adma.201806484.

(4) Daniel, W. F. M.; Burdyńska, J.; Vatankhah-Varnoosfaderani, M.; Matyjaszewski, K.; Paturej, J.; Rubinstein, M.; Dobrynin, A. V; Sheiko, S. S. Solvent-Free, Supersoft and Superelastic Bottlebrush Melts and Networks. *Nat Mater* 2016, *15* (2), 183–189. https://doi.org/10.1038/nmat4508.

(5) M. Miyake, G.; A. Weitekamp, R.; A. Piunova, V.; H. Grubbs, R. Synthesis of Isocyanate-Based Brush Block Copolymers and Their Rapid Self-Assembly to Infrared-Reflecting Photonic Crystals. *J Am Chem Soc* 2012, *134* (34), 14249–14254. https://doi.org/10.1021/ja306430k.

(6) Verduzco, R.; Li, X.; Pesek, S. L.; Stein, G. E. Structure, Function, Self-Assembly, and Applications of Bottlebrush Copolymers. *Chem. Soc. Rev.* 2015, *44* (8), 2405–2420. https://doi.org/10.1039/C4CS00329B.

(7) Pesek, S. L.; Lin, Y. H.; Mah, H. Z.; Kasper, W.; Chen, B.; Rohde, B. J.; Robertson, M. L.; Stein, G. E.; Verduzco, R. Synthesis of Bottlebrush Copolymers Based on Poly(Dimethylsiloxane) for Surface Active Additives. *Polymer (Guildf)* 2016, *98*, 495–504. https://doi.org/10.1016/j.polymer.2016.01.057.

(8) A. Johnson, J.; Y. Lu, Y.; O. Burts, A.; Xia, Y.; C. Durrell, A.; A. Tirrell, D.; H. Grubbs, R. Drug-Loaded, Bivalent-Bottle-Brush Polymers by Graft-through ROMP. *Macromolecules* 2010, *43* (24), 10326–10335. https://doi.org/10.1021/ma1021506.

(9) Matyjaszewski, K.; Xia, J. Atom Transfer Radical Polymerization. *Chem Rev* 2001, *101* (9). https://doi.org/10.1021/cr940534g.

(10) Jakubowski, W.; Matyjaszewski, K. Activator Generated by Electron Transfer for Atom Transfer Radical Polymerization. *Macromolecules* 2005, *38* (10). https://doi.org/10.1021/ma047389l.

(11) Börner, H. G.; Matyjaszewski, K. Graft Copolymers by Atom Transfer Polymerization. In *Macromolecular Symposia*; 2002; Vol. 177. https://doi.org/10.1002/1521-3900(200201)177:1<1::AID-MASY1>3.0.CO;2-V.

(12) Sheiko, S. S.; Sumerlin, B. S.; Matyjaszewski, K. Cylindrical Molecular Brushes: Synthesis, Characterization, and Properties. *Progress in Polymer Science (Oxford)* 2008, *33* (7), 759–785. https://doi.org/10.1016/j.progpolymsci.2008.05.001.

(13) Lee, H.; Pietrasik, J.; Sheiko, S. S.; Matyjaszewski, K. Stimuli-Responsive Molecular Brushes. *Prog Polym Sci* 2010, *35* (1–2), 24–44. https://doi.org/10.1016/j.progpolymsci.2009.11.002.

(14) Neugebauer, D.; Zhang, Y.; Pakula, T.; Sheiko, S. S.; Matyjaszewski, K. Densely-Grafted and Double-Grafted PEO Brushes via ATRP. A Route to Soft Elastomers. *Macromolecules* 2003, *36* (18). https://doi.org/10.1021/ma0345347.

(15) Savin, D. A.; Pyun, J.; Patterson, G. D.; Kowalewski, T.; Matyjaszewski, K. Synthesis and Characterization of Silica-Graft-Polystyrene Hybrid Nanoparticles: Effect of Constraint on the Glass-Transition Temperature of Spherical Polymer Brushes. *J Polym Sci B Polym Phys* 2002, *40* (23), 2667–2676. https://doi.org/10.1002/polb.10329.

(16) Peterson, G. I.; Choi, T. L. The Influence of Polymer Architecture in Polymer Mechanochemistry. *Chemical Communications* 2021, *57* (53), 6465–6474. https://doi.org/10.1039/d1cc02501e.

(17) Bhattacharya, A.; Misra, B. N. Grafting: A Versatile Means to Modify Polymers: Techniques, Factors and Applications. *Prog Polym Sci* 2004, *29* (8), 767–814. https://doi.org/10.1016/J.PROGPOLYMSCI.2004.05.002.

(18) Kremer, F.; Schonhals, A. *Broadband Dielectric Spectroscopy*; Springer, 2003. https://doi.org/10.1016/B978-0-12-823518-8.00001-3.

(19) Vigier, G.; Tatibouet, J. Physical Ageing of Amorphous and Semicrystalline Poly(Ethylene Terephthalate). *Polymer (Guildf)* 1993, *34* (20). https://doi.org/10.1016/0032-3861(93)90186-E.

(20) Hutchinson, J. M. Polymer Glasses, Mechanical Properties of: Physical Aging of Polymer Glasses. In *Encyclopedia of Materials: Science and Technology*; 2001. https://doi.org/10.1016/b0-08-043152-6/01305-x.

(21) Napolitano, S.; Glynos, E.; Tito, N. B. Glass Transition of Polymers in Bulk, Confined Geometries, and near Interfaces. *Reports on Progress in Physics* 2017, *80* (3). https://doi.org/10.1088/1361-6633/aa5284.

(22) Sillescu, H. Heterogeneity at the Glass Transition: A Review. *J Non Cryst Solids* 1999, *243* (2–3), 81–108. https://doi.org/10.1016/S0022-3093(98)00831-X.

(23) Priestley, R. D.; Ellison, C. J.; Broadbelt, L. J.; Torkelson, J. M. Materials Science: Structural Relaxation of Polymer Glasses at Surfaces, Interfaces, and in Between. *Science (1979)* 2005, *309* (5733). https://doi.org/10.1126/science.1112217.

(24) Wu, X.; Liu, C.; Zhu, Z.; Ngai, K. L.; Wang, L. M. Nature of the Sub-Rouse Modes in the Glass-Rubber Transition Zone of Amorphous Polymers. *Macromolecules* 2011, *44* (9). https://doi.org/10.1021/ma102897e.

(25) Debenedetti, P. G.; Stillinger, F. H. Supercooled Liquids and the Glass Transition. *Nature* 2001, *410* (6825), 259–267. https://doi.org/10.1038/35065704.

(26) *Volume VI Collected Experimental Papers, Volume VI*; Harvard University Press, 1964. https://doi.org/doi:10.4159/harvard.9780674287839.

(27) Ediger, M. D.; Angell, C. A.; Nagel, S. R. Supercooled Liquids and Glasses. *J Phys Chem* 1996, *100* (31), 13200–13212. https://doi.org/10.1021/jp953538d.

(28) C. A. Angell. Relaxation in Liquids, Polymers and Plastic Crystals - Strong/Fragile Patterns and Problems. *J Non Cryst Solids* 1991, *131*, 13–31.

(29) Austen Angell, C.; Sivarajan, S. Glass Transition. *Reference Module in Materials Science and Materials Engineering* 2017. https://doi.org/10.1016/B978-0-12-803581-8.03155-6.

(30) Adachi, K.; Kotaka, T. Dielectric Normal Mode Relaxation. *Prog Polym Sci* 1993, *18* (3), 585–622. https://doi.org/10.1016/0079-6700(93)90018-8.

(31) Floudas, G.; Reisinger, T. Pressure Dependence of the Local and Global Dynamics of Polyisoprene. *Journal of Chemical Physics* 1999, *111* (11). https://doi.org/10.1063/1.479774.

(32) Floudas, G.; Gravalides, C.; Reisinger, T.; Wegner, G. Effect of Pressure on the Segmental and Chain Dynamics of Polyisoprene. Molecular Weight Dependence. *Journal of Chemical Physics* 1999, *111* (21). https://doi.org/10.1063/1.480327.

(33) Casalini, R.; Roland, C. M. Temperature and Density Effects on the Local Segmental and Global Chain Dynamics of Poly(Oxybutylene). *Macromolecules* 2005, *38* (5). https://doi.org/10.1021/ma0476902.

(34) Se, K.; Adachi, K.; Kotaka, T. Dielectric Relaxations in Poly(Ethylene Oxide): Dependence on Molecular Weight. *Polym J* 1981, *13* (11). https://doi.org/10.1295/polymj.13.1009.

(35) Mierzwa, M.; Floudas, G.; Dorgan, J.; Knauss, D.; Wegner, J. Local and Global Dynamics of Polylactides.: A Dielectric Spectroscopy Study. *J Non Cryst Solids* 2002, *307–310*, 296–303. https://doi.org/10.1016/S0022-3093(02)01480-1.

(36) Hirose, Y.; Adachi, K. Type-A Dipole Moment and Segmental Dynamics of Poly(Styrene Oxide). *Polymer (Guildf)* 2005, *46* (6), 1913–1920. https://doi.org/10.1016/J.POLYMER.2004.12.003.

(37) Hirai, T.; Fujimura, N.; Urakawa, O.; Adachi, K.; Donkai, M.; Se, K. Dielectric Relaxation of Poly(n-Hexyl Isocyanate) in Concentrated Solutions of Polybutadiene. *Polymer (Guildf)* 2001, *43* (4). https://doi.org/10.1016/S0032-3861(01)00710-8.

(38) Cochrane, J.; Harrison, G.; Lamb, J.; Phillips, D. W. Creep, Creep Recovery and Dynamic Mechanical Measurements of a Poly(Propylene Glycol) Oligomer. *Polymer (Guildf)* 1980, *21* (7), 837–844. https://doi.org/10.1016/0032-3861(80)90306-7.

(39) Grzybowska, K.; Grzybowski, A.; Ziolo, J.; Rzoska, S. J.; Paluch, M. Anomalous Behavior of Secondary Dielectric Relaxation in Polypropylene Glycols. *Journal of Physics: Condensed Matter* 2007, *19* (37). https://doi.org/10.1088/0953-8984/19/37/376105.

(40) Gainaru, C.; Hiller, W.; Böhmer, R. A Dielectric Study of Oligo- and Poly(Propylene Glycol). *Macromolecules* 2010, *43* (4). https://doi.org/10.1021/ma9026383.

(41) Eckert-Kastner, S.; Meier, G.; Alig, I. Phase Behaviour of Mixtures of Polyethylene Glycol and Polypropylene Glycol: Influence of Hydrogen Bond Clusters on Critical Composition Fluctuations. *Physical Chemistry Chemical Physics* 2003, *5* (15). https://doi.org/10.1039/b304935n.

(42) Talik, A.; Tarnacka, M.; Dzienia, A.; Kaminska, E.; Kaminski, K.; Paluch, M. High-Pressure Studies on the Chain and Segmental Dynamics of a Series of Poly(Propylene Glycol) Derivatives. *Macromolecules* 2019, *52* (15), 5658–5669. https://doi.org/10.1021/acs.macromol.9b00692.

(43) Talik, A.; Tarnacka, M.; Geppert-Rybczyńska, M.; Hachuła, B.; Kaminski, K.; Paluch, M. Impact of Confinement on the Dynamics and H-Bonding Pattern in Low-Molecular Weight Poly(Propylene Glycols). *The Journal of Physical Chemistry C* 2020, *124* (32), 17607–17621. https://doi.org/10.1021/acs.jpcc.0c04062.

(44) Swenson, J.; Köper, I.; Telling, M. T. F. Dynamics of Propylene Glycol and Its 7-Mer by Neutron Scattering. *Journal of Chemical Physics* 2002, *116* (12). https://doi.org/10.1063/1.1453400.

(45) Stockmayer, W. H. Dielectric Dispersion in Solutions of Flexible Polymers. *Pure and Applied Chemistry* 1967, *15* (3–4), 539–554. https://doi.org/10.1351/pac196715030539.

(46) Paluch, M. Dielectric and Mechanical Relaxation in Epoxy Systems with Molecules of Differing Topology. *Journal of Physics Condensed Matter* 2000, *12* (45). https://doi.org/10.1088/0953-8984/12/45/312.

(47) Roland, C. M.; Psurek, T.; Pawlus, S.; Paluch, M. Segmental- and Normal-Mode Dielectric Relaxation of Poly(Propylene Glycol) under Pressure. *J Polym Sci B Polym Phys* 2003, *41* (23), 3047–3052. https://doi.org/10.1002/polb.10634.

(48) Colmenero, J.; Alegroia, A.; Santangelo, P. G.; Ngai, K. L.; Roland, C. M. Detailed Correspondences between Dielectric and Mechanical Relaxations in Poly(Vinylethylene). *Macromolecules* 1994, *27* (2). https://doi.org/10.1021/ma00080a013.

(49) Gerstl, C.; Schneider, G. J.; Pyckhout-Hintzen, W.; Allgaier, J.; Richter, D.; Alegría, A.; Colmenero, J. Segmental and Normal Mode Relaxation of Poly(Alkylene Oxide)s Studied by Dielectric Spectroscopy and Rheology. *Macromolecules* 2010, *43* (11). https://doi.org/10.1021/ma100384j.

(50) Schwartz, G. A.; Bergman, R.; Swenson, J. Relaxation Dynamics of a Polymer in a 2D Confinement. *Journal of Chemical Physics* 2004, *120* (12), 5736–5744. https://doi.org/10.1063/1.1650289.

(51) Boese, D.; Momper, B.; Meier, G.; Kremer, F.; Hagenah, J. U.; Fischer, E. W. Molecular Dynamics in Poly(Methylphenylsiloxane) As Studied by Dielectric Relaxation Spectroscopy and Quasielastic Light Scattering. *Macromolecules* 1989, *22* (12), 4416–4421. https://doi.org/10.1021/ma00202a005.

(52) Paluch, M.; Roland, C. M.; Pawlus, S. Temperature and Pressure Dependence of the α-Relaxation in Polymethylphenylsiloxane. *Journal of Chemical Physics* 2002, *116* (24). https://doi.org/10.1063/1.1478767.

(53) Pawlus, S.; Rzoska, S. J.; Ziolo, J.; Paluch, M.; Roland, C. M. Effect of Temperature and Pressure on Segmental Relaxation in Polymethylphenylsiloxane. *Rubber Chemistry and Technology* 2003, *76* (5). https://doi.org/10.5254/1.3547790.

(54) Kriegs, H.; Gapinski, J.; Meier, G.; Paluch, M.; Pawlus, S.; Patkowski, A. Pressure Effects on the α and A′ Relaxations in Polymethylphenylsiloxane. *Journal of Chemical Physics* 2006, *124* (10). https://doi.org/10.1063/1.2177242.

(55) Dlubek, G.; Shaikh, M. Q.; Krause-Rehberg, R.; Paluch, M. Effect of Free Volume and Temperature on the Structural Relaxation in Polymethylphenylsiloxane: A Positron Lifetime and Pressure-Volume-Temperature Study. *Journal of Chemical Physics* 2007, *126* (2). https://doi.org/10.1063/1.2406077.

(56) Tu, W.; Ngai, K. L.; Paluch, M.; Adrjanowicz, K. Dielectric Study on the Well-Resolved Sub-Rouse and JG β-Relaxations of Poly(Methylphenylsiloxane) at Ambient and Elevated Pressures. *Macromolecules* 2020, *53* (5), 1706–1715. https://doi.org/10.1021/acs.macromol.9b02332.

(57) Adrjanowicz, K.; Winkler, R.; Chat, K.; Duarte, D. M.; Tu, W.; Unni, A. B.; Paluch, M.; Ngai, K. L. Study of Increasing Pressure and Nanopore Confinement Effect on the Segmental, Chain, and Secondary Dynamics of Poly(Methylphenylsiloxane). *Macromolecules* 2019, *52* (10), 3763–3774. https://doi.org/10.1021/acs.macromol.9b00473.

(58) Plazek, D. J.; Bero, C. A.; Neumeister, S.; Floudas, G.; Fytas, G.; Ngai, K. L. Viscoelastic Properties of Amorphous Polymers 3: Low Molecular Weight Poly(Methylphenylsiloxane). *Colloid Polymer Science* 1994, *272*, 1430–1438.

(59) Bischoff, R.; Cray, S. E. Polysiloxanes in Macromolecular Architecture. *Progress in Polymer Science (Oxford)* 1999, *24* (2), 185–219. https://doi.org/10.1016/S0079-6700(99)00006-4.

(60) Yi, B.; Liu, P.; Hou, C.; Cao, C.; Zhang, J.; Sun, H.; Yao, X. Dual-Cross-Linked Supramolecular Polysiloxanes for Mechanically Tunable, Damage-Healable and Oil-Repellent Polymeric Coatings. *ACS Appl Mater Interfaces* 2019, *11* (50), 47382–47389. https://doi.org/10.1021/acsami.9b17199.

(61) Brook, M. Silicon in Organic, Organometallic, and Polymer Chemistry / M.A. Brook. 2000.

(62) Colas, A.; Curtis, J. Silicone Biomaterials: History and Chemistry & Medical Applications of Silicones. *Computer Law and Security Report* 2004, *20* (1).

(63) De Buyl, F. Silicone Sealants and Structural Adhesives. *Int J Adhes Adhes* 2001, *21* (5). https://doi.org/10.1016/S0143-7496(01)00018-5.

(64) Mojsiewicz-Pienkowska, K.; Jamrógiewicz, M.; Szymkowska, K.; Krenczkowska, D. Direct Human Contact with Siloxanes (Silicones) - Safety or Risk Part 1.

Characteristics of Siloxanes (Silicones). *Front Pharmacol* 2016, *7* (MAY), 1–8. https://doi.org/10.3389/fphar.2016.00132.

(65) Stoddard, R. J.; Arielle, L. Recent Developments in Silicones for Topical and Transdermal Drug Delivery. *Ther Deliv* 2015, *6* (7), 827–839.

(66) Fytas, G.; Dorfmuller, T.; Chu, B. PHOTON CORRELATION SPECTRA OF POLY(PHENYLMETHYL SILOXANE) UNDER HIGH PRESSURES. *Journal of polymer science. Part A-2, Polymer physics* 1984, *22* (8). https://doi.org/10.1002/pol.1984.180220811.

(67) Plazek, D. J.; Chay, I. C.; Ngai, K. L.; Roland, C. M. Viscoelastic Properties of Polymers. 4. Thermorheological Complexity of the Softening Dispersion in Polyisobutylene. *Macromolecules* 1995, *28* (19), 6432–6436. https://doi.org/10.1021/ma00123a007.

(68) Ngai, K. L.; Plazek, D. J. Identification of Different Modes of Molecular Motion in Polymers That Cause Thermorheological Complexity. *Rubber Chemistry and Technology* 1995, *68* (3), 376–434. https://doi.org/https://doi.org/10.5254/1.3538749.

(69) Plazek, D. J.; Ngai, K. L. Resolving the Sub-Rouse Modes by Creep Compliance Measurements in Poly(Methyl- Para-Tolyl-Siloxane). *Macromolecules* 2020, *53* (10), 3940–3945. https://doi.org/10.1021/acs.macromol.0c00536.

(70) Patkowski, A.; Gapinski, J.; Pakula, T.; Meier, G. Physical Nature of Complex Structural Relaxation in Polysiloxane - PMpTS: α and A′ Relaxations. *Polymer (Guildf)* 2006, *47* (20), 7231–7240. https://doi.org/10.1016/j.polymer.2006.05.065.

(71) Tarnacka, M.; Jurkiewicz, K.; Hachuła, B.; Wojnarowska, Z.; Wrzalik, R.; Bielas, R.; Talik, A.; Maksym, P.; Kaminski, K.; Paluch, M. Correlation between Locally Ordered (Hydrogen-Bonded) Nanodomains and Puzzling Dynamics of Polymethysiloxane Derivative. *Macromolecules* 2020, *53* (22), 10225–10233. https://doi.org/10.1021/acs.macromol.0c01289.

(72) Xing, K.; Chatterjee, S.; Saito, T.; Gainaru, C.; Sokolov, A. P. Impact of Hydrogen Bonding on Dynamics of Hydroxyl-Terminated Polydimethylsiloxane. *Macromolecules* 2016, *49* (8), 3138–3147. https://doi.org/10.1021/acs.macromol.6b00262.

(73) Politidis, C.; Alexandris, S.; Sakellariou, G.; Steinhart, M.; Floudas, G. Dynamics of Entangled Cis-1,4-Polyisoprene Confined to Nanoporous Alumina. *Macromolecules* 2019, *52* (11), 4185–4195. https://doi.org/10.1021/acs.macromol.9b00523.

(74) Zimny, S.; Tarnacka, M.; Kamińska, E.; Wrzalik, R.; Adrjanowicz, K.; Paluch, M.; Kamiński, K. Studies on the Molecular Dynamics at High Pressures as a Key to Identify the Sub-Rouse Mode in PMMS. *Macromolecules* 2022, *55* (13), 5581–5590. https://doi.org/10.1021/acs.macromol.2c00378.

(75) Zimny, S.; Tarnacka, M.; Maksym, P.; Wojnarowska, Ż.; Paluch, M.; Kamiński, K. The Influence of Graft Rigidity on the Dynamical Behavior of PMMS-Based Polymer Brushes at Ambient and High Pressures. *Macromolecules* 2024. https://doi.org/10.1021/acs.macromol.4c01779.